ROLES OF THE UNFOLDED PROTEIN RESPONSE IN CULTURED CELLS AND TRANSGENIC MURINE MODELS

by

Jun Wu

A dissertation submitted in partial fulfillment
of the requirements for the degree of
Doctor of Philosophy
(Biological Chemistry)
in The University of Michigan
2007

Doctoral Committee:

Professor Randal J. Kaufman, Chair
Professor Robert S. Fuller
Professor David Ginsburg
Professor Miriam H. Meisler
Professor Alan R. Saltiel
Associate Professor Zhaohui Xu

To my parents and my sister

Acknowledgements

I would like to thank my thesis advisor, Dr. Randal J. Kaufman. First of all, for his great scientific guidance and inspiration to this work, his broad knowledge and critical thinking helped me carry the projects through. I have been trained as an independent researcher, learning from how to identify an interesting and significant question, design well-controlled experiments to scientific writing and presentation. Secondly, I am grateful that he provided the best research environment and resource as well as his efforts in communicating and collaborating with other leading groups in the field. Last but not least, I thank him for this wonderful role model: I have witnessed the passion and the perseverance of a true scientist in him. He is the best mentor a graduate student could ask for.

I would like to thank my thesis committee, Drs. Alan Saltiel, David Ginsburg, Meriam Meisler, Robert Fuller and Zhaohui Xu, for their time, suggestions and encouragements. I thank Drs. Kun-liang Guan and Benjamin Margolis for their help and advice during my rotations in their laboratories.

I am in debt to my collaborators and former/current coworkers for their supports. Dr. D. Thomas Rutkowski, who taught me a great deal about experimental design, critical interpretation of raw data and scientific writing, helped me through my graduate study. His knowledge, enthusiasm towards science and dedicated working attitude made him a marvelous person to work and be friends with. Thanks to Drs. Kezhong Zhang, Sung Hoon Back, Robert Clark, Donalyn Scheuner, Jingcheng Yu, Alan Cheng and Benbo Song for their collaborations and/or discussions.

I would like to thank Junying Wang, Meghan Dubois and Jayanth Swathirajan for all their help along the way.

My sincere thanks also go to my friends: Xiaohua Shen, Hongmin Sun, Shuling Fan, Hongjiao Ouyang, Hetty Wong and Kathryn Gunnison for their friendship and

encouragements. Thanks to Janet Mitchell in Kaufman laboratory and Beth Goodwin in the department office for their excellent assistance.

Finally, I would like to thank my family, my parents — Li Hui, Wu Changhong, and my sister — Wu Zhen, who always believe in me. Without their everlasting love and unconditional support, I will never come this far.

Preface

The introduction (Chapter I) is a review of our current understanding of the UPR field. (*Cell Death Differ. 2006 Mar;13(3):374-84.*) Chapter II is a copy of publication by Jun Wu et al. (*Developmental Cell, 2007 Sep;13(3):351-64,* J. Wu, D.T. Rutkowsk and R. Kaufman jointly conceived and designed the experiments, performed experiments, analyzed data and wrote the paper). Chapter III is composed of the mouse genetics part of a research article (*Cell. 2006 Feb 10;124(3):587-99*) and further work on ER stress and inflammation that is being prepared for submission for publication and will be credited to Jun Wu, Kezhong Zhang, Sung Hoon Back, D. Thomas Rutkowski and Randal Kaufman et. al.

TABLE OF CONTENTS

Dedication…..……..…ii
Acknowledgements……iii
Preface…..……v
List of Figures…….……...vii

CHAPTER
I. INTRODUCTION…….……1
Figures……..……20
Table……22
References……23

II. ATF6 ALPHA OPTIMIZES LONG-TERM ENDOPLASMIC RETICULUM FUNCTION TO PROTECT CELLS FROM CHRONIC STRESS……32
Abstract……32
Introduction……..32
Results and Discussion……..…….…….34
Conclusions and Perspectives……..45
Experimental Procedures…….50
Figures……..59
References……75

III. ENDOPLASMIC RETICULUM STRSS AND INFLAMMATION……..80
Part I. UPR and the acute phase response…...……..80
Part II. Lipopolysaccharide+Galactosamine (LPS+GalN) induced acute liver injury requires phosphorylation of the alpha subunit of eukaryotic translation initiation factor 2…….94
Figures……105
References……..115

IV. CONCLUSIONS, PERSPECTIVES AND FUTURE DIRECTIONS…..…119
Figures……128
References……..131

List of Figures

Figure

1-1. Adaptive signaling of the unfolded protein response……..…20

1-2. ER stress mediated apoptotic pathways……..21

2-1. Generation of *Atf6*α deficient mice……59

2-2. Further molecular characterization of ATF6α deficient mice……60

2-3. *Atf6*α deficient MEFs are responsive to ER stress but defective in chaperone upregulation……61

2-4. Attenuated upregulation of UPR targets by TM and TG in *Atf6*α-/- cells….62

2-5. Direct regulation of ERSE-dependent expression by ATF6α……63

2-6. ATF6α-XBP1 pathway interactions……...64

2-7. The PERK and IRE1α pathways functionally overlap with ATF6α…….65

2-8. *Atf6*β knockdown does not exacerbate *Atf6*α-/- defects in BiP and CHOP upregulation……66

2-9. Transcriptional profiling reveals defective induction of a subset of ER stress-dependent genes in *Atf6*α-/- fibroblasts…….67

2-10. Additional validation of microarray data…….68

2-11. *Atf6*α deficient cells are defective in ER protein processing……...69

2-12. *Atf6*α-/- MEFs do not efficiently adapt to chronic ER stress……...70

2-13. Impaired adaptation to chronic stress in *Atf6*α-/- cells…….71

2-14. Persistence of UPR signaling in *Atf6*α-/- cells exposed to chronic stress…72

2-15. ATF6α regulates stress-dependent chaperone expression in vivo……...73

2-16. Lack of upregulation of *Edem1* in *Atf6*α-/- mice…….74

3-1. Generation of CREBH knockdown mice…….105

3-2. CREBH is required to up-regulate expression of the CRP and SAP genes.106

3-3. Attenuated secretion of SAP in TM challenged *Atf6α-/-* mice……107

3-4. *Atf6α*-deficient mice are responsive to LPS challenge……108

3-5. *Ire1α*-deficient mice are defective in up-regulation of acute phase response marker genes upon LPS challenge…….……..109

3-6. Generation of hepatocyte-specific eIF2α Ser51Ala knockin mice……..110

3-7. LPS+GalN challenge induces eIF2α phosphorylation in vivo…….111

3-8. Disruption of eIF2α phosphorylation ameliorates acute liver injury induced by LPS+GalN challenge…….….112

3-9.CHOP upregulation is defective in the LPS+GalN challenged eIF2α$^{A/A}$:tg/+:Alb-cre mice…….……..113

3-10.Diagrammatic representation of the cross talk of macrophages and hepatocytes during LPS+GalN induced liver apoptosis in eIF2α$^{A/A}$:tg/+:Alb-cre mice……114

4-1. A schematic diagram depicting the relative roles of PERK, ATF6α and IRE1α in regulating the functions responsible for adaptation to stress…....128

4-2. *Atf6α*-/- primary splenic B cells do not efficiently adapt to physiological stress during plasma cell differentiation……....129

4-3. Basal pancreatic expression level of BiP is lower in *Atf6α*-/- mice…….130

CHAPTER I

INTRODUCTION

The Endoplasmic Reticulum (ER) is the entry site for proteins destined to the endo/exocytotic pathway, and provides an optimal and unique environment for protein folding, assembly and disulfide bond formation prior to exposure to the extracellular space. The concentration of proteins within the ER lumen is extremely high, approximately 100mg/ml [1]. The protein synthesis rate is also astonishingly high in professional secretory cells, where it is estimated that hepatocytes and pancreatic exocrine cells synthesize approximately 13 million and 2.6 million secretory proteins per minute, respectively [2]. To accomplish such a thermodynamically unfavorable process in an overwhelmingly crowded environment, the cell expends a large amount of energy to ensure that this quantitative achievement does not come at the price of quality. Homeostasis within the ER lumen is meticulously monitored and elegantly maintained. A broad spectrum of insults can lead to the activation of a coordinated adaptive program called the unfolded protein response (UPR). In response to the accumulation of unfolded proteins in the ER, the rate of general translation initiation is attenuated, the expression of ER resident protein chaperones and protein foldases is induced, the ER compartment proliferates, and ER-associated degradation (ERAD) is activated to eliminate the irreparably misfolded proteins. When the pro-survival efforts are exhausted, ER-stress related apoptosis commences. A number of insults lead to protein misfolding in the ER.

These include nutrient deprivation, alterations in the oxidation-reduction balance, changes in calcium concentration, failure of post-translational modifications, or simply increases in secretory protein synthesis [3]. Pharmacological reagents were initially employed to elucidate how cells cope with immediate and severe challenges to the protein folding quality control system. These approaches have led to our present knowledge of the molecular logic of UPR signaling pathways, which has been thoroughly reviewed [4]. However, as analysis of increasing numbers of murine genetic models created with mutations in major UPR components proceeds, it is becoming apparent that a wide diversity of physiological fluctuations and pathological conditions can also disrupt the protein folding efficiency in the ER in a relatively subtle and chronic manner to activate the UPR. For professional secretory cells that harbor an extensive, highly-evolved ER structure, such as antibody-secreting plasma cells, collagen-secreting osteoblasts, and cells within the endocrine/exocrine organs, emerging evidence suggests the UPR is indispensable and actively involved to ensure proper function and survival.

I. The temporal sequential activation of UPR sub-pathways upon acute ER stress

a. Response initiation: one master regulator

During the pre-stress state, nascent, folding-competent polypeptides are maintained in a soluble form by interaction with ER lumenal chaperones. BiP/GRP78 (immunoglobulin heavy chain binding protein/glucose regulated protein of molecular weight 78 kDa) is one of the most highly expressed ER resident chaperones. BiP is a member of the heat-shock protein (Hsp70) family, and is localized to the ER through an N-terminal cleaved signal peptide and a C-terminal ER retention motif (KDEL). The C-terminal domain of BiP binds to exposed hydrophobic patches on protein-folding

intermediates with rather low substrate specificity. The N-terminal domain of BiP functions as a peptide-dependent ATPase that uses ATP hydrolysis to promote a conformational change in the C-terminal region that promotes high affinity peptide binding. Upon exchange of ATP for bound ADP, BiP reverts back to the low-affinity peptide binding state. In this way, the cell couples substrate binding and release with the expenditure of cellular energy [5-7].

To date there are three identified proximal sensors of the UPR: the PKR-like ER protein kinase/pancreatic eIF2α (eukaryotic translation initiation factor 2, α subunit) kinase (PERK/PEK); the activating transcription factor 6 (ATF6); and the inositol-requiring enzyme 1 (IRE1) (Figure 1-1). All of these sensors associate with BiP in their inactive states. It is proposed that when ER homeostasis is perturbed, BiP preferentially binds to and is sequestered by unfolded/misfolded proteins that accumulate in the ER lumen. As a consequence, BiP dissociates from the UPR transducers to permit their signaling. The major support for this hypothesis is that BiP is found in association with each stress transducer under non-stress conditions and is released upon accumulation of unfolded proteins [8-11]. In addition, over-expression of BiP inhibits signaling through all three sub-pathways [12]. Unfortunately, there is little direct data to support this model where BiP inhibits UPR activation. However, it remains an attractive hypothesis because this model implies that the peptide-dependent ATPase activity of BiP can function as an unfolded protein sensor to mechanistically link UPR activation with the cellular energy status and/or nutrient level.

In contrast to the simultaneous activation of the three UPR transducers upon severe, acute ER stress, selective UPR sub-pathways function under various

physiological and pathological ER stresses (see section II). Two groups recently proposed that the ER stress transducers Ire1p and ATF6 themselves are actively involved in the dissociation from BiP and the consequent activation, contrary to being passively competitive deprived of BiP [13,14]. It is also conceivable that there are other regulators involved in response initiation, for example, co-chaperones such as the DnaJ family members that stimulate the ATPase activity of the Hsp70 family members, or other tissue-specific adaptor proteins that may facilitate activation of specific UPR sub-pathways in response to different physiological conditions. Alternatively, it is possible that the affinity of each UPR transducer for BiP varies from cell type to cell type.

b. Signal diversification: unique signal transduction from three proximal transducers

Although the three UPR sub-pathways are simultaneously activated upon severe ER stress, the immediate response occurs through the PERK/eIF2α pathway. PERK is a type I ER transmembrane protein kinase. Upon release from BiP, PERK dimerizes to promote its autophosphorylation and activation. Activated PERK phosphorylates eIF2α to attenuate the rate of general translation initiation [15,16]. The rapid and reversible regulation of mRNA translation provides an "emergency brake" to prevent further synthesis of proteins when the ER lumen is compromised in its protein-folding capacity. Paradoxically, phosphorylation of eIF2α preferentially increases the translation of selective mRNAs that contain inhibitory upstream open-reading frames (uORFs) within their 5' untranslated region (UTR). The best studied example in mammalian cells is the eIF2α phosphorylation-dependent translation of activating transcription factor 4 (ATF4) mRNA [17,18].

Coincident with PERK activation upon BiP release, BiP release from IRE1 permits its dimerization and autophosphorylation to activate its site-specific endoribonuclease (RNase) activity [19]. The RNase activity of IRE1 initiates splicing of a 26 base intron from X-box binding protein 1 (XBP1) mRNA. This non-conventional splicing reaction introduces a translational frameshift into the XBP1 mRNA that alters the C-terminus of the protein to create a potent transcription factor [20-23].

ATF6 is a type II transmembrane protein of the ER. BiP release allows the transit of ATF6 to the *cis*-Golgi compartment, where it is cleaved by site-1 protease (S1P) and site-2 protease (S2P), the same enzymes that process the sterol-response-element binding protein (SREBP) upon cholesterol deprivation [24-26]. The cleaved cytosolic N-terminal fragment of ATF6 migrates to the nucleus and acts as an active transcription factor, together with ATF4 and XBP1 derived from spliced *Xbp1* mRNA, to increase the expression of the genes encoding proteins that function to augment the ER protein-folding capacity. These gene targets include ones encoding ER chaperones such as BiP/GRP78, GRP94, calreticulin, and ones encoding proteins that catalyze protein-folding such as the protein disulfide isomerases PDI, ERP57, and ERP72. In addition, UPR-activated genes stimulate ER biogenesis to compensate for the increased demand for the protein-folding machinery and accelerate ERAD to remove terminally misfolded proteins [27-31]. The specificity and diversity of downstream transcriptional responses upon different conditions is likely a result of combinatorial interactions between these transcription factors at the promoters of target genes.

This transcriptional adaptive program requires mRNA translation and therefore, a mechanism to recover from the PERK-mediated translational suppression.

c. Termination of the UPR signaling: negative feedback regulators

Translational recovery is mediated through dephosphorylation of PERK and/or eIF2α. To preclude the destructive translation attenuation mediated by eIF2α phosphorylation upon cell stress, mammalian cells evolved both a constitutively active regulator of p-eIF2α phosphatase, e.g. CreP (constitutive repressor of eIF2α phosphorylation) and a stress-induced regulator of p-eIF2α phosphatase, GADD34 (growth arrest and DNA damage gene 34). Both proteins act as subunits of the protein phosphatase holoenzyme PP1. In addition, $p58^{IPK}$ (58 kDa PKR inhibitor) is a UPR-induced gene product that inhibits the eIF2α kinases PERK and the double stranded-RNA activated protein kinase PKR [32-36]. It is unknown how the mRNAs of GADD34 and $p58^{IPK}$ escape translational repression before dephosphorylation of eIF2α occurs, but CreP may mediate this function.

In yeast, inactivation of Ire1p/Hac1p pathway is achieved by an Ire1p phosphatase, Ptc2p [37]. The mechanism of deactivation of the ATF6 and IRE1/XBP1 pathways in higher eukaryotes has not been established. However, as the UPR remains activated, the level of BiP increases so that it can bind and prevent further activation of ATF6, IRE1, as well as PERK. The mechanisms for inactivation of ATF6 and XBP1 transcriptional functions are also not known, but may involve targeted degradation by the proteasome.

d. ER stress-mediated apoptosis

When all the pro-survival efforts fail to correct the protein-folding defect, apoptosis is activated. It is not clear at what point and by which mechanism the cell commits to death in response to excessive ER stress. Both mitochondrial- dependent and

independent cell death pathways likely mediate apoptosis in response to ER stress. The ER might actually serve as a site where apoptotic signals are generated through several mechanisms including Bak/Bax regulated Ca^{2+} release from the ER, cleavage and activation of procaspase-12, and IRE1-mediated activation of ASK1 (apoptosis signal-regulating kinase 1) / JNK (c-Jun amino terminal kinase) (Figure 1-2).

The available data suggest that upon encountering ER stress, pro-apoptotic Bcl2-related proteins, Bak and Bax undergo conformational alteration in the ER membrane to permit Ca^{2+} efflux into the cytoplasm [38,39]. *In vitro* experiments support the idea that the increase in Ca^{2+} concentration (from micromolar to millimolar) in the cytoplasm activates the calcium-dependent protease m-Calpain, that subsequently cleaves and activates the ER-resident procaspase-12 [40]. Activated caspase-12 cleaves and activates procaspase-9 and consequently leads to activation of the caspase cascade [41]. The Ca^{2+} released from the ER enters mitochondria leading to depolarization of the inner membrane, cytochrome *c* release, and activation of Apaf-1(apoptosis protease activating factor 1)/procaspase-9 regulated apoptosis [42,43]. CHOP (CEBP homologous protein) is a downstream transcriptional target of ATF6 and PERK/ eIF2α/ATF4. CHOP is a basic leucine zipper-containing transcription factor that inhibits the expression of Bcl-2 and thereby is proposed to promote apoptosis [44,45].

IRE1α is proposed to play a role in ER stress-mediated apoptosis by interaction with TRAF2 (TNF receptor associated factor-2) and ASK1 leading to the activation of ASK1 and JNK, and subsequent cell death [46]. It has also been suggested that IRE1/TRAF2 association releases procaspase-12 from TRAF2, which is required for the activation of procaspase-12 [47].

Analysis of gene-deleted mice has provided insight into ER stress-induced apoptosis. Cells from *Apaf-1* deficient mice are susceptible to ER stress-induced apoptosis, indicating that non-mitochondrial death pathways exist. Bak/Bax double knock-out, *caspase-12*-/- and *chop*-/- murine embryonic fibroblasts (MEFs) all show partial resistance to ER stress induced apoptosis, further supporting the idea that they facilitate the apoptotic response upon ER stress [44,48,49]. Although, caspase-12-deficient and CHOP-deficient mice show no developmental defects, they display protection to genetically-imposed or environmentally-imposed ER stress [49,50].

II. The role of the UPR in professional secretory cell development and function

The adaptive aspects of the UPR signaling are better understood than the apoptotic pathways. However, *in vivo* analyses of these pathways under physiological and pathological contexts constantly surprise researchers and have inspired the current popular hypothesis that UPR pathways are regulated in a finely-tuned manner with selectivity and additional specificity to meet the complexity of various developmental and metabolic demands. The best understood physiological requirements for the UPR were elucidated in studies performed in professional secretory cells, which are under greater demand to fold and process large quantities of proteins (Table 1-1).

a. Lessons from plasma cell differentiation

Analysis of the differentiation of B lymphocytes into plasma cells has suggested that the UPR drives ER biogenesis in response to high-level secretory protein synthesis [51]. Extensive studies have elucidated the relationship between the UPR and plasma cell differentiation. The results from these studies established the fundamental principle that

the UPR provides an essential physiological role in professional secretory cell differentiation.

It was reported over 20 years ago that the expression level of chaperones in the ER lumen is increased during lipopolysaccharide (LPS)-induced B cell differentiation [52,53]. BiP was originally characterized as a protein that interacts with immunoglobulin (Ig) heavy chains to prevent their secretion in pre-B lymphocytes prior to light chain gene rearrangement [54]. Subsequent studies demonstrated that BiP acts as a chaperone to assist Ig heavy chains interact with Ig light chains. In parallel studies, it was observed that GRP78 is one of a number of gene products that reside in the ER and that are induced upon glucose deprivation. The products of these genes were thus termed glucose-regulated proteins. When it was discovered that BiP is the same protein as GRP78, it became evident that many of the GRPs provide protein chaperone function in the ER. At that point, investigators began to test whether the UPR may be involved in the process of B lymphocyte differentiation into high-level Ig secreting plasma cells. B cell lymphopoiesis consists of an antigen-independent phase in the bone marrow (pro-B cell, pre-B cell) and an antigen-driven phase of differentiation that is completed in the periphery (mature B cell, plasma cell). In pre-B cells, the ER exists as a minimal structure, most of which is nuclear envelope. Plasma cell differentiation in the periphery is accompanied by a 5-fold expansion of the ER compartment, into stereotyping ribosome-studded stacked membrane sheets, presumably to accommodate the high level of Ig secretion. The first factor identified to be required for B lymphocyte differentiation into plasma cells was the transcription factor XBP1. When it was discovered that the mammalian substrate for the endoribonuclease activity of IRE1 is XBP1 mRNA, it was

proposed that the IRE1 sub-pathway of the UPR provides an important physiological role to drive plasma cell differentiation [55].

LPS- or interleukin-4 induced differentiation of B lymphoma cells into plasma cells provides a unique experimental system to study the general involvement of the UPR. Results from *in vitro* lymphoma or splenic B cell differentiation assays showed that the classical UPR target genes, such as BiP and GRP94 are dramatically induced [55,56]. Stimulation of primary splenic B cells from different mouse genetic backgrounds can identify the unique requirements for individual gene products in this differentiation. In addition, the ability to reconstitute the B cell lineage in immunodeficient mice (such as recombination activating gene RAG1- or RAG2- deficient mice), provides a method to directly test the role of different genes in B cell differentiation. RAG-1 and RAG-2 are essential for the rearrangement of Ig (immunoglobin) heavy and light chain gene loci [57], as well as the T cell receptor gene loci. As a consequence, RAG-2-deficient mice lack mature T cells and B cells. Analysis of chimeric mice created by injection of homozygous deficient embryonic stem cells into RAG-2-deficient blastocysts or of RAG-2 deficient mice transplanted with hematopoietic stem cells deleted in specific components of the UPR pathway has provided insights into the requirement of the IRE1α/XBP1 pathway in this system.

XBP1 transcription is induced during B cell differentiation and *xbp1*-/- B cells fail to differentiate into antibody-secreting plasma cells *in vivo* [58]. XBP1 splicing correlates with plasma cell differentiation and ectopic expression of the spliced form of XBP1 restores Ig production in XBP1-deficient B cells *in vitro* [55]. The important role that XBP1 plays in plasma cell differentiation suggested that IRE1α is also essential for this process.

This idea was well supported by the observation that *Ire1α*-/- B cells did not differentiate into antibody secreting plasma cells [59]. Unexpectedly, the same set of experiments discovered that IRE1α is also required at the first stage of B cell lymphopoiesis to induce Ig gene rearrangements. More intriguing, is that the cytoplasmic domain, but not the protein kinase or endoribonuclease catalytic activities, was required for this novel function [59]. The IRE1α protein was required to activate expression of Rag1, Rag2, and terminal deoxynucleotidyl transferase (TDT).

These findings have led to several important questions. First, what signals activate IRE1α to promote Ig gene rearrangement? Second, is BiP dissociation from IRE1αrequired? Certainly, the analysis of plasma cell differentiation in B cells that express different mutants of IRE1α will provide important insight into this process [55].

Finally, what role does IRE1α/XBP1 play in the late stage of B cell differentiation? To address these issues, it is important to elucidate the temporal hierarchy of the increase in antibody production to create ER load and the expansion of the protein folding capacity. Does ER stress actually drive the ER differentiation process? Although this question has created a considerable debate, most reports support the hypothesis that expansion of the ER protein-folding capacity occurs at least simultaneously, if not prior to, initiation of Ig protein secretion [56,60], suggesting that the UPR activation may not solely depend on BiP dissociation from IRE1 in this case. However, it should be noted that Ig gene rearrangements associated with B cell differentiation produce a number of non-productive alleles that would produce misfolded Ig chains. It is possible that expression of folding-defective Ig intermediates from incorrectly rearranged alleles potently activates the UPR to contribute to ER expansion at

an early time in differentiation, after the first Ig heavy chain gene V-D rearrangement occurs.

The unsolved mysteries of B cell differentiation also raise the question of why the PERK/eIF2α pathway is not as essential as the IRE1α/XBP1 pathway. In the absence of eIF2α phosphorylation, B cells can completely differentiate into functional plasma cells [59]. Since BiP appears to associate with the lumenal domains of IRE1α and PERK in a similar manner to regulate the UPR upon severe ER stress [61], the *in vivo* disparity in the roles of these two pathways supports the idea that a more sophisticated mechanism of regulation exists for the physiological UPR in specific cell types. The other UPR transducer, ATF6 is cleaved and activated during B cell differentiation into plasma cells [56]. In addition, inhibition of the ATF6 pathway by expression of a dominant-negative form of ATF6 reduced IgM production in differentiating B cells [62].

The physiological function of ATF6 in the UPR and plasma cell differentiation is under question because knock-down of both isoforms of ATF (ATF6α and ATF6β) did not interfere with UPR gene induction [63], despite the finding that over-expression of ATF6 induced a significant set of UPR target genes. Cells lacking both XBP1 and ATF6α are defective in UPR activation [63], suggesting that these two pathways may overlap.

Another very appealing possibility is that the UPR is activated through interplay between the conventional UPR pathway and other signal transduction pathways. During plasma cell differentiation, XBP1 is downstream of BLIMP1 (B lymphocyte-induced maturation protein 1), a transcription factor required for plasma cell differentiation which is regulated by interleukin (IL)-4 at a transcriptional level [55,64]. It has also been proposed

that XBP1 is upstream of IL-6 during plasma cell differentiation [55]. Meanwhile, activated XBP1 increases the protein-folding machinery in the cell, at least in part by increasing the expression of ER chaperones and foldases. A recent report links XBP1 activation to ER membrane biogenesis [65].

b. Pancreatic beta cell function and survival

The pancreatic beta cell has been under intense investigation ever since its pivotal role in the pathogenesis of diabetes mellitus was recognized [66]. Extensive research is directed to understand what unique properties beta cells have to confer glucose responsive insulin production and secretion. The hallmark of pancreas dysfunction in non-insulin dependent diabetes mellitus is diminished glucose-responsive insulin secretion, which is regulated by signals derived from mitochondrial metabolism [67]. In order to maintain adequate intracellular insulin stores, beta cells must adapt their acute and chronic rates of insulin biosynthesis to compensate for insulin release. Chronic elevation in extra-cellular glucose concentration further stimulates the synthesis of insulin by increasing expression of the mRNA encoding preproinsulin, increasing proinsulin translation and processing, and induction of additional components of the secretory pathway to support processing, transport and glucose-regulated secretion of insulin. Type 2 diabetes results from failure of beta cells to adequately adapt to the increasing demand for insulin production as a consequence of peripheral insulin resistance.

i. ER overload leads to beta cell dysfunction.

As a professional secretory cell, the vulnerability of the beta cell to ER stress was suggested in early studies that induced beta-cell damage by over-expression of major histocompatibility complex (MHC) class II protein in islets of transgenic mice [68].

Characterization of the Akita mouse further supported the hypothesis that ER stress could be one cause for beta cell death. There are two insulin genes in the murine genome (Ins1 and Ins2). In the Akita mouse, a highly conserved cysteine in the Ins2 gene is replaced by a tyrosine, thereby disrupting formation of one essential disulfide bond in proinsulin-2. The mutant protein cannot be processed and secreted normally and is retained within the ER. Although the islets from newborn Akita mice do not show detectable defects, later in development a progressive beta cell loss occurs that correlates with early onset diabetes [69]. Since the complete absence of Ins2 expression does not lead to a similar diabetic phenotype and the Akita phenotype is dominant, the Akita mutation represents a gain-of-function. It is believed that the mutant protein is toxic due to induction of the ER stress response [70]. This notion is further supported by the findings that the ER in the Akita beta cells is distended and the UPR target genes BiP and CHOP are induced. In addition, deletion of the CHOP gene delayed the onset of beta-cell destruction and of hyperglycemia in heterozygous Akita mice [69,71]. The absence of CHOP was also reported to increase resistance to nitric oxide-induced apoptosis in pancreatic beta cells [72]. Since nitric oxide production is implicated in the pathogenesis of type I diabetes [73], development of specific inhibitors that either block CHOP expression or its transcription factor activity, for example preventing CHOP dimerization or DNA binding activity, may yield potential therapeutics for the prevention of diabetes.

ii. Defective regulation of the PERK/eIF2α pathway leads to beta cell dysfunction

Recent studies also indicate that the UPR is required to maintain beta cell function. Compared to other differentiated cells, the beta cell requires periodic increases in the capacity to fold and secrete insulin in response to post-prandial increases in blood

glucose. This regulation of insulin synthesis is immediate and reversible and may be mediated by the PERK/eIF2α UPR sub-pathway. PERK was first identified as a highly expressed eIF2α protein kinase in the pancreas. Deletion of PERK results in progressive destruction of pancreatic beta cells in both humans and mice [15,74,75]. In humans, mutations in the PERK gene cause Wolcott-Rallison syndrome which manifests as an infantile-onset, insulin-requiring diabetes [74]. *perk*-/- mice experience a progressive loss of beta cells and develop diabetes within the first few weeks after birth [75]. It is proposed that in the absence of PERK, mRNA translation cannot be attenuated so the protein-folding load cannot be properly coupled with the protein-folding capacity of the ER. As a consequence, *perk*-/- mice have defects in beta cells as well as in other highly specialized secretory cells, such as exocrine pancreatic acinar cells, hepatocytes and osteoblasts [75]. Islets isolated from *perk*-/- mice secrete more insulin when they are switched from low glucose to high glucose conditions [75]. This is presumably due to the inability to down-regulate protein synthesis in response to increased insulin production. The eventual outcome results in accumulation of unfolded proinsulin in the ER with loss of beta cell secretion potential.

Mice that are resistant to regulation by all eIF2α kinases were generated by introducing a serine51alanine point mutation, the residue phosphorylated by all eIF2α kinases, into the eIF2α gene [31]. Homozygous eIF2α S51A knock-in mice develop a more severe β-cell dysfunction prior to birth, compared to *perk*-/- mice [31]. The more severe beta cell defect in the eIF2α mutant mice may indicate that other eIF2α kinases, such as the general control of amino acid biosynthesis kinase GCN2 or the double-stranded (ds)

RNA-activated protein kinase PKR, may partially compensate for eIF2α phosphorylation in the absence of PERK [76-78].

Heterozygous eIF2α S51A mice, where eIF2α phosphorylation regulation is reduced to approximately 50%, have no significant phenotype. However, when these mice are challenged with a high-fat diet, they develop insulin resistance, obesity, and diabetes with pancreatic beta cell failure associated with a loss of glucose-stimulated insulin secretion. The beta cells in the heterozygous high-fat fed mice exhibit abnormal distension of the ER lumen, defective folding and trafficking of proinsulin, and a reduced number of insulin granules [79]. The reduced number of insulin granules can account for the loss of glucose-stimulated insulin secretion. It is proposed that the partial defect in the PERK/eIF2α pathway compromises the ability to couple proinsulin synthesis with proinsulin folding in the ER, leading to defective insulin secretion.

Mice with a defect in down-regulating PERK-mediated eIF2α phosphorylation by deletion of $p58^{IPK}$ also show increased pancreatic beta cell apoptosis concurrent with a gradual onset of glucosuria and hyperglycemia [80]. On the other hand, developmental or metabolic defects were not observed in mice with homozygous GADD34 mutation to prevent regulated p-eIF2α dephosphorylation [81]. The divergence between the $gadd34^{\Delta c/\Delta c}$- and $p58^{IPK}$- deleted mice may indicate that these two negative regulators play different physiological roles *in vivo*.

c. The UPR in hepatocytes

The liver is one of the major secretory organs in the body. Its functions include regulation of glucose homeostasis, lipid metabolism and drug detoxification. Although

the role of the UPR in the liver has not been significantly studied, preliminary results suggest that the UPR is essential for hepatocyte function.

Both IRE1α– and XBP1- deficient mice display a hypoplastic fetal liver. Growth is severely diminished and prominent apoptosis occurs in XBP1-null hepatocytes [59,82]. UPR activation is observed in the livers of diet-induced or genetically obese and/or diabetic mice [83,84]. For example, PERK activation, eIF2α phosphorylation, and BiP expression were increased compared to lean controls. In addition, heterozygous XBP1-deleted mice were more susceptible to insulin resistance, associated with chronic ER stress and JNK1 hyperactivation [83]. It has been reported that ER stress leads to JNK activation [85] and inhibition of JNK1 signaling was shown to increase insulin sensitivity [86]. In hepatoma cells, it is proposed that the UPR initiates activation of JNK1 which subsequently phosphorylates serine residue 307 of the insulin receptor substrate-1 (IRS-1), consequently reducing insulin receptor signaling [83]. Recent work has shown that protein-tyrosine phosphatase 1B (PTP-1B) interacts with the IRE1/XBP1 pathway [87]. The absence of PTP-1B attenuates ER stress-induced apoptosis, JNK-activation and XBP1-splicing. The potential involvement of PTP-1B in the physiological UPR is particularly interesting because of its predominant localization to the ER [88], and its role in insulin signaling and metabolism [89]. Although data support a role for XBP1 and JNK1 in insulin signaling, it is presently not known whether signaling from these transducers emanates from ER stress and activation of IRE1.

Recent work has shown that ATF6 antagonizes the lipogenic functions of SREBP2 in the liver [90]. Glucose deprivation to induce ATF6 cleavage and activation, as well as ectopic expression of the cleaved form of ATF6, attenuates the activity of the

transcription factor SREBP2. This inhibitory effect can be reversed by over-expression of BiP, suggesting the signal emanates from the ER.

The *Caenorhabditis elegans* homologue of Creb-H, a liver-specific b-ZIP transcription factor that shares significant homology with ATF6, is a UPR responsive gene and is regulated by *ire-1* and *xbp-1* in the nematode [91]. Like ATF6, mammalian CREBH is cleaved upon ER stress by S1P/S2P, and the liberated N-terminal cytosolic fragment transits to the nucleus. Instead of inducing expression of the UPR target genes, CREBH acts with ATF6 to synergistically activate the transcription of the acute phase response genes, including serum amyloid P-component (SAP) and C-reative protein (CRP) in response to ER stress. CREBH knockdown in transgenic mice demonstrated CREBH may not be required for hepatocyte differentiation, although there was a defect in the acute inflammatory response [92]. These observations identify a novel link between ER stress and some previously-thought-non-related physiological processes.

The mechanism by which misfolded proteins affect liver function is also illustrated in some cases of α1-antititrypsin deficiency. The Z allele of the α1-antitrypsin (α1-AT)(Glu342Lys mutation) produces a protein that polymerizes and is retained in the ER. Although this protein interacts with calnexin, there is questions about whether it significantly interacts with BiP and activates the UPR [93]. However, analysis of α1-AT expression in transfected fibroblasts isolated from affected patients suggests that defects in ERAD are associated with a greater severity of liver pathology [94].

d. The physiological role of the UPR in osteoblasts

The osteoblast is the only cell type responsible for extracellular matrix deposition during bone formation. One of the major ER stress markers, ATF4 has been reported to

regulate the onset of osteoblast differentiation, type I collagen synthesis, osteoblast-specific gene expression, and osteoblast terminal differentiation [95]. Osteoblasts express high levels of ATF4 protein compared to most other tissues [96]. This observation is surprising given that ATF4 mRNA is present in a rather broad range of organs [96]. It is tempting to speculate that this discrepancy is related to stress-induced translational regulation. Mice and humans deficient in PERK have the same abnormal thinning of bone trabeculae that was observed in ATF4-deficient mice [74,97]. It will be informative to investigate whether tissue-specific knock-in of the eIF2α S51A mutation in osteoblasts produces a similar defect as the ATF4-null and PERK-null mice. In contrast, osteoporosis and deficient bone mineralization occur during osteogenesis imperfecta (OI), which is a disease where misfolded mutant procollagen binds to BiP and activates the UPR [98]. Therefore, a proper balance of UPR activation may be required for optimal osteoblast function.

The initial stage of tooth enamel development is a secretory event. The columnar ameloblast cells of the enamel organ are responsible for dental enamel development. During the secretory stage, the ameloblasts are tall, contain an extensive ER and secret large amounts of protein into the enamel matrix. It was reported that the UPR plays a role in the ameloblast, especially for its susceptibility to the toxic effects of fluoride exposure [99].

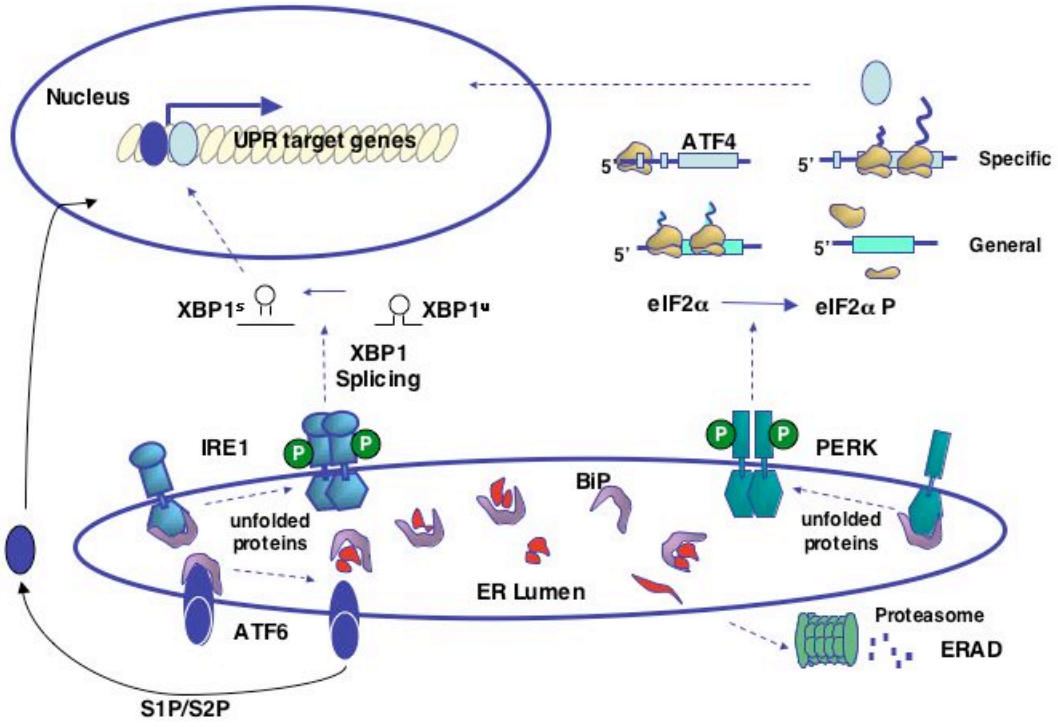

Figure 1-1. Adaptive signaling of the unfolded protein response. The three proximal UPR transducers, ATF6, IRE1 and PERK all associate with BiP in their inactivate state. Upon accumulation of unfolded/misfolded proteins in the ER lumen, these sensors are released and activated. ATF6 transits to the Golgi where it is cleaved by S1P/S2P and the cytosolic fragment of ATF6 migrates to the nucleus. Both IRE1 and PERK are oligomerized and autophosphorylated. Phosphorylated IRE1 catalyzes the splicing of XBP1 mRNA, which generates a more potent transcription factor. Activated PERK phosphorylates eIF2α, which attenuates the general translation rate while inducing the translation of selective mRNAs with inhibitory uORFs in their 5'UTR. The downstream effectors of these three sub-pathways combinatorially induce the expression of the genes encoding proteins that function to augment the ER protein-folding capacity. Meanwhile, ERAD is accelerated to remove terminally misfolded proteins.

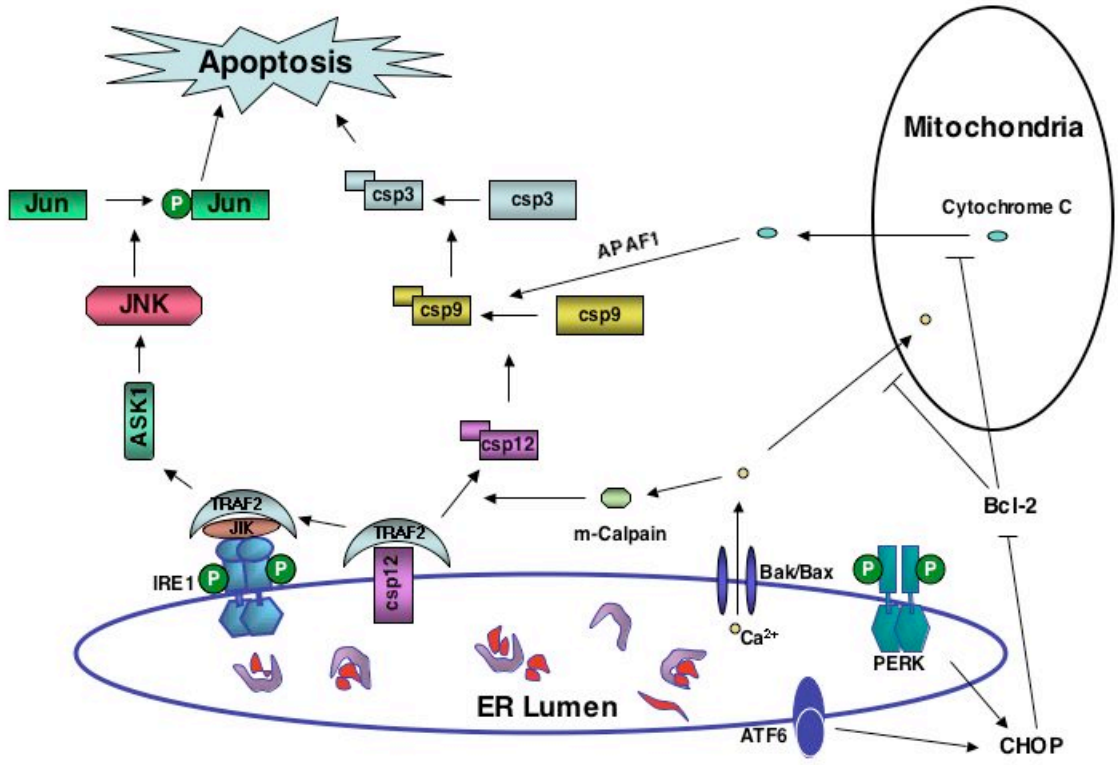

Figure 1-2. ER stress mediated apoptotic pathways. Upon ER stress, Bak and Bax in the ER membrane undergo conformational alteration and permit Ca^{2+} efflux, which activates m-Calpain in the cytoplasm and subsequently cleaves and activates ER-resident procaspase-12 and leads to activation of the caspase-cascade. The Ca^{2+} efflux also leads to the activation of Mitochondria-dependent apoptosis. CHOP, one of the UPR downstream effectors, inhibits the expression of Bcl-2 and thus promotes apoptosis. Activated IRE1 binds to c-Jun-N-terminal inhibitory kinase (JIK) and recruits TRAF2, which leads to the activation of ASK1/JNK and also the release of the procaspase-12 from the ER.

Table 1-1. Genetic models studied for the physiological roles of the unfolded protein response.

	Cells/tissues/organs	Genetic Models	References
Professional secretory cell development/differentiation	B cell	IRE1α-/-, RAG2-/- XBP1-/-, RAG2-/-	59 58
Professional secretory cell function	Pancreatic beta cell	Akita CHOP-/-Akita PERK-/- eIF2αAA eIF2αSA $p58^{IPK}$-/-	69 71 74, 75 31 79 80
	Liver	eIF2αAA IRE1α-/- XBP1-/- XBP1+/-	31 59 82 83
	Osteoblast	PERK-/- ATF4-/-	74, 97 95
Professional secretory cell death	Renal tubular epithelium	Caspase12-/- CHOP-/- GADD34 mutant	49 50, 81 81

References:

1. Stevens, FJ and Argon, Y, (1999) Protein folding in the ER. Semin Cell Dev Biol 10: 443-54.

2. Snapp, E, (2005) Endoplasmic Reticulum Biogenesis Proliferation and Differentiation In *The Biogenesis of Cellular Organelles* Mullins, C. ed. (Kluwer Academic/Plenum Publishers, New York) pp. 63-95.

3. Rutkowski, DT and Kaufman, RJ, (2004) A trip to the ER: coping with stress. Trends Cell Biol 14: 20-8.

4. Schroder, M and Kaufman, RJ, (2005) The Mammalian Unfolded Protein Response. Annu Rev Biochem 74: 739-789.

5. Flynn, GC, Pohl, J, Flocco, MT and Rothman, JE, (1991) Peptide-binding specificity of the molecular chaperone BiP. Nature 353: 726-30.

6. Blond-Elguindi, S, Cwirla, SE, Dower, WJ, Lipshutz, RJ, Sprang, SR, Sambrook, JF et al., (1993) Affinity panning of a library of peptides displayed on bacteriophages reveals the binding specificity of BiP. Cell 75: 717-28.

7. Kassenbrock, CK and Kelly, RB, (1989) Interaction of heavy chain binding protein (BiP/GRP78) with adenine nucleotides. Embo J 8: 1461-7.

8. Ma, K, Vattem, KM and Wek, RC, (2002) Dimerization and release of molecular chaperone inhibition facilitate activation of eukaryotic initiation factor-2 kinase in response to endoplasmic reticulum stress. J Biol Chem 277: 18728-35.

9. Shen, J, Chen, X, Hendershot, L and Prywes, R, (2002) ER stress regulation of ATF6 localization by dissociation of BiP/GRP78 binding and unmasking of Golgi localization signals. Dev Cell 3: 99-111.

10. Liu, CY, Xu, Z and Kaufman, RJ, (2003) Structure and intermolecular interactions of the luminal dimerization domain of human IRE1alpha. J Biol Chem 278: 17680-7.

11. Bertolotti, A, Zhang, Y, Hendershot, LM, Harding, HP and Ron, D, (2000) Dynamic interaction of BiP and ER stress transducers in the unfolded-protein response. Nat Cell Biol 2: 326-32.

12. Dorner, AJ, Wasley, LC and Kaufman, RJ, (1992) Overexpression of GRP78 mitigates stress induction of glucose regulated proteins and blocks secretion of selective proteins in Chinese hamster ovary cells. Embo J 11: 1563-71.

13. Kimata, Y, Oikawa, D, Shimizu, Y, Ishiwata-Kimata, Y and Kohno, K, (2004) A role for BiP as an adjustor for the endoplasmic reticulum stress-sensing protein Ire1. J Cell Biol 167: 445-56.

14. Shen, J, Snapp, EL, Lippincott-Schwartz, J and Prywes, R, (2005) Stable binding of ATF6 to BiP in the endoplasmic reticulum stress response. Mol Cell Biol 25: 921-32.

15. Shi, Y, Vattem, KM, Sood, R, An, J, Liang, J, Stramm, L et al., (1998) Identification and characterization of pancreatic eukaryotic initiation factor 2 alpha-subunit kinase, PEK, involved in translational control. Mol Cell Biol 18: 7499-509.

16. Harding, HP, Zhang, Y and Ron, D, (1999) Protein translation and folding are coupled by an endoplasmic-reticulum-resident kinase. Nature 397: 271-4.

17. Harding, HP, Novoa, I, Zhang, Y, Zeng, H, Wek, R, Schapira, M et al., (2000) Regulated translation initiation controls stress-induced gene expression in mammalian cells. Mol Cell 6: 1099-108.

18. Lu, PD, Harding, HP and Ron, D, (2004) Translation reinitiation at alternative open reading frames regulates gene expression in an integrated stress response. J Cell Biol 167: 27-33.

19. Tirasophon, W, Welihinda, AA and Kaufman, RJ, (1998) A stress response pathway from the endoplasmic reticulum to the nucleus requires a novel bifunctional protein kinase/endoribonuclease (Ire1p) in mammalian cells. Genes Dev 12: 1812-24.

20. Shen, X, Ellis, RE, Lee, K, Liu, CY, Yang, K, Solomon, A et al., (2001) Complementary signaling pathways regulate the unfolded protein response and are required for C. elegans development. Cell 107: 893-903.

21. Yoshida, H, Matsui, T, Yamamoto, A, Okada, T and Mori, K, (2001) XBP1 mRNA is induced by ATF6 and spliced by IRE1 in response to ER stress to produce a highly active transcription factor. Cell 107: 881-91.

22. Calfon, M, Zeng, H, Urano, F, Till, JH, Hubbard, SR, Harding, HP et al., (2002) IRE1 couples endoplasmic reticulum load to secretory capacity by processing the XBP-1 mRNA. Nature 415: 92-6.

23. Lee, K, Tirasophon, W, Shen, X, Michalak, M, Prywes, R, Okada, T et al., (2002) IRE1-mediated unconventional mRNA splicing and S2P-mediated ATF6 cleavage merge to regulate XBP1 in signaling the unfolded protein response. Genes Dev 16: 452-66.

24. Haze, K, Yoshida, H, Yanagi, H, Yura, T and Mori, K, (1999) Mammalian transcription factor ATF6 is synthesized as a transmembrane protein and activated by proteolysis in response to endoplasmic reticulum stress. Mol Biol Cell 10: 3787-99.

25. Ye, J, Rawson, RB, Komuro, R, Chen, X, Dave, UP, Prywes, R et al., (2000) ER stress induces cleavage of membrane-bound ATF6 by the same proteases that process SREBPs. Mol Cell 6: 1355-64.

26. Yoshida, H, Okada, T, Haze, K, Yanagi, H, Yura, T, Negishi, M et al., (2000) ATF6 activated by proteolysis binds in the presence of NF-Y (CBF) directly to the cis-acting element responsible for the mammalian unfolded protein response. Mol Cell Biol 20: 6755-67.

27. Harding, HP, Zhang, Y, Bertolotti, A, Zeng, H and Ron, D, (2000) Perk is essential for translational regulation and cell survival during the unfolded protein response. Mol Cell 5: 897-904.

28. Yoshida, H, Haze, K, Yanagi, H, Yura, T and Mori, K, (1998) Identification of the cis-acting endoplasmic reticulum stress response element responsible for transcriptional induction of mammalian glucose-regulated proteins. Involvement of basic leucine zipper transcription factors. J Biol Chem 273: 33741-9.

29. Li, M, Baumeister, P, Roy, B, Phan, T, Foti, D, Luo, S et al., (2000) ATF6 as a transcription activator of the endoplasmic reticulum stress element: thapsigargin stress-induced changes and synergistic interactions with NF-Y and YY1. Mol Cell Biol 20: 5096-106.

30. Yoshida, H, Okada, T, Haze, K, Yanagi, H, Yura, T, Negishi, M et al., (2001) Endoplasmic reticulum stress-induced formation of transcription factor complex ERSF including NF-Y (CBF) and activating transcription factors 6alpha and 6beta that activates the mammalian unfolded protein response. Mol Cell Biol 21: 1239-48.

31. Scheuner, D, Song, B, McEwen, E, Liu, C, Laybutt, R, Gillespie, P et al., (2001) Translational control is required for the unfolded protein response and in vivo glucose homeostasis. Mol Cell 7: 1165-76.

32. Jousse, C, Oyadomari, S, Novoa, I, Lu, P, Zhang, Y, Harding, HP et al., (2003) Inhibition of a constitutive translation initiation factor 2alpha phosphatase, CReP, promotes survival of stressed cells. J Cell Biol 163: 767-75.

33. Novoa, I, Zeng, H, Harding, HP and Ron, D, (2001) Feedback inhibition of the unfolded protein response by GADD34-mediated dephosphorylation of eIF2alpha. J Cell Biol 153: 1011-22.

34. Novoa, I, Zhang, Y, Zeng, H, Jungreis, R, Harding, HP and Ron, D, (2003) Stress-induced gene expression requires programmed recovery from translational repression. Embo J 22: 1180-7.

35. Yan, W, Frank, CL, Korth, MJ, Sopher, BL, Novoa, I, Ron, D et al., (2002) Control of PERK eIF2alpha kinase activity by the endoplasmic reticulum stress-induced molecular chaperone P58IPK. Proc Natl Acad Sci U S A 99: 15920-5.

36. van Huizen, R, Martindale, JL, Gorospe, M and Holbrook, NJ, (2003) P58IPK, a novel endoplasmic reticulum stress-inducible protein and potential negative regulator of eIF2alpha signaling. J Biol Chem 278: 15558-64.

37. Welihinda, AA, Tirasophon, W, Green, SR and Kaufman, RJ, (1998) Protein serine/threonine phosphatase Ptc2p negatively regulates the unfolded-protein response by dephosphorylating Ire1p kinase. Mol Cell Biol 18: 1967-77.

38. Zong, WX, Li, C, Hatzivassiliou, G, Lindsten, T, Yu, QC, Yuan, J et al., (2003) Bax and Bak can localize to the endoplasmic reticulum to initiate apoptosis. J Cell Biol 162: 59-69.

39. Scorrano, L, Oakes, SA, Opferman, JT, Cheng, EH, Sorcinelli, MD, Pozzan, T et al., (2003) BAX and BAK regulation of endoplasmic reticulum Ca2+: a control point for apoptosis. Science 300: 135-9.

40. Nakagawa, T and Yuan, J, (2000) Cross-talk between two cysteine protease families. Activation of caspase-12 by calpain in apoptosis. J Cell Biol 150: 887-94.

41. Rao, RV, Castro-Obregon, S, Frankowski, H, Schuler, M, Stoka, V, del Rio, G et al., (2002) Coupling endoplasmic reticulum stress to the cell death program. An Apaf-1-independent intrinsic pathway. J Biol Chem 277: 21836-42.

42. Crompton, M, (1999) The mitochondrial permeability transition pore and its role in cell death. Biochem J 341 (Pt 2): 233-49.

43. Boya, P, Cohen, I, Zamzami, N, Vieira, HL and Kroemer, G, (2002) Endoplasmic reticulum stress-induced cell death requires mitochondrial membrane permeabilization. Cell Death Differ 9: 465-7.

44. McCullough, KD, Martindale, JL, Klotz, LO, Aw, TY and Holbrook, NJ, (2001) Gadd153 sensitizes cells to endoplasmic reticulum stress by down-regulating Bcl2 and perturbing the cellular redox state. Mol Cell Biol 21: 1249-59.

45. Ma, Y, Brewer, JW, Diehl, JA and Hendershot, LM, (2002) Two distinct stress signaling pathways converge upon the CHOP promoter during the mammalian unfolded protein response. J Mol Biol 318: 1351-65.

46. Nishitoh, H, Matsuzawa, A, Tobiume, K, Saegusa, K, Takeda, K, Inoue, K et al., (2002) ASK1 is essential for endoplasmic reticulum stress-induced neuronal cell death triggered by expanded polyglutamine repeats. Genes Dev 16: 1345-55.

47. Yoneda, T, Imaizumi, K, Oono, K, Yui, D, Gomi, F, Katayama, T et al., (2001) Activation of caspase-12, an endoplastic reticulum (ER) resident caspase, through tumor necrosis factor receptor-associated factor 2-dependent mechanism in response to the ER stress. J Biol Chem 276: 13935-40.

48. Wei, MC, Zong, WX, Cheng, EH, Lindsten, T, Panoutsakopoulou, V, Ross, AJ et al., (2001) Proapoptotic BAX and BAK: a requisite gateway to mitochondrial dysfunction and death. Science 292: 727-30.

49. Nakagawa, T, Zhu, H, Morishima, N, Li, E, Xu, J, Yankner, BA et al., (2000) Caspase-12 mediates endoplasmic-reticulum-specific apoptosis and cytotoxicity by amyloid-beta. Nature 403: 98-103.

50. Zinszner, H, Kuroda, M, Wang, X, Batchvarova, N, Lightfoot, RT, Remotti, H et al., (1998) CHOP is implicated in programmed cell death in response to impaired function of the endoplasmic reticulum. Genes Dev 12: 982-95.

51. Rush, JS, Sweitzer, T, Kent, C, Decker, GL and Waechter, CJ, (1991) Biogenesis of the endoplasmic reticulum in activated B lymphocytes: temporal relationships between the induction of protein N-glycosylation activity and the biosynthesis of membrane protein and phospholipid. Arch Biochem Biophys 284: 63-70.

52. Lewis, MJ, Mazzarella, RA and Green, M, (1985) Structure and assembly of the endoplasmic reticulum. The synthesis of three major endoplasmic reticulum proteins during lipopolysaccharide-induced differentiation of murine lymphocytes. J Biol Chem 260: 3050-7.

53. Wiest, DL, Burkhardt, JK, Hester, S, Hortsch, M, Meyer, DI and Argon, Y, (1990) Membrane biogenesis during B cell differentiation: most endoplasmic reticulum proteins are expressed coordinately. J Cell Biol 110: 1501-11.

54. Haas, IG and Wabl, M, (1983) Immunoglobulin heavy chain binding protein. Nature 306: 387-9.

55. Iwakoshi, NN, Lee, AH, Vallabhajosyula, P, Otipoby, KL, Rajewsky, K and Glimcher, LH, (2003) Plasma cell differentiation and the unfolded protein response intersect at the transcription factor XBP-1. Nat Immunol 4: 321-9.

56. Gass, JN, Gifford, NM and Brewer, JW, (2002) Activation of an unfolded protein response during differentiation of antibody-secreting B cells. J Biol Chem 277: 49047-54.

57. Fugmann, SD, Lee, AI, Shockett, PE, Villey, IJ and Schatz, DG, (2000) The RAG proteins and V(D)J recombination: complexes, ends, and transposition. Annu Rev Immunol 18: 495-527.

58. Reimold, AM, Iwakoshi, NN, Manis, J, Vallabhajosyula, P, Szomolanyi-Tsuda, E, Gravallese, EM et al., (2001) Plasma cell differentiation requires the transcription factor XBP-1. Nature 412: 300-7.

59. Zhang, K, Wong, HN, Song, B, Miller, CN, Scheuner, D and Kaufman, RJ, (2005) The unfolded protein response sensor IRE1alpha is required at 2 distinct steps in B cell lymphopoiesis. J Clin Invest 115: 268-81.

60. van Anken, E, Romijn, EP, Maggioni, C, Mezghrani, A, Sitia, R, Braakman, I et al., (2003) Sequential waves of functionally related proteins are expressed when B cells prepare for antibody secretion. Immunity 18: 243-53.

61. Liu, CY, Schroder, M and Kaufman, RJ, (2000) Ligand-independent dimerization activates the stress response kinases IRE1 and PERK in the lumen of the endoplasmic reticulum. J Biol Chem 275: 24881-5.

62. Gunn, KE, Gifford, NM, Mori, K and Brewer, JW, (2004) A role for the unfolded protein response in optimizing antibody secretion. Mol Immunol 41: 919-27.

63. Lee, AH, Iwakoshi, NN and Glimcher, LH, (2003) XBP-1 regulates a subset of endoplasmic reticulum resident chaperone genes in the unfolded protein response. Mol Cell Biol 23: 7448-59.

64. Shaffer, AL, Shapiro-Shelef, M, Iwakoshi, NN, Lee, AH, Qian, SB, Zhao, H et al., (2004) XBP1, downstream of Blimp-1, expands the secretory apparatus and other organelles, and increases protein synthesis in plasma cell differentiation. Immunity 21: 81-93.

65. Sriburi, R, Jackowski, S, Mori, K and Brewer, JW, (2004) XBP1: a link between the unfolded protein response, lipid biosynthesis, and biogenesis of the endoplasmic reticulum. J Cell Biol 167: 35-41.

66. Lingohr, MK, Buettner, R and Rhodes, CJ, (2002) Pancreatic beta-cell growth and survival--a role in obesity-linked type 2 diabetes? Trends Mol Med 8: 375-84.

67. Lowell, BB and Shulman, GI, (2005) Mitochondrial dysfunction and type 2 diabetes. Science 307: 384-7.

68. Lo, D, Burkly, LC, Widera, G, Cowing, C, Flavell, RA, Palmiter, RD et al., (1988) Diabetes and tolerance in transgenic mice expressing class II MHC molecules in pancreatic beta cells. Cell 53: 159-68.

69. Wang, J, Takeuchi, T, Tanaka, S, Kubo, SK, Kayo, T, Lu, D et al., (1999) A mutation in the insulin 2 gene induces diabetes with severe pancreatic beta-cell dysfunction in the Mody mouse. J Clin Invest 103: 27-37.

70. Leroux, L, Desbois, P, Lamotte, L, Duvillie, B, Cordonnier, N, Jackerott, M et al., (2001) Compensatory responses in mice carrying a null mutation for Ins1 or Ins2. Diabetes 50 Suppl 1: S150-3.

71. Oyadomari, S, Koizumi, A, Takeda, K, Gotoh, T, Akira, S, Araki, E et al., (2002) Targeted disruption of the Chop gene delays endoplasmic reticulum stress-mediated diabetes. J Clin Invest 109: 525-32.

72. Oyadomari, S, Takeda, K, Takiguchi, M, Gotoh, T, Matsumoto, M, Wada, I et al., (2001) Nitric oxide-induced apoptosis in pancreatic beta cells is mediated by the endoplasmic reticulum stress pathway. Proc Natl Acad Sci U S A 98: 10845-50.

73. Chan, NN, Vallance, P and Colhoun, HM, (2000) Nitric oxide and vascular responses in Type I diabetes. Diabetologia 43: 137-47.

74. Delepine, M, Nicolino, M, Barrett, T, Golamaully, M, Lathrop, GM and Julier, C, (2000) EIF2AK3, encoding translation initiation factor 2-alpha kinase 3, is mutated in patients with Wolcott-Rallison syndrome. Nat Genet 25: 406-9.

75. Harding, HP, Zeng, H, Zhang, Y, Jungries, R, Chung, P, Plesken, H et al., (2001) Diabetes mellitus and exocrine pancreatic dysfunction in perk-/- mice reveals a role for translational control in secretory cell survival. Mol Cell 7: 1153-63.

76. Berlanga, JJ, Santoyo, J and De Haro, C, (1999) Characterization of a mammalian homolog of the GCN2 eukaryotic initiation factor 2alpha kinase. Eur J Biochem 265: 754-62.

77. Sood, R, Porter, AC, Olsen, DA, Cavener, DR and Wek, RC, (2000) A mammalian homologue of GCN2 protein kinase important for translational control by phosphorylation of eukaryotic initiation factor-2alpha. Genetics 154: 787-801.

78. Scarim, AL, Arnush, M, Blair, LA, Concepcion, J, Heitmeier, MR, Scheuner, D et al., (2001) Mechanisms of beta-cell death in response to double-stranded (ds) RNA and interferon-gamma: dsRNA-dependent protein kinase apoptosis and nitric oxide-dependent necrosis. Am J Pathol 159: 273-83.

79. Scheuner, D, Mierde, DV, Song, B, Flamez, D, Creemers, JW, Tsukamoto, K et al., (2005) Control of mRNA translation preserves endoplasmic reticulum function in beta cells and maintains glucose homeostasis. Nat Med 11: 757-64.

80. Ladiges, WC, Knoblaugh, SE, Morton, JF, Korth, MJ, Sopher, BL, Baskin, CR et al., (2005) Pancreatic beta-cell failure and diabetes in mice with a deletion mutation of the endoplasmic reticulum molecular chaperone gene P58IPK. Diabetes 54: 1074-81.

81. Marciniak, SJ, Yun, CY, Oyadomari, S, Novoa, I, Zhang, Y, Jungreis, R et al., (2004) CHOP induces death by promoting protein synthesis and oxidation in the stressed endoplasmic reticulum. Genes Dev 18: 3066-77.

82. Reimold, AM, Etkin, A, Clauss, I, Perkins, A, Friend, DS, Zhang, J et al., (2000) An essential role in liver development for transcription factor XBP-1. Genes Dev 14: 152-7.

83. Ozcan, U, Cao, Q, Yilmaz, E, Lee, AH, Iwakoshi, NN, Ozdelen, E et al., (2004) Endoplasmic reticulum stress links obesity, insulin action, and type 2 diabetes. Science 306: 457-61.

84. Nakatani, Y, Kaneto, H, Kawamori, D, Yoshiuchi, K, Hatazaki, M, Matsuoka, TA et al., (2005) Involvement of endoplasmic reticulum stress in insulin resistance and diabetes. J Biol Chem 280: 847-51.

85. Urano, F, Wang, X, Bertolotti, A, Zhang, Y, Chung, P, Harding, HP et al., (2000) Coupling of stress in the ER to activation of JNK protein kinases by transmembrane protein kinase IRE1. Science 287: 664-6.

86. Hirosumi, J, Tuncman, G, Chang, L, Gorgun, CZ, Uysal, KT, Maeda, K et al., (2002) A central role for JNK in obesity and insulin resistance. Nature 420: 333-6.

87. Gu, F, Nguyen, DT, Stuible, M, Dube, N, Tremblay, ML and Chevet, E, (2004) Protein-tyrosine phosphatase 1B potentiates IRE1 signaling during endoplasmic reticulum stress. J Biol Chem 279: 49689-93.

88. Frangioni, JV, Beahm, PH, Shifrin, V, Jost, CA and Neel, BG, (1992) The nontransmembrane tyrosine phosphatase PTP-1B localizes to the endoplasmic reticulum via its 35 amino acid C-terminal sequence. Cell 68: 545-60.

89. Cheng, A, Dube, N, Gu, F and Tremblay, ML, (2002) Coordinated action of protein tyrosine phosphatases in insulin signal transduction. Eur J Biochem 269: 1050-9.

90. Zeng, L, Lu, M, Mori, K, Luo, S, Lee, AS, Zhu, Y et al., (2004) ATF6 modulates SREBP2-mediated lipogenesis. Embo J 23: 950-8.

91. Shen, X, Ellis, RE, Sakaki, K and Kaufman, RJ, (2005) Genetic Interactions Due to Constitutive and Inducible Gene Regulation Mediated by the Unfolded Protein Response in C. elegans. PLoS Genet 1: e37.

92. Zhang, K, Shen, X, Wu, J, Sakaki, K, Saunders, T, Rutkowski, DT et al., (2006) Endoplasmic reticulum stress activates cleavage of CREBH to induce a systemic inflammatory response. Cell 124: 587-99.

93. Rudnick, DA and Perlmutter, DH, (2005) Alpha-1-antitrypsin deficiency: a new paradigm for hepatocellular carcinoma in genetic liver disease. Hepatology 42: 514-21.

94. Wu, Y, Whitman, I, Molmenti, E, Moore, K, Hippenmeyer, P and Perlmutter, DH, (1994) A lag in intracellular degradation of mutant alpha 1-antitrypsin correlates with the liver disease phenotype in homozygous PiZZ alpha 1-antitrypsin deficiency. Proc Natl Acad Sci U S A 91: 9014-8.

95. Yang, X, Matsuda, K, Bialek, P, Jacquot, S, Masuoka, HC, Schinke, T et al., (2004) ATF4 is a substrate of RSK2 and an essential regulator of osteoblast biology; implication for Coffin-Lowry Syndrome. Cell 117: 387-98.

96. Yang, X and Karsenty, G, (2004) ATF4, the osteoblast accumulation of which is determined post-translationally, can induce osteoblast-specific gene expression in non-osteoblastic cells. J Biol Chem 279: 47109-14.

97. Zhang, P, McGrath, B, Li, S, Frank, A, Zambito, F, Reinert, J et al., (2002) The PERK eukaryotic initiation factor 2 alpha kinase is required for the development of the skeletal system, postnatal growth, and the function and viability of the pancreas. Mol Cell Biol 22: 3864-74.

98. Lamande, SR and Bateman, JF, (1999) Procollagen folding and assembly: the role of endoplasmic reticulum enzymes and molecular chaperones. Semin Cell Dev Biol 10: 455-64.

99. Kubota, K, Lee, DH, Tsuchiya, M, Young, CS, Everett, ET, Martinez-Mier, EA et al., (2005) Fluoride induces endoplasmic reticulum stress in ameloblasts responsible for dental enamel formation. J Biol Chem 280: 23194-202.

CHAPTER II

ATF6 ALPHA OPTIMIZES LONG-TERM ENDOPLASMIC RETICULUM FUNCTION TO PROTECT CELLS FROM CHRONIC STRESS

Abstract

In vertebrates, three proteins—PERK, IRE1α, and ATF6α—sense protein misfolding stress in the ER and initiate ER-to-nucleus signaling cascades to improve cellular function. The mechanism by which this unfolded protein response (UPR) protects ER function during stress is not clear. To address this issue, we have deleted *Atf6α* in the mouse. ATF6α is neither essential for basal expression of ER protein chaperones nor for embryonic or postnatal development. However, ATF6α is required in both cells and tissues to optimize protein folding, secretion, and degradation during ER stress, and thus to facilitate recovery from acute stress and tolerance to chronic stress. Challenge of *Atf6α*-null animals *in vivo* compromises organ function and survival despite functional overlap between UPR sensors. These results suggest that the vertebrate ATF6α pathway evolved to maintain ER function when cells are challenged with chronic stress, and provide a rationale for the overlap amongst the three UPR pathways.

Introduction

The potential toxicity of accumulated unfolded or misfolded proteins demands that cells respond to protein folding stresses with adaptive programs that restore homeostasis, or with the initiation of apoptosis to protect the organism. Stresses may be of two general types: either acute stresses that require immediate adjustments to the

cellular protein folding environment, or chronic stresses that persistently tax the folding apparatus and necessitate long-term changes in gene expression to improve the folding capacity in a quasi-permanent manner.

Protein folding stress in the endoplasmic reticulum (ER) is sensed principally by three ER-resident transmembrane proteins—PERK, IRE1α, and ATF6α—that initiate a series of signaling cascades known as the unfolded protein response (UPR) [1,2]. The UPR alleviates protein folding stress in two ways, one of which is by reduction in ER protein influx. Classically, this reduction is mediated by activation of PERK, which phosphorylates the alpha subunit of the eukaryotic translation initiation factor eIF2, bringing about a rapid but reversible inhibition of global protein synthesis [3-5]. More recently described are ER-selective mechanisms for reducing protein load [6,7]. None of these events requires changes in gene expression, and so each is ideally suited to the alleviation of acute stress.

Activation of PERK, IRE1α, and ATF6α also initiates ER-to-nucleus signaling cascades that culminate in the transcriptional upregulation of genes that enhance the protein processing capacity of the cell, which encompasses processes such as protein folding, degradation, and trafficking. ATF6α-dependent transcriptional induction is regulated by ER stress-induced trafficking of ATF6α from the ER to the Golgi. In the Golgi, ATF6α is cleaved by the proteases S1P and S2P to release a cytosolic fragment that migrates to the nucleus to activate transcription [8-14]. ATF6β, which is weakly homologous to ATF6α, is activated in a similar fashion, and might function as a transcriptional repressor [15-17]. PERK activation and subsequent eIF2α phosphorylation lead to production of the ATF4 transcription factor [18-20], while IRE1α activation results in

splicing of *Xbp1* mRNA and its subsequent translation into the XBP1 transcription factor [21-24].

Paradoxically, activation of PERK, IRE1α, and ATF6α also leads to the initiation of apoptotic signaling cascades [25]. While the mechanisms that allow cells to escape apoptosis and adapt are not well understood, this "decision" appears to require, at a minimum, the improvement of ER protein folding and processing, that serves to attenuate further UPR signaling even as a stressful stimulus persists [26]. How the three limbs of the UPR manage adaptation to chronic stress is not understood.

Although it is proposed that ATF6α mediates UPR transcriptional activation [16,27-29], the actual requirement for ATF6α in the ER stress response is not known, because *Atf6*α-deleted cells were not heretofore available. To understand the role of ATF6α in UPR signaling, we characterized cells and mice that are deleted in *Atf6*α. ATF6α is not essential for embryonic or postnatal development. However, despite functional overlap between gene targets of ATF6α and those of the IRE1α and PERK UPR subpathways, ATF6α is needed both in cells and animals for induction of the protein folding, processing, and degradation capacity of the ER. ATF6α deletion compromises the functionality of the secretory pathway during conditions of ER stress and impairs adaptation to chronic ER stress. These results suggest that the UPR evolved as a three-limbed stress-sensing pathway to protect against both acute and chronic stress, and that ATF6α provides an essential role in the chronic adaptive response.

Results and Discussion

ATF6α is dispensable for embryonic and postnatal development

The strategy for creating an ATF6α conditional allele in the mouse is outlined in Figure 2-1A. Exon IV was targeted for Cre-mediated deletion, which should alter the reading frame of the *Atf6*α transcript and result in a nonsense mutation and production of a truncated protein product (containing only the 72 N-terminal amino acids of ATF6α) that lacks the functional elements of the protein. Exon IV was targeted directly in C57BL/6J animals (see Experimental Procedures) (Figure 2-1B), and was deleted by mating with EIIa-Cre-expressing transgenic mice in the C57BL/6J background. Intercrossing of *Atf6*α+/- animals produced progeny in the expected genotypic ratios (Figure 2-1C).

Timed matings were used to isolate several lines of *Atf6*α-/- and littermate-matched wild-type mouse embryonic fibroblasts (MEFs). Northern blot of total RNA from these cells, and also from liver tissue isolated from wild-type and *Atf6*α-/- animals, revealed a reduction in full-length *Atf6*α mRNA from *Atf6*α-/- cells (probably attributable to nonsense-mediated decay), and no evidence for a knockout-specific alternatively spliced mRNA (Figures 2-1D and 2-2). Quantitative real-time RT-PCR using Exon IV-specific primers confirmed the deletion of this region in the knockout MEFs, and amplification with primers specific for other regions of *Atf6*α mRNA confirmed that expression of a putative *Atf6*α transcript was significantly reduced in the knockouts (Figure 2-1E). Immunoblot of total protein lysates from *Atf6*α-/- MEFs did not detect ATF6α protein (Figure 2-1F and data not shown).

Mice lacking *Atf6*α show no obvious developmental defects through 7 months of age. Thus, *Atf6*α is not essential for embryonic or postnatal development, although a more detailed characterization is ongoing. Likewise, *Atf6*α-/- MEFs displayed normal

growth and morphology relative to wild-type controls, and no significant alteration in the basal expression of a sampling of stress-related proteins (Figure 2-1G). These data suggest that *Atf6*α is not essential for basal chaperone expression, leading us to investigate its role in response to ER stress.

_Atf6_α optimizes ER stress-mediated induction of UPR target genes

Previous studies describing UPR-mediated transcriptional regulation have suggested that it might be possible to categorize many UPR target genes as *Atf6*α-dependent, *Ire1*α-dependent, or *Perk*-dependent [20,28,30,31]. Our deletion of *Atf6*α allowed us to more directly describe the contribution of *Atf6*α to changes in the expression of these genes.

Of most interest was the expression of the ER chaperone *BiP*, which is the classic sentinel for UPR gene activation [32], and which can be upregulated by overexpression of the active form of ATF6α [28,31]. Quantitative real-time RT-PCR showed that *BiP* upregulation was reduced, though not completely abrogated, in *Atf6*α-/- cells challenged with the ER stress-inducing agents tunicamycin (TM) or thapsigargin (TG) (Figure 2-3A and data not shown). Real-time RT-PCR analysis also showed a reduction in *Chop* mRNA upregulation, consistent with a proposed role for *Atf6*α in coregulating this *Atf4*-dependent gene [33,34]. Surprisingly, we also found *Atf6*α-/- cells largely defective in the upregulation of the *Edem1* and *p58*^{IPK} genes as well (Figure 2-3A), both of which were previously described as *Ire1*α/*Xbp1*-dependent [31,35,36]. In contrast, upregulation of the presumptively *Atf4*-dependent tryptophanyl tRNA synthetase [30,31] (*Wars*) was not attenuated in *Atf6*α-/- cells (Figure 2-3A), and the putative CHOP target *Gadd34* [37] was

more highly induced in *Atf6*α-/- cells. The attenuated upregulation of *BiP*, *p58*^{IPK}, and *Chop* was confirmed by immunoblot (Figures 2-3B and 2-4).

Because of possible overlap in the binding specificities of ATF6α, XBP1, and ATF4 for the various stress-dependent promoter regulatory sequences [13,22,29,38,39], the role of ATF6α in their regulation is not known. Using reporter constructs driven by tandem copies of either a UPR element (UPRE) [13,22] or by the *BiP* promoter, which contains three ER stress response element (ERSE) sites [29,40], we found that *Atf6*α deletion compromised stress-dependent upregulation through both elements (Figures 2-3C). Confirming the role of ATF6α in the regulation of *BiP* expression, the *BiP* promoter could be immunopurified by antisera to crosslinked ATF6α in wild-type but not *Atf6*α-/- cells, and *BiP* regulation was directly dependent upon the *BiP* ERSE sites (Figure 2-5). The attenuation of ERSE- and UPRE-dependent upregulation was seen regardless of whether the stressor was pharmacological or caused by overexpression of the null Hong Kong (NHK) variant of α1-antitrypsin, a misfolded secretory protein [41] (Figure 2-3D). The stress inducibility of both of these reporter constructs could be restored by transfection of *Atf6*α-/- cells with a plasmid encoding full-length human *Atf6*α (Figure 2-3E), and regulation of the UPRE-dependent reporter, but not the *BiP* promoter reporter, could also be restored by overexpression of XBP1 (Figure 2-6 and data not shown). Taken together, our data suggest that genes containing either ERSE or UPRE sequences in their promoters require ATF6α binding for their full stress-dependent activation.

Functional overlap between the ATF6α and the PERK and IRE1α pathways

Our data suggest that *Atf6*α is necessary for the full upregulation of a subset of UPR target genes, but that other mechanisms regulate UPR gene expression in its

absence. We found that ATF6β cleavage (Figure 2-7A), PERK activation (measured by translational inhibition—Figure 2-7B), and IRE1α activation (assessed by *Xbp1* mRNA splicing—Figure 2-7C) all occurred to similar extents in *Atf6*α+/+ and *Atf6*α-/- cells soon after challenge by diverse ER stressors. We then monitored the stress-dependent upregulation of UPR sentinel genes in *Perk*-/- and *Ire1*α-/- MEFs. *Ire1*α deletion had little effect on the upregulation of most genes analyzed in response to TM challenge, with the exception of *Edem* (Figure 2-7D and data not shown), consistent with previous reports [31,36]. In contrast, *Perk* was required for upregulation of a broad group of UPR genes (Figure 2-7E) [20,30,42]. siRNA knockdown of *Atf6*β in *Atf6*α-/- cells had no effect on the stress-dependent upregulation of BiP and CHOP, which is consistent with the protein having a non-redundant role with ATF6α [16,17] (Figure 2-8). Taken together, these data suggest that the ATF6α pathway at least partially overlaps functionally with the PERK pathway and to a lesser extent the IRE1α pathway.

ATF6α regulates genes that protect ER protein processing capacity

To characterize the global function of *Atf6*α and its relative contribution to UPR signaling, we used mRNA expression profiling to identify *Atf6*α-dependent genes. Remarkably, no gene except for *Atf6*α itself was significantly altered in its expression in *Atf6*α-/- cells in the absence of ER stress (Figure 2-9A and data not shown). Conversely, TM treatment of wild-type cells resulted in the upregulation of approximately 250 genes. Of these, at least 45 were upregulated by TM to a significantly lesser extent in *Atf6*α-/- MEFs, approximately half of which lost stress-dependent upregulation completely in knockout cells (Figures 2-9B and 2-9C). Importantly, our array data for specific genes (Figure 2-10), such as *BiP*, *Edem*, etc., agree well with the *Atf6*α-dependencies identified

by our real-time analysis, and were only excluded from Figure 2-9C based on our statistical criteria. These results suggest that the data presented in Figure 2-9C represent a conservative estimate of putative ATF6α-dependent genes. Notably, nearly half of the genes with known or likely functions have roles in preserving ER function, including protein folding, protein degradation, and maintenance of general ER homeostasis (Figure 2-9C). Taken together, our gene expression experiments suggest a role for ATF6α in optimizing the protein folding and processing capacity of the ER during stress.

Impaired protein degradation and processing in *Atf6*α-/- cells

Most surprising among the genes identified as *Atf6*α-dependent in our array and real-time analyses were those involved in ERAD, as this function was proposed to be controlled by the IRE1α/XBP1 pathway [31,36]. To test whether the ERAD capacity of *Atf6*α-/- cells was compromised, we monitored the degradation of NHK, which is a well-characterized ERAD substrate. NHK overexpression itself activates the UPR (Figure 2-3D), yet in the absence of an exogenous stress, its rate of degradation was no different in wild-type versus *Atf6*α-/- cells (Figure 2-11A). However, when NHK-expressing cells were pretreated with a low concentration of TG, the rate of NHK degradation was slowed in *Atf6*α-/- cells relative to wild-type counterparts (Figure 2-11B). We also observed that, despite comparable levels of NHK synthesis in TG-treated cells, the steady-state expression of intracellular NHK was greater in *Atf6*α-/- cells than in wild-type cells, which supports the idea that its degradation is attenuated (Figure 2-11B).

We also monitored the maturation of a cell-surface glycoprotein, the transferrin receptor (TfR), by its acquisition of resistance to deglycosylation by endoglycosidase H (EndoH). TfR was quantitatively resistant to EndoH digestion in untreated wild-type or

*Atf6*α-/- cells. ER stress led to accumulation of a significant amount of EndoH-sensitive TfR in *Atf6*α-/- cells, but much less-so in wild-type cells (Figure 2-11C).

Finally, we compared the efficiency of protein secretion in *Atf6*α-/- versus wild-type cells by monitoring the secreted and intracellular amounts of overexpressed secreted alkaline phosphatase (SEAP). SEAP was secreted with similar efficiencies in *Atf6*α-/- cells and wild-type cells in the absence of stress. However, after cells were treated with TG, the ratio of secreted to intracellular SEAP was reduced in *Atf6*α-/- cells compared to wild-type cells (Figure 2-11D), suggesting *Atf6*α-/- cells are defective in secretion in response to ER stress. Collectively, these observations support the notion that ER protein processing operates suboptimally in stressed *Atf6*α-/- cells.

Compromised adaptation in *Atf6*α-/- cells

Improved protein processing function of the ER has been proposed to suppress the perpetuation of UPR signaling and prevent the stressed cell from committing to execution of UPR-dependent apoptotic programs during exposure to chronic stress [26]. To assess the consequences of *Atf6*α deletion in terms of cell survival, recovery, and adaptation, we took advantage of the rapid reversibility of the reducing agent dithiothreitol (DTT), which disrupts oxidative protein folding in the ER but can be readily removed by washing. As cells recover from acute exposure to stress, or adapt to chronic stress, splicing of *Xbp1* mRNA is downregulated [26,37]. Thus, we measured the relative abundance of spliced *Xbp1* mRNA as one indicator of whether *Atf6*α-/- cells were less able to recover from acute DTT treatment. While treatment of cells with DTT for 1 hour resulted in similar levels of *Xbp1* mRNA splicing in wild-type and *Atf6*α-/- cells, the knockout cells returned to homeostasis much more slowly than wild-type cells, as seen in

the persistence of *Xbp1* mRNA splicing 4 and 8 hours after removal of DTT (Figure 2-12A).

Expression of the CHOP protein is also rapidly downregulated as the cellular stress burden diminishes, as a consequence of the rapid degradation of the mRNAs and proteins encoding both CHOP and its upstream effector ATF4 [26]. *Atf6*α-/- cells upregulated CHOP to a lesser extent than wild-type cells following acute exposure to DTT. However, despite this initially attenuated induction of CHOP (up to 8 hours after DTT removal), *Atf6*α-/- cells failed to fully suppress CHOP expression at 24 hours after DTT removal (Figure 2-12B). Therefore, by these two independent assays we conclude that UPR activation is prolonged in *Atf6*α-/- cells, and that ATF6α therefore facilitates recovery from stress. In comparison, *Perk*-deficient cells were profoundly deficient in their recovery from DTT treatment (Figure 2-12C), while *Ire1*α-/- cells, despite a defect in ERAD, recovered from DTT treatment with kinetics similar to wild-type cells (Figure 2-12D). These results are consistent with the nature of the genes regulated by ATF6α, versus the relatively small group that requires XBP1 and the relatively large and diverse group that requires PERK.

Exposure to either brief or persistent but mild ER stress protects cells against subsequent challenge by the same or a heterologous stress agent [26,43,44]. This phenomenon, termed preconditioning, can be observed most readily as a reduced activation of ER stress sensors in response to exposure to a given stress, relative to non-preconditioned cells. The impaired ability of *Atf6*α-/- cells to restore homeostasis after acute exposure to ER stress predicts that they will also be less able to tolerate challenge with a secondary stressor. To test this prediction, we pretreated cells with DTT for one

hour, allowed them to recover, and then challenged them with either TM or TG. As expected, DTT pretreatment protected wild-type cells from challenge by either TM or TG, assessed by *Xbp1* mRNA splicing (Figure 2-12E). However, *Atf6*α-/- cells failed to fully recover from DTT pretreatment, and as a consequence showed little or no protection from secondary stress (Figure 2-12E).

The inability of *Atf6*α-/- cells to be preconditioned suggests that they should be less able to tolerate and adapt to persistent or repeated stress. To test this hypothesis, we cultured wild-type or *Atf6*α-/- cells for up to 4 days in the continued presence of low concentrations of either TG or TM that allowed for the adaptation and proliferation of wild-type cells [26]. In the absence of stress, both cell types proliferated at comparable rates (Figure 2-12F, NT 4d). However, chronic exposure to either TG or TM significantly reduced the proliferative capacity of *Atf6*α-/- cells relative to wild-type cells (Figure 2-12F, compare 1d and 4d to 0d). Repeated DTT treatment produced similar results. A single exposure to DTT did not alter the growth of *Atf6*α-/- cells relative to wild-type cells (Figure 2-12G; 4d 1x); however, wild-type cells were able to tolerate repeated DTT exposure and proliferate over the time-course, while *Atf6*α-/- cells could not (Figure 2-12G; 4d). Similar results were obtained in both clonogenic and MTT-based proliferative assays (Figure 2-13). Therefore, *Atf6*α deletion impairs the ability of cells to tolerate persistent exposure to mild ER stress.

We also found that, while wild-type cells suppressed CHOP expression concomitant with adaptation to persistent mild stress (10 or 25 ng/ml TM for 3 days), *Atf6*α-/- cells did not do so fully (Figure 2-12H). This result is consistent with our previous observation that expression of CHOP serves as a sentinel for the failure of cells

to adapt to chronic stress [26], and correlates with ongoing activation of the UPR in *Atf6*α-/-, but not wild-type cells (Figure 2-14). Upon chronic exposure to relatively mild stress, *Atf6*α-/- cells also displayed more PARP cleavage, a late marker of apoptosis (Figure 2-12I). We conclude from these results that functional redundancy within the UPR allows *Atf6*α-/- cells to tolerate brief mild stresses, but that the cellular effects of *Atf6*α deletion are exacerbated by repeated insult, possibly as a cumulative consequence of defects in protein folding, degradation, and trafficking.

ATF6α protects from ER stress in vivo

Our results in MEFs lead to the conclusion that ATF6α is required to protect cells against ongoing stress despite the ability of other UPR signaling pathways to partially compensate for its absence. To determine whether these conclusions could be extended to protection from stress *in vivo*, we challenged mice by intraperitoneal injection with TM, which leads to ER stress in both the liver and kidney [37,45,46], and the ER stress response in both organs was monitored. Inhibition of glycosylation of the ER-resident glycoprotein TRAPα confirmed the efficacy of injection. As in MEFs, the upregulation of BiP, GRP94, and $p58^{IPK}$ was attenuated in *Atf6*α-/- livers compared to wild-type and heterozygous controls over the entire time course (Figure 2-15A). These results were also seen in *Atf6*α-/- mice in which the neomycin selection cassette was deleted by FLP-mediated recombination, confirming that the phenotype is not due to secondary effects of the neomycin cassette (Figure 2-15A and 2-2). Similar results were observed in the kidney (Figure 2-15B). These results were corroborated by real-time RT-PCR analysis, as was a defect in *Edem1* mRNA upregulation in the livers of *Atf6*α-/- animals (Figure 2-16 and data not shown).

As in cultured cells, we observed that CHOP expression was lower in *Atf6*α-/- animals early after injection (8 hours) but was elevated relative to wild-type and heterozygous animals at later time-points (Figures 2-15A, 2-15B). Also as in cultured cells, expression of the negative regulator of eIF2α, GADD34, was higher in *Atf6*α-/- animals at all time points (Figures 2-15A and 2-14); consistent with this result, eIF2α phosphorylation was reduced to basal (i.e., non-stressed) levels in the livers of *Atf6*α-/- animals, despite persistent splicing of *Xbp1* mRNA selectively in these animals, suggesting ongoing stress (Figures 2-15A, B). These results reveal that, while ATF6α is not strictly necessary for eIF2α phosphorylation in the immediate aftermath of exposure to stress (Figure 2-7B and data not shown), it does appear to potentiate the ability of eIF2α to remain persistently phosphorylated during chronic stress.

TM was found to be markedly more toxic to *Atf6*α-/- animals than wild-type or heterozygous controls. We found that, even fairly shortly after injection (18 hours), TM elicited more cell death, assessed by histological staining to detect cleaved caspase-3, in knock-out than in wild-type livers (Figures 2-15C and 2-15D). Increased toxicity was also observed at the organismal level; while all wild-type and heterozygous animals survived TM challenge (n = 8), most *Atf6*α-/- animals succumbed (n = 4/5) (Figure 2-15E). By 72 hours after injection, the livers of *Atf6*α-/- animals were grossly discolored consistent with hepatic lipidosis (Figure 2-15F). The most likely explanation for these results is that wild-type animals are better protected from ER stress *in vivo* than *Atf6*α-/- animals, and so an equivalent pharmacological insult produces adaptation (i.e., higher expression of chaperones and maintenance of organ function) and less overall stress (less splicing of *Xbp1* mRNA, lower expression of CHOP, and less apoptosis) in wild-type

animals. As in cultured cells, this difference in sensitivity to ER stress is manifested more at later points after insult when *Atf6*α-/- animals are unable to recover and/or adapt. Taken together, these data support a role for ATF6α in regulating ER protein processing capacity to protect tissues from ER stress *in vivo*.

Conclusions and Perspectives

By deleting *Atf6*α in the mouse and exploring the responsiveness to stress of *Atf6*α-/- cells, we have uncovered a role for ATF6α in mediating adaptation to chronic stress. This role is likely filled by ATF6α because of its function in regulating the expression of genes that facilitate ER protein folding and processing. At first glance, functional overlap between the PERK, IRE1α and ATF6α pathways would seem to make ATF6α dispensable for the ER stress response, since many of the genes downstream of this protein are nonetheless upregulated by stress in its absence, albeit to a lesser extent. Accordingly, *Atf6*α-/- cells do not show evidence of basal stress (Figure 2-1G and 2-9A), do not appear to initially suffer a greater stress burden than wild-type cells given an equivalent stimulus (Figure 2-7A-C), and appear to be no more sensitive to short term stresses (Figure 2-12F, G). Yet *Atf6*α-/- cells do not return to equilibrium as efficiently as wild-type cells when a stressor is removed (Figure 2-12A, B, E). Accordingly, persistent or recurring stress exacts a cumulative toll on *Atf6*α-deficient cells such that they are less able to survive. This impairment correlates with lower chaperone expression, more persistent CHOP expression, and increased apoptosis (Figure 2-12F-I). This impairment is manifested dramatically as failure to recover from challenge *in vivo* (Figure 2-15). Thus, the absence of *Atf6*α appears to adjust the threshold of tolerable chronic cellular stress. While there is no overt phenotype in *Atf6*α-/- animals, the fact that ATF6α

protects tissues against pharmacological ER stress suggests that unmasking of a phenotype *in vivo* awaits only the proper challenge.

While each limb of the UPR doubtless regulates at least some genes and controls some physiological responses uniquely [47,48], the overlap between the pathways appears to be considerable. We propose, then, that ATF6α has evolved not to discretely regulate a subset of genes during acute exposures to stress, but instead to augment the protective mechanisms upregulated by the PERK and IRE1α (and perhaps ATF6β) pathways. This augmentation raises the likelihood that the protein folding and processing capacity of the cell will be able to withstand persistent insult and suppress apoptotic UPR signaling cascades. It is telling that each limb of the UPR contributes to the protein folding, maturation, and/or degradation capacity of the ER during stress. To the extent that enhancement of these processes is the most critical element of adaptation to ER stress, overlap ensures that cells have the greatest opportunity possible to adapt to stress rather than succumb to it.

Beyond its role in regulating the long-term protein processing capacity of the ER, ATF6α can also modulate the cellular response to chronic stress though its effects on the other UPR pathways, in particular the PERK/eIF2α axis. Although the mechanism is not yet clear, ATF6α appears to suppress production of GADD34 during ER stress, allowing PERK/eIF2α signaling to persist and presumably contribute to maintenance of ER and general cellular function during chronic stress (Figure 2-15A). Interestingly, ATF6α has the opposite effect on IRE1α signaling, as ATF6α deletion causes IRE1α to remain activated during chronic stress (Figures 2-15 and 2-14), although it is not yet clear whether this effect arises from direct interaction between the pathways or as an indirect

consequence of alterations in the ER folding capacity in *Atf6*α-/- cells. These results raise the possibility that activation of the proximal sensors of ER stress is managed differently during chronic stress versus acute stress, and that one function of ATF6α is to regulate this altered responsiveness.

From this work, we conclude that the idea that each limb of the UPR regulates the functionality of discrete cellular processes needs to be reconsidered. Perhaps multiple stress sensing pathways have evolved not so much for the division of labor as for the generation of fail-safe mechanisms for surviving both short-term and long-term environmental insult.

Supplemental notes

1. Deletion of exon IV of the *Atf6*α mRNA results in a shift of the reading frame, resulting in a nonsense mutation. The predicted protein product contains the first 72 amino acids of ATF6α, followed by seven additional amino acids and a stop codon. Thus, the predicted protein product ends …HFCSGGVGFVV-Stop. This protein contains neither the transactivation domain of ATF6α, nor the bZIP dimerization domain; consequently, it should have none of the normal function of ATF6α, nor should it function as a dominant negative. In support of this, heterozygous animals and cells behave similarly to wild-type, and do not show any evidence of a dominant negative effect (Figure 2-15 and data not shown). Alternative splicing could potentially restore the reading frame of the targeted mRNA, producing a fully or partially functional protein product. However, we detected no RNA species in heterozygous or knockout animals other than those present in the wild-type (exon IV is 101 nucleotides, and so its loss from the mRNA would not likely result in a significant shift of the ~7.5 kb primary transcript

in an agarose gel), and real-time RT-PCR revealed similar expression levels of several exons within the *Atf6*α mRNA (Figures 2-1 and 2-2). The reduction in the amount of full-length *Atf6*α mRNA in the knockout cells and liver is most likely attributable to nonsense-mediated degradation of the targeted species. Finally, cryptic splice donor/acceptor sites in the neomycin cassette could conceivably result in a protein that was essentially like wild-type ATF6α, but with a portion of exon IV replaced in frame by sequence from the cassette. However, *Atf6*α-/- mice with a deleted neomycin cassette responded to TM challenge essentially identically to *Atf6*α-/- mice with the neomycin cassette intact (Figure 2-15A). We also observed that the expression of *Atf6*α mRNA was similar in the livers of *Atf6*α-/- neomycin-deleted and neomycin nondeleted animals (Figure 2-2), ruling out any indirect effect of the neomycin cassette on *Atf6*α mRNA expression. In addition, immunoblot using an antibody that recognizes amino acids 242-253 of ATF6α, which is downstream of exon IV and recognizes both full-length and cleaved ATF6α, failed to recognize any specific species in *Atf6*α-/- cells, during either unstressed or stressed conditions (Figure 2-1). A polyclonal antiserum raised against the active form of ATF6α gave similar results (data not shown). Thus, although we cannot exclude that a small protein product is made from the targeted *Atf6*α mRNA, we conclude that we have generated a true *Atf6*α-null allele.

2. It was previously proposed that ATF6α-dependent transcriptional activation from the UPRE is indirect and mediated through transcriptional activation of *Xbp1* mRNA during ER stress [22,24]. However, our analysis demonstrated that the induction of *Xbp1* mRNA during either mild or severe ER stress is quite modest, and not significantly attenuated in *Atf6*α-/- cells (Figure 2-6). Further, the levels of XBP1 protein translated from the spliced

mRNA were actually higher in *Atf6*α-/- cells than in wild-type cells upon stress (Figure 2-6). Therefore, it seems likely that UPRE-dependent transcription requires direct activation by both XBP1 and ATF6α, consistent with the original identification of the UPRE as an ATF6α binding site [13].

3. GADD34 protein upregulation is observed in TM-injected *Atf6*α-/- animals but not in wild-type or heterozygous controls (Figure 2-15). This result mirrors an elevation of *Gadd34* mRNA and protein in *Atf6*α-/- MEFs (Figures 2-3A and 2-14). While CHOP has been proposed to regulate *Gadd34* expression, and CHOP is also elevated in *Atf6*α-/- cells and animals at later points after ER stress, the increase in *Gadd34* seems to precede *Chop* upregulation in the knockouts, as it is evident at early time points when expression of *Chop* is lower in the *Atf6*α-/- cells and animals than wild-type controls (for example, only 8h after TM injection—Figure 2-15A). Thus, it seems likely that a protein in addition to CHOP is capable of regulating *Gadd34* expression. Indeed, this result is consistent with the observation that *Chop*-/- cells still upregulate *Gadd34*, albeit to a lesser extent than wild-type cells [37]. The apparent consequence of persistently elevated GADD34 in the *Atf6*α-/- animals is attenuated eIF2α phosphorylation despite enhanced *Xbp1* splicing (a parallel phenomenon probably operates in MEFs as well, but the overall increase in eIF2α phosphorylation in response to chronic TM treatment falls below the level of detection—Figure 2-14 and [26]. CHOP is short-lived at both the mRNA and protein levels [26], which suggests that its persistence in *Atf6*α-/- animals and cells reflects active and ongoing synthesis. Therefore, absent both eIF2α phosphorylation and ATF6α, which have been proposed as the regulators of CHOP expression, we conclude that there is also an additional as yet unidentified regulator of CHOP. The putative role of such a

regulator might be to ensure the perpetuation of an apoptotic signal during unresolved stress, as a way of circumventing GADD34-mediated negative feedback of eIF2α signaling.

4.The efficacy of TM injection is monitored by inhibition of glycosylation of the ER-resident protein TRAPα (Figure 2-15A). All mice were given a uniform dose of TM (1 mg/kg body weight). The *apparent* difference in inhibition of glycosylation for *Atf6*α-/- animals is likely due to ER stress-related differences in the turnover of TRAPα [49] and not to any difference in pharmacological sensitivity to TM. Note that the increased production of CHOP in the livers of *Atf6*α-/- animals 24h after injection (Figure 2-15A) would be inconsistent with a lower sensitivity to TM.

Experimental Procedures:

General notes. A total of three wild-type and three *Atf6*α-/- MEF lines were isolated. Most of the experiments using *Atf6*α+/+ and -/- cells were confirmed in at least one other independent pair of cell lines, and in all cases the resultant data were essentially identical. All experiments were carried out using cells plated at similar confluence, the night prior to stress treatments. Both immunoblots and autoradiographs were collected on film, documented by scanning, and quantitated by densitometric analysis of scanned films when all quantitated bands of interest were within the linear range of intensity. Band arrangement was in some instances altered by cut-and-paste manipulations. Bands shown together were always taken from the same exposure, except where indicated in the figure legend.

Targeting the ATF6 alpha gene in mice. A targeting vector was constructed to replace the ATF6α gene exon IV, with the sequence of exon IV flanked by *LoxP* sites, for *in vivo*

specific-promoter-Cre recombinase-mediated deletion [50]. The G418 resistance gene cassette was inserted in the sense orientation and was flanked by *FRT* sites, for *in vivo* FLP recombinase-mediated deletion. The target sequence and the homologous arms were PCR amplified from C57BL/6J mouse genomic DNA and confirmed by sequencing comparing to the NCBI mouse genome sequences. An Embryonic Stem (ES)-cell line derived from the C57BL/6J substrain BL/6 [51] was used for homologous recombination [52]. Electroporated ES cells were subjected to G418 selection. The surviving clones were screened by southern blot analysis of genomic DNA. The 5' end was determined by digestion with HindIII and probing of the blot with a 436 bp external fragment, which results in a 7.327 kb endogenous and a 6.673 kb homologous recombinant band. The 3' end was determined by digestion of DNA with PstI and probing of the blot with a 475 bp external fragment which results in a 6.432 kb endogenous and a 5.158 kb homologous recombinant band. The correctly targeted ES cells were injected into Albino B6 (C57BL/6J-Tyr<c-2J>) blastocysts to generate chimeric mice. The chimeras were mated with Albino B6 (C57BL/6J-Tyr<c-2J>) mice. Male offspring showing germ line transmission of the mutant allele were crossed with female EIIa-Cre transgenic mice that had been highly backcrossed into C57BL/6J. The heterozygous progeny bearing a knockout *Atf6*α allele are therefore in a pure C57BL/6J genetic background (from C57BL/6J embryonic stem cell lines), and no further backcrossing is needed. Routine genotyping was performed by PCR. All protocols for animal use were reviewed and approved by the University Committee on Use and Care of Animals at the University of Michigan.

Materials. All purchased materials were of the highest quality available commercially. TM and TG were from EMD Biosciences, and were dissolved in DMSO and aliquoted before use. DTT was from Invitrogen, and was made fresh prior to use. Antibody sources have been previously described [26], except as follows: anti-α1-antirypsin was from Dako; anti-PARP was from Cell Signaling Technologies; anti-TRAPα was a gift of R. S. Hegde (NICHD, NIH). ATF6α polyclonal antiserum was raised against a KLH-conjugated peptide with the amino acid sequence NGKLSVTKPVLQC corresponding to amino acids 242-253 of murine ATF6α; it was then purified by peptide affinity chromatography. Polyclonal ATF6β antiserum was raised against a KLH-conjugated peptide with the amino acid sequence EIADPTRFFTDNC corresponding to amino acids 9-20 of murine ATF6β. Antibody specificities were verified by overexpression and/or knockout controls wherever possible. Plasmid pcDNA hα1-AT_{HK} was created using Quickchange Site Directed Mutagenesis Kit (Stratagene) to reproduce a CT dinuncleotide deletion within the Leu_{318} codon that results in a frameshift and early termination of the wild-type α1-AT gene [41].

Preparation and characterization of MEFs. MEFs derived from 14.5 day embryos were prepared as described [20]. MEFs were maintained in Dulbecco's Modified Eagle Medium containing 4.5-g/l glucose (Invitrogen catalog 11995–065; Carlsbad, California, United States) supplemented with 10% FBS, L-glutamine, 1% penicillin G/streptomycin, at 37 °C in a 5% CO_2 incubator. For *Perk*-/- and matched wild-type cells, βME was added to a final concentration of 50 μM.

Genotype analysis. Isolated embryonic stem (ES) cell DNA or mouse tail DNA was digested with the appropriate restriction enzyme, electrophoresed in a 1% agarose gel,

and transferred to positively charged nylon membranes (Roche). The blot was hybridized sequentially with digoxigenin (DIG)-labeled DNA probes as indicated in Figure 2-1 prepared with the PCR DIG probe synthesis kit according to the manufacturer's instructions (Roche). Figure 2-2 shows the locations of primer sets designed to identify different locus modifications. The PCR primers used for genotyping were: WT: ctactgggcactgaggaagc and ggtggccagtctcttgtgat; Deleted: aaggggggaggattgggaagaca and actgggcactgaggaagcaagaac. To delete the G418 resistance gene cassette, male offspring with one mutant allele were crossed with female *FLP1* mice. (B6; J-Tg(ACTFLPe)9205Dym/J from the Jackson Laboratory). The Exon IV-deleted, Neo-deleted allele was genotyped by PCR using the following primers: gctgctgcttattcatggttcctg and actgggcactgaggaagcaagaac.

Array analysis. Passage 3 primary fibroblasts from three separate pairs of wild-type and *Atf6*α-/- embryos were left untreated or treated with tunicamycin (50 ng/ml) for 24 hours. Total RNA was isolated using RNeasy (QIAgen). cDNA synthesis, hybridization, and laser scanning of the array were carried out at the University of Michigan Comprehensive Cancer Center (UMCCC) Affymetrix and cDNA Microarray Core Facility with the GeneChip Mouse Genome 430v2.0 Array that had over 39,000 transcripts (Affymetrix) as recommended by the manufacturer. The primary image analysis was done using GCOS (Affymetrix). Raw data were analyzed using Bioconductor [53]. One TM-treated sample of each genotype was discarded before analysis because of a failure to pass internal quality control standards. Statistical significance was assessed by two-tailed student's t-test.

RNA analysis. RNA was isolated using TRIzol RNA reagent (Invitrogen) or RNeasy (QIAgen), according to the manufacturers' protocols. Poly(A) mRNA was isolated from total RNA using the Oligotex mRNA kit (QIAgen). For Northern analysis, total RNA from MEFs (5 μg) or poly(A) RNA from liver (0.5 μg) was denatured, electrophoresed, and transferred to positively charged nylon membranes (Roche). The blot was hybridized sequentially with digoxigenin (DIG)-labeled DNA probes prepared with the PCR DIG probe synthesis kit (Roche). The probes hybridized to either nucleotides 719-1149 (exons 7-9) or 1592-2208 (exons 13-16) of the *Atf6*α cDNA. Before hybridization the membrane was stained in 0.03% (w/v) methylene blue in 0.3M sodium acetate, pH 5.2, for 45 seconds and destained in diethyl pyrocarbonate treated water for 2 min to visualize *18S* and *28S* rRNA. Real-time RT-PCR analysis, including primer sequences and applicable control/piloting experiments, has been described [26]. Additional real-time primer sequences were as follows: *Edem*: aagtctcaggagctcagagtcattaa and cgatctggcgcatgtagatg; *Wars*: ccttggactacacagccagga and ctaggaccgaggcctgcag; *Ero1*β: gggccaagtcattaaaggaa and tttatcgcacccaacacagt; *Erp72*: agtcaaggtggtggtgggaaag and tgggagcaaaatagatggtaggg; *Herpud1*: agcagccggacaactctaat and cttggaaagtctgctggaca; *Atf6*α exons 2/3: gagtcgacgttgtttgctga and ccaaggcatcaaatccaaat; *Atf6*α exons 12/13: ccaacagaaagcccgcatt and tggacagccatcagctgaga; *Atf6*α exons 4/5: cttcctccagttgctccatc and caactcctcaggaacgtgct; *Atf6*α 3' UTR: ccaccctcagtgttggaact and aggagtatgctctgggctga. For *Xbp1* RT-PCR, the Titan One-Tube RT-PCR kit (Roche) was used along with primers flanking the *Xbp1* intron to amplify both spliced and unspliced *Xbp1* [26].

Cell culture and analysis. Treatment of cells with TM or TG was as described [26], including chronic treatments. The cell proliferative rate was measured by washing cells

twice in PBS, perfectly aspirating the second wash, lysing in 1% SDS, and heating to 100°C for 10 minutes with intermittent vortexing. The protein concentration of the lysate was then measured using the BioRad RC-DC protein assay kit. Results obtained in this way closely mirrored cell proliferative rate measured by cell counting (data not shown). For the clonogenic assay, 5,000 cells were seeded onto 10 cm dishes, allowed to rest overnight, and then treated either continuously for three days with TM or vehicle (with media and stressor refreshed daily), or for one hour out of every twelve hours with 10 mM DTT, followed by rinsing and washing, for three days. Cells were then allowed to recover in complete media for seven additional days before staining with crystal violet. MTT assays used the CellTiter Aqueous One kit (Promega). Immunoblots were carried out as described [26]. For luciferase assays, cells were transfected using FuGene 6 (Roche), with plasmids pcDNA CMV-lacZ and either 5x UPRE-luciferase (formerly known as 5x ATF6-luciferase), or BiP-luciferase (containing the proximal 340 bp of the rat *BiP* promoter), as well as overexpression constructs where indicated. The Grp78-luciferase construct (Figure 2-5) contained the proximal rat *BiP* promoter up to position –169 [54] or –79. Luciferase activity was measured using the Dual Light assay kit (Applied Biosystems) according to the manufacturer's instructions. Chromatin immunoprecipitation (Figure 2-5) was carried out exactly according to a protocol from Upstate Biotechnology using primers tactggccgagacaacactg and cagacgaagcacagaggagg (BiP promoter) or tggagagatggctggttagg and aaaattcgtaggtgtaccgt (control sequence). Antibodies used were the affinity-purified ATF6α peptide antibody described above, a polyclonal ATF6α antibody (Santa Cruz), or an irrelevant antiserum against interferon gamma (Pierce).

For SEAP assays, cells were cotransfected with pcDNA CMV-lacZ (to verify equivalent efficiency of transfection) and a vector encoding SEAP driven by a CMV promoter (pcDNA 3.1 SEAP). This construct was subcloned from pSEAP2-Control (Clontech) by standard methods. 24 hours after transfection, transfection media was replaced with fresh media containing or lacking 5 nM TG, and after a further 24 hours media and lysates were collected and SEAP activity was monitored using the Phospha-Light System kit (Applied Biosystems) according to the manufacturer's instructions. For NHK immunoprecipitations, cells were transfected with pcDNA hα1-AT$_{HK}$ using FuGene 6. The next day, transfection media was replaced with normal or TG-containing media and cells were incubated overnight. For pulse labeling, cells were preincubated in Met/Cys-free media for 20 minutes, followed by labeling for 1 hour using 200 μCi/ml of TranSlabel (MP Biomedicals). Cells were rinsed twice in complete media and chased in complete media for the indicated times before lysis in Tris/SDS as described above. Lysates were diluted in 10 volumes of IP buffer (1% Triton X-100, 100 mM NaCl, 100 mM Hepes pH 7.5) precleared for 30 minutes with protein A-agarose (Pierce), and the supernatants, equalized by the total amount of TCA-precipitable radioactivity for each time point, were incubated overnight with anti-α1-antitrypsin antibody (Dako). Protein A-agarose was then added for 2 hours, and beads were washed twice in IP buffer and once in distilled deionized H_2O before elution in loading buffer. Gels were stained with coomassie blue to verify equivalent antibody recovery; experiments with unequal recovery were not analyzed further. For EndoH digestion (Figure 2-11C), cells were lysed in unbuffered 1% SDS with 100 mM DTT, denatured by boiling for 10 minutes, and diluted into an equal volume of 100 mM NaCitrate pH 5.2 prior to digestion with 500

U of EndoH (NEB) at 37°C for 1 hour. To measure the rate of protein synthesis (Figure 2-3B), cells were treated with TG for 30 minutes and labeled with TranSlabel for 10 minutes, followed by lysis in Tris/SDS, and precipitation of aliquots on a filter and scintillation counting as described [20].

Tissue preparation and analysis. Mice were injected intraperitoneally with 1 mg/kg body weight of TM, or vehicle, exactly as described [46] and liver and kidney were isolated at the indicated times after injection. Briefly, tissue was homogenized using an electronic homogenizer in RIPA buffer containing protease inhibitors, and centrifuged twice at 15,000 rpm for 10 minutes in a microfuge at 4°C. Samples were diluted into 1% SDS, 0.1 M Tris pH 8.8 prior to addition of loading buffer and electrophoresis.

Histological analysis of tissues. Liver specimens were fixed in 10% formalin for embedding in paraffin. Sections of 4 μm were cut and mounted on slides. The cleaved form of caspase 3 was detected using a kit (Abcam) according to the manufacturer's instructions, by the University of Michigan Morphology Core Facility. Livers were visualized in situ using a Leica MZ16FA stereomicroscope.

Knockdown of *Atf6*β in wild-type and *Atf6*α -/- MEFs. A vector that expresses hairpin siRNAs under the control of the mouse U6 promoter was constructed by inserting a pair of annealed DNA oligonucleotides into the LentiLox3.7 vector (provided by Dr. Luk Van Parijs) between the HpaI and XhoI restriction sites [55]. The sequence used for ATF6β RNAi is: GCTCAGAGTCCTCACATCTTT. The clone and packaging vectors including VSVG, RSV-REV, and pMDL g/p RRE were cotransfected into 293T cells. The supernatants containing virus were concentrated by ultracentrifugation. Then the wild-type and *Atf6*α-/- MEFs were infected at 50% confluence with polybrene (8 μg/ml)-

supplemented virus. High infection efficiency (>95%) was achieved by second infection 3 days after first infection. Infected cells were sorted by GFP expression from the RNAi vector.

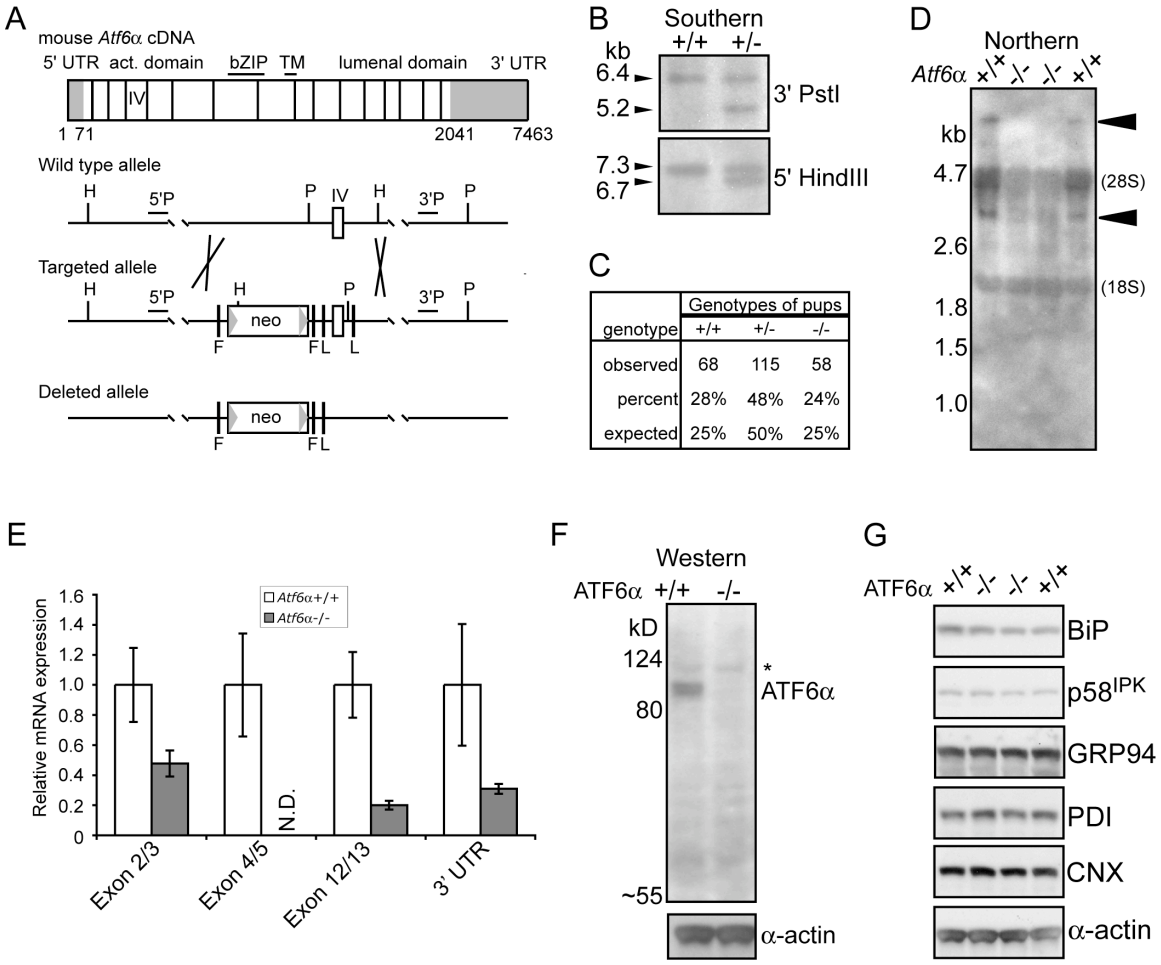

Figure 2-1. Generation of *Atf6α* deficient mice. (A) Schematic drawings of the structure of *Atf6α* cDNA, the wild-type allele showing Exon IV, the targeted allele and the deleted allele. The exons encoding the basic region leucine zipper domain (bZIP) and transmembrane domain (TM) of ATF6α, the *neo* cassette, the *FRT* (F) and *loxP* (L*)* sites, the restriction sites used for Southern screening (PstI: P, HindIII: H), and the 5'/3' external probes (5'P/3'P) are indicated. (B) Southern blot analysis of control and correctly targeted ES clones. The size of each band (in kilobases) is indicated. (C) The genotypes of pups from *Atf6α*+/- intercrosses were tabulated and compared against expected percentages. (D) *Atf6α*+/+ and -/- MEFs were probed by Northern blot for expression of *Atf6α* mRNA. Non-specific probe hybridization to *18S* and *28S* rRNA is indicated. The *18S* background band demonstrates equivalent loading. Note that Northern hybridization produces two species (arrowheads), one of the predicted ~7.5 kb length and another minor species of ~4 kb. Relatively inefficient transfer of large RNAs (>5 kb) means that the full-length *Atf6α* mRNA is probably underrepresented. The probe was complementary to exons 13-16 of *Atf6α* mRNA. (E) Total RNA was isolated from wild-type and *Atf6α-/-* MEFs and the expression of *Atf6α* mRNA was analyzed by real-time RT-PCR, using primers either targeting exons 2/3, exons 4/5 (overlapping the deleted region), exons 12/13, or the 3' UTR. Expression was normalized against *18S* rRNA. N.D. = Not Detected. (F) *Atf6α*+/+ and -/- MEFs were probed by immunoblot for expression of ATF6α protein and α-actin as a loading control. Asterisk represents a nonspecific band. (G) Cellular lysates from two pairs of independent wild-type and *Atf6α-/-* MEFs were probed by immunoblot for BiP, $p58^{IPK}$, GRP94, PDI and CNX to compare the basal expression levels of these ER chaperones and cochaperones, with α-actin as a loading control.

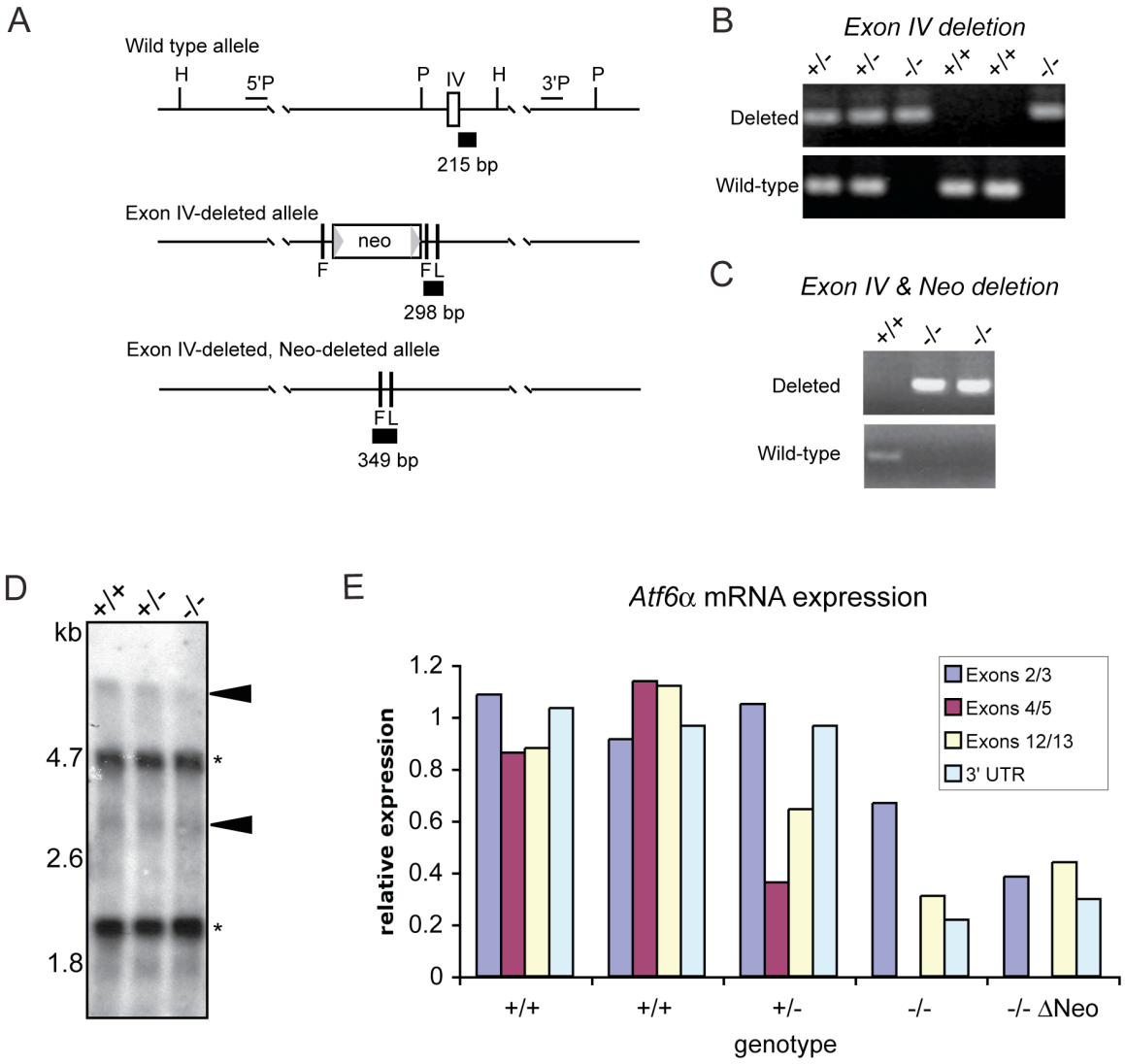

Figure 2-2. Further molecular characterization of ATF6α deficient mice. (A) Schematic drawings of the structures of the wild-type *Atf6*α allele, the Exon IV-deleted allele, and the Exon IV- and Neo-deleted allele, with the locations of genotyping PCR products shown (black bars). (B) Results of PCR analysis of wild-type and Exon IV-deleted *Atf6*α alleles from tail genomic DNA. (C) Results of PCR analysis of wild-type and Exon IV-deleted, Neo-deleted alleles from tail genomic DNA. (D) Mouse liver poly(A) mRNA was probed by Northern blot as in Figure 2-1D, using a probe specific for exons 7-9 of the *Atf6*α mRNA. Asterisks denote nonspecific hybridization to residual *18S* and *28S* rRNA. (E) Exon IV-deleted mice were mated with FLP recombinase-expressing mice to delete the neomycin cassette (genotyping as in (C) above). Total RNA was isolated from the livers of wild-type, heterozygous, Exon IV-deleted (-/-), and Exon IV-deleted, Neo-deleted (-/- ΔNeo) animals and the expression of *Atf6*α mRNA was analyzed by real-time RT-PCR, using primers either targeting exons 2/3, exons 4/5 (overlapping the deleted region), exons 12/13, or the 3' UTR. Expression was normalized against *18S* rRNA.

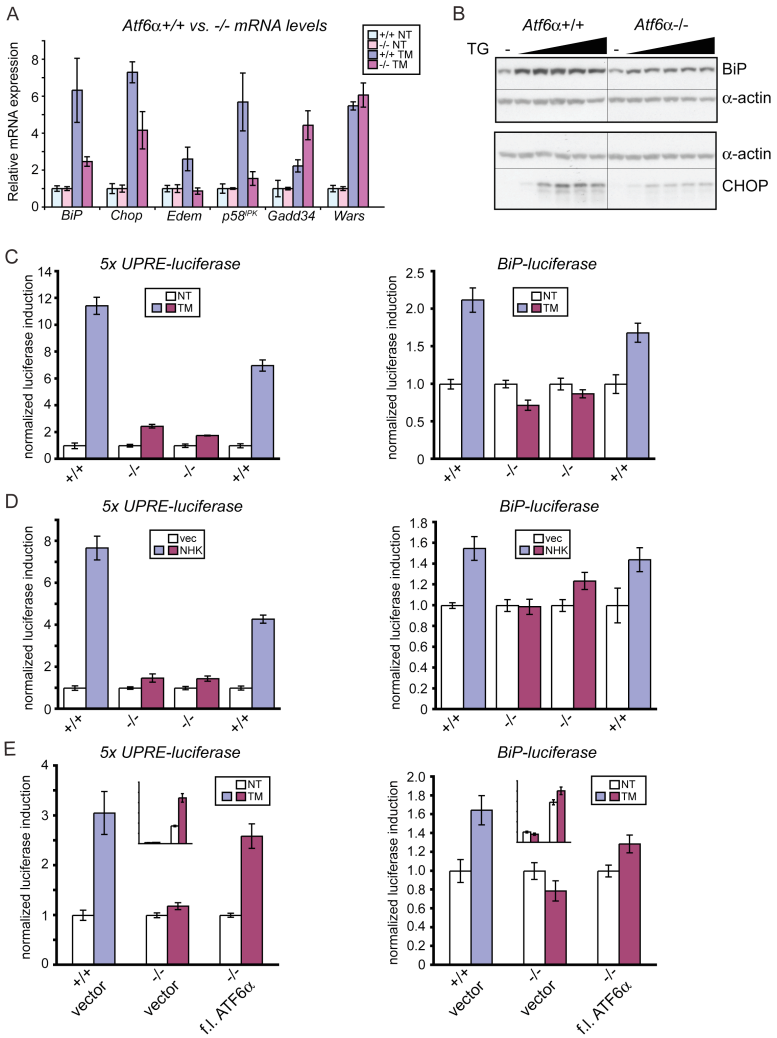

Figure 2-3. *Atf6α* deficient MEFs are responsive to ER stress but defective in chaperone upregulation. (A) Wild-type and *Atf6α-/-* MEFs were treated with 50 ng/ml TM for 24 hours. Total RNA was isolated and the expression of *BiP, Chop, Edem, p58*^{IPK}*, Gadd34* and *Wars* was quantitated by real-time RT-PCR, normalizing against *18S* rRNA expression. Error bars represent means ± SDM from RNA isolated from three independent plates. Basal expression of these genes was not found to consistently vary between experiments. (B) Wild-type and *Atf6α-/-* MEFs were treated for 16 hours with increasing concentrations of TG (2.5-100 nM), followed by cell lysis and immunoblot for BiP, CHOP or α-actin. (C) Two separate lines each of wild-type and *Atf6α-/-* MEFs were cotransfected with *5XUPRE*- or *BiP* promoter-dependent luciferase reporters and a constitutive β-galactosidase reporter. Cells were treated with 50 ng/ml TM 24 hrs post-transfection and lysates were analyzed for luciferase expression, normalized against β-galactosidase, after 24 hrs of TM treatment. Luciferase expression is given as a fold-change relative to untreated cells of the same genotype. Luciferase expression after treatment is shown in blue for wild-type cells and purple for knockout cells. Note that the basal expression of the BiP-luciferase reporter is high, and its stress inducibility low, likely because this construct contains approximately 340 bp of the rat *BiP* promoter, which encompasses regulatory regions upstream of the ERSE sites. A construct driven by a more minimal *BiP* promoter was more robustly induced by ER stress (Figure 2-5). (D) Wild-type and *Atf6α-/-* MEFs were transfected as in (C), and also with an α1-antitrypsin null Hong Kong (NHK) variant or empty vector control. Lysates were analyzed for luciferase expression 48 hrs post-transfection and normalized as in (C). (E) Wild-type and *Atf6α-/-* MEFs were transfected as in (C), a constitutive β-galactosidase reporter, and also with full-length human *Atf6α* or empty vector. Cells were treated with TM and assayed and normalized as in (C). The inset panel shows the non-normalized luciferase expression in vector-transfected (left pair) or *Atf6α*-transfected (right pair) *Atf6α-/-* cells, which demonstrates that *Atf6α* transfection stimulates significant reporter transcription even in the absence of stress. Error bars represent means ± SDM from three independent plates. The variation in inducibility of each construct varies between experiments, but the relative effects of ATF6α deletion remain consistent.

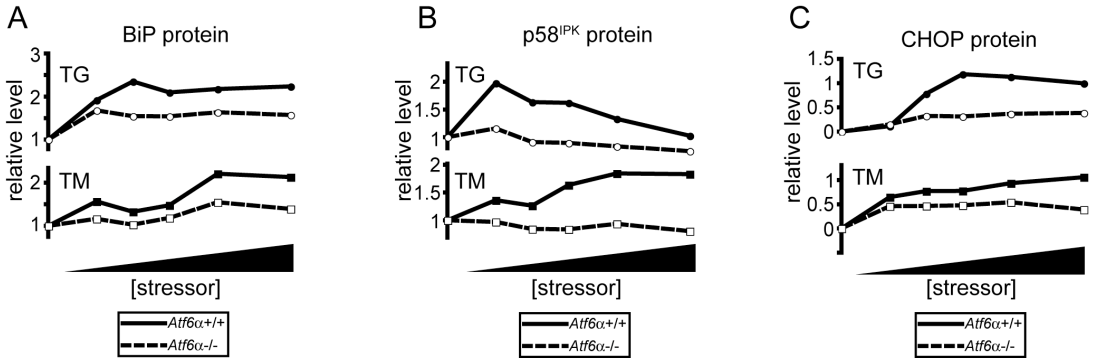

Figure 2-4. Attenuated upregulation of UPR targets by TM and TG in *Atf6*α-/- cells. Wild-type and *Atf6*α-/- MEFs were treated with increasing concentrations of TG (2.5-100 nM) or TM (25-1000 ng/ml) for 16 hrs, followed by cell lysis and immunoblot for BiP (A), $p58^{IPK}$ (B), and CHOP (C). The expression of these three ER stress marker proteins was quantitated by densitometry and normalized against α-actin expression, and is shown in graphical form for each concentration.

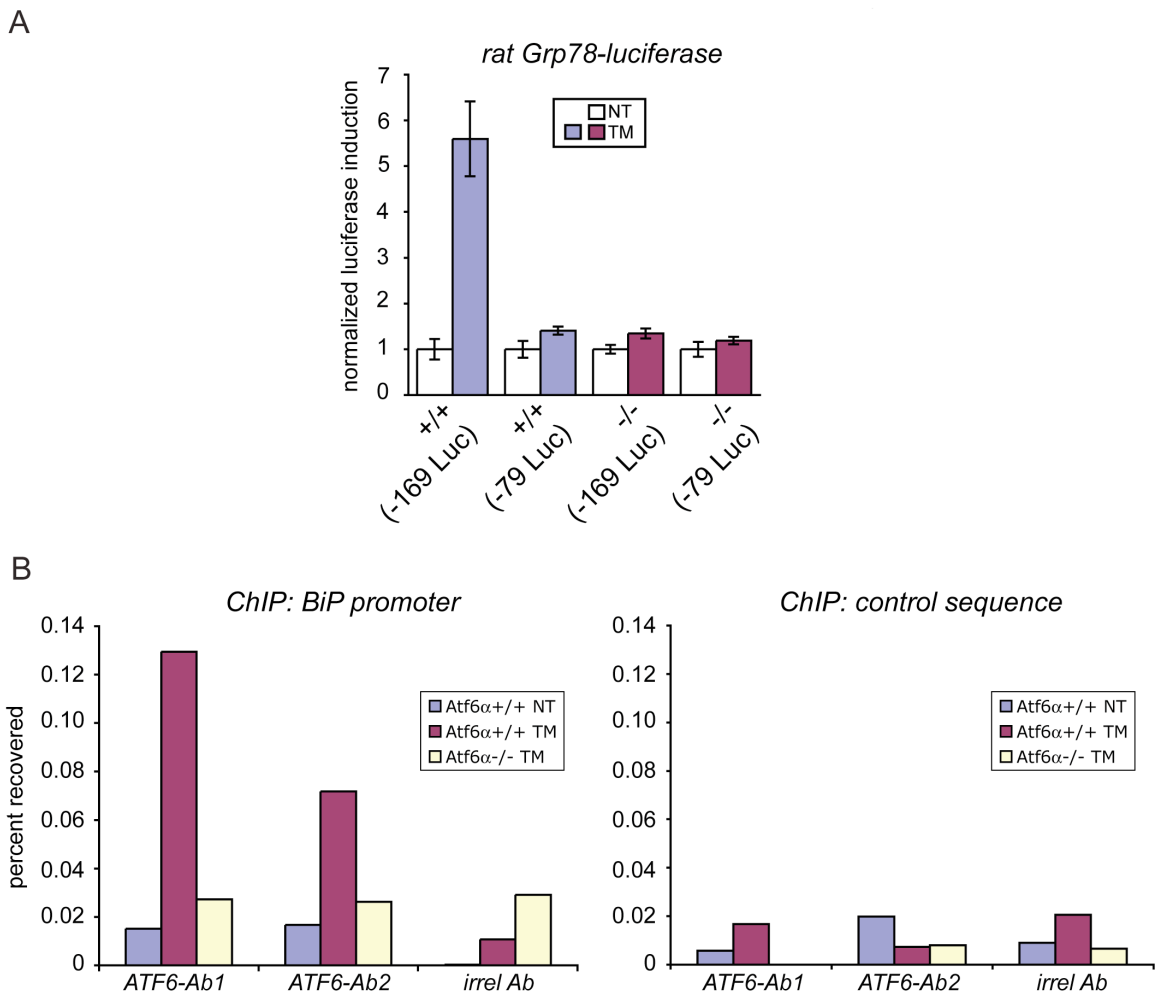

Figure 2-5. Direct regulation of ERSE-dependent expression by ATF6α. (A) A minimal version of the rat *BiP* promoter, containing only the proximal 169 nucleotides of the promoter which encompasses the three ERSE sites, could be upregulated by overnight TM treatment in wild-type but not *Atf6*α-/- cells. Deletion of these sites (-79 Luc) renders the construct unresponsive to ER stress. (B) Protein-DNA complexes in wild-type or *Atf6*α-/- cells were crosslinked using formaldehyde, followed by denaturation and chromatin immunoprecipitation using either of two antibodies against ATF6α (Ab1 and Ab2) or an irrelevant antiserum against interferon gamma (irrel). Recovered material was quantitated by real-time RT-PCR with primers specific for either the *BiP* promoter or a control sequence located 6 kb upstream of the *BiP* promoter. Recovery was quantitated as a percentage of immunoprecipitation input. Note that the *BiP* promoter but not the control sequence is enriched with ATF6α antisera but not irrelevant antisera, that this interaction is strengthened by ER stress, and that this enrichment is lost in *Atf6*α-/- cells.

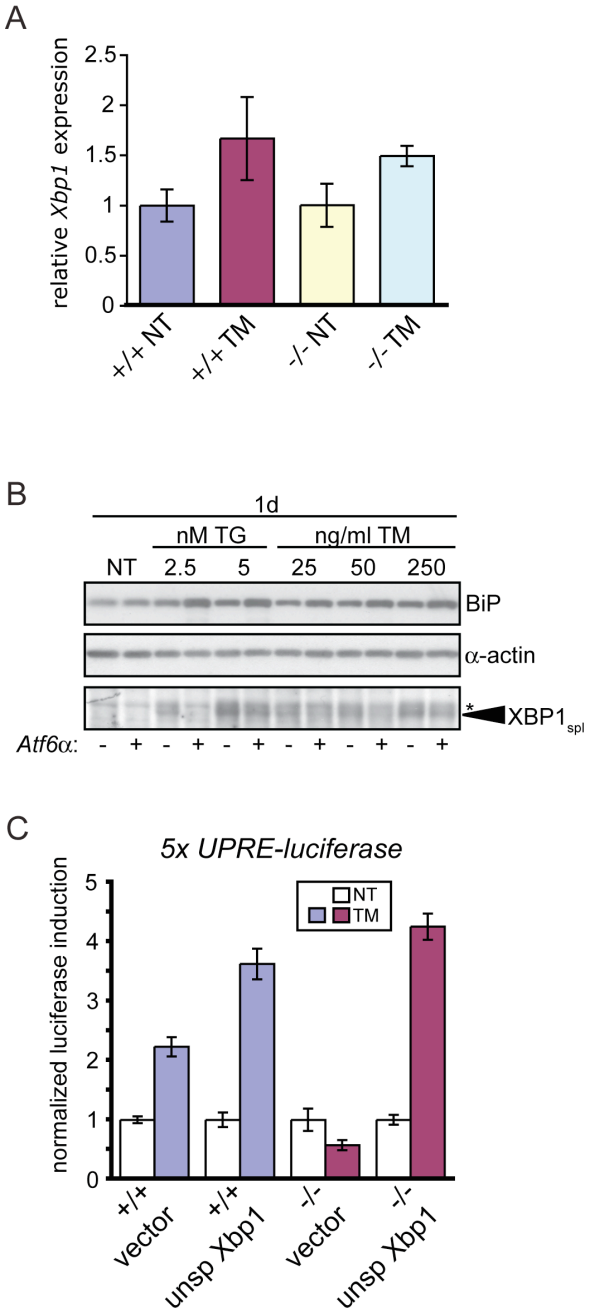

Figure 2-6. ATF6α-XBP1 pathway interactions. (A) The expression of *Xbp1* mRNA was determined in the presence or absence of 50 ng/ml TM for 24 hours using array expression profiling. Error bars represent means ± S.D.M. from one plate each of three independent *Atf6*α+/+ or *Atf6*α-/- cell lines. (B) Wild-type and *Atf6*α-/- MEFs were treated with TG or TM at the indicated concentrations for 24 hours, followed by cell lysis and immunoblot for BiP, XBP1 derived from spliced *Xbp1* mRNA, and α-actin. The asterisk represents a nonspecific band. Note that the wild-type is shown on the right for each pair. (C) Wild-type and *Atf6*α-/- MEFs were cotransfected with a *5XUPRE* dependent luciferase reporter, a constitutive β-galactosidase reporter, and either the unspliced form of mouse *Xbp1* or empty vector control. Cells were treated with TM and assayed as in Figure 2-3E.

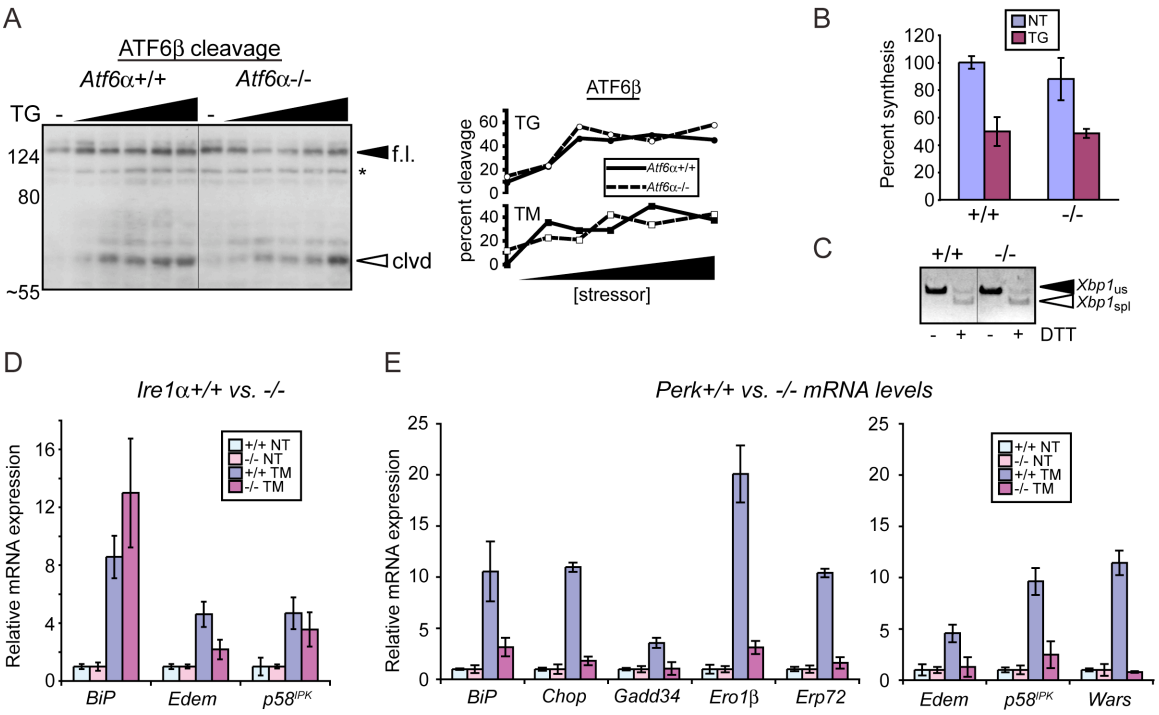

Figure 2-7. The PERK and IRE1α pathways functionally overlap with ATF6α. (A) Wild-type and *Atf6*α*-/-* MEFs were treated with increasing concentrations of TG (2.5-100 nM) or TM (25-1000 ng/ml; blot not shown) for 16 hrs, followed by cell lysis and immunoblot for ATF6β. Uncleaved (f.l.) and cleaved (clvd) forms are indicated, as well as a non-specific band (asterisk). The extent of ATF6β cleavage relative to full-length was quantitated by densitometry, and is shown in graphical form for each concentration to the right of the blots. (B) Wild-type and *Atf6*α*-/-* MEFs were treated for 30 minutes with 5 nM TG. Cells were then pulse-labeled for 10 min with ^{35}S Cys/Met. Precipitable counts were normalized against incorporation for nontreated *Atf6*α+/+ cells. Error bars represent means ± SDM from three independent plates. (C) Total RNA was isolated from wild-type and *Atf6*α*-/-* MEFs treated for 1 hr with 10 mM DTT. RT-PCR was used to simultaneously detect both spliced (spl) and unspliced (us) *Xbp1* mRNA. The image is presented in black-and-white inverted form for greater visual clarity. (D) and (E) Total RNA was isolated from *Ire1*α+/+ and -/- MEFs (D) and *Perk* +/+ and -/- MEFs (E) treated with 50 ng/ml TM for 24 hrs and the expression levels of the indicated genes were quantitated by real-time RT-PCR, normalizing against *18S* rRNA expression. Data from *Perk* cells were taken from two separate experiments. Error bars represent means ± SDM from RNA isolated from three independent plates.

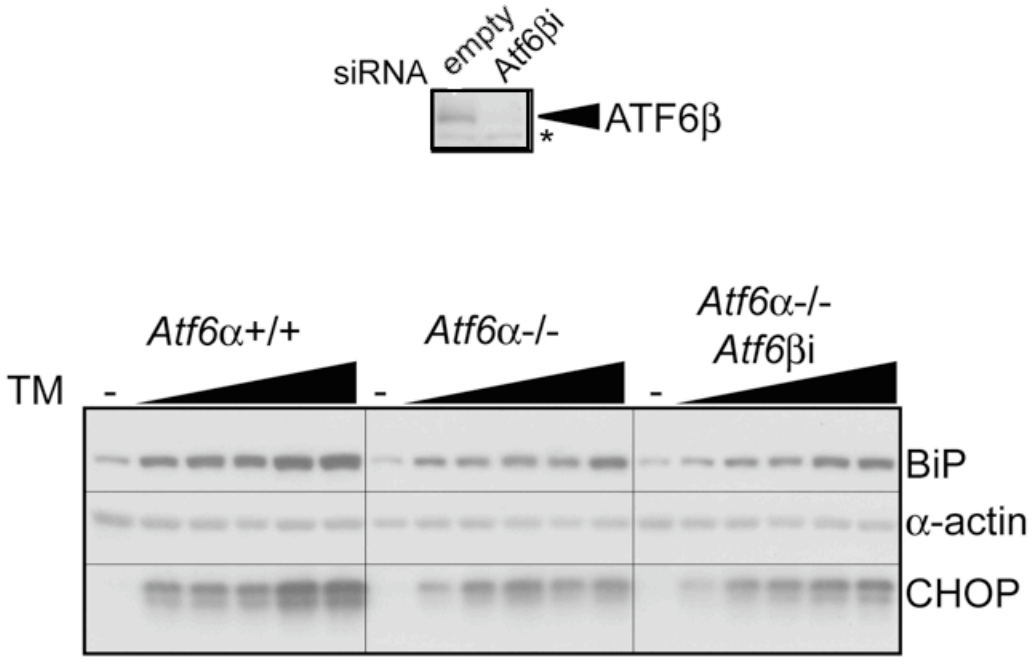

Figure 2-8. *Atf6*β knockdown does not exacerbate *Atf6*α-/- defects in BiP and CHOP upregulation. *Atf6*α-/-: *Atf6*βi MEFs were generated as described in experimental procedures. (A) Cellular lysates were collected and probed for expression of ATF6β. The asterisk indicates a nonspecific band that demonstrates equal protein loading. (B) *Atf6*α+/+, *Atf6*α-/-, and *Atf6*α-/-:*Atf6*βi MEFs were treated with increasing concentrations of TM for 24 hours. Protein lysates were collected and probed for the expression of BiP, CHOP and α-actin.

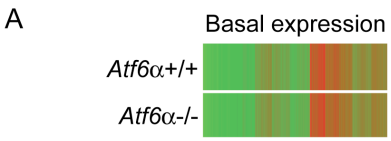

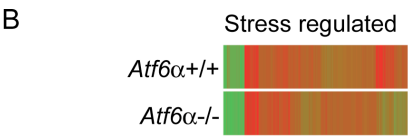

C

Gene	Locus Name	Accession #	Expression relative to wild-type NT: *Atf6*α+/+ TM	*Atf6*α-/- NT	*Atf6*α-/- TM	Probable Function
Protein folding						
ERO1-like beta (S. cerevisiae)	Ero1lb	BB234316	6.6 ± 0.1	1.0 ± 0.2	1.6 ± 0.0	ER redox
protein disulfide isomerase associated 4	Pdia4	J05186	6.6 ± 0.1	1.1 ± 0.4	1.1 ± 0.0	Oxidative folding (ERp72)
DnaJ (Hsp40) homolog, subfamily C, member 3	Dnajc3	BE624323	3.4 ± 0.1	1.0 ± 0.1	1.4 ± 0.0	BiP cochaperone (p58^{IPK})
hypoxia up-regulated 1	Hyou1	BM231738	3.3 ± 0.0	1.2 ± 0.1	1.7 ± 0.1	ER protein folding
DnaJ (Hsp40) homolog, subfamily B, member 11	Dnajb11	AK010861	2.2 ± 0.1	0.9 ± 0.1	1.0 ± 0.0	BiP cochaperone
protein disulfide isomerase associated 6	Pdia6	AK005989	1.8 ± 0.1	1.0 ± 0.1	1.3 ± 0.1	Oxidative folding
Protein degradation						
HCy- and ER stress-inducible, ubiq.-like domain 1	Herpud1	NM_022331	8.4 ± 0.1	1.0 ± 0.1	3.0 ± 0.1	ERAD
Der1-like domain family, member 3	Derl3	AK007348	6.4 ± 0.1	1.0 ± 0.1	0.9 ± 0.1	ERAD
synovial apoptosis inhibitor 1, synoviolin	Syvn1	AK004688	3.6 ± 0.1	1.0 ± 0.1	1.6 ± 0.1	E3 ligase; ERAD
Sel1 (suppressor of lin-12) 1 homolog	Sel1h	AK005023	3.0 ± 0.0	0.9 ± 0.0	1.2 ± 0.0	ERAD
cylindromatosis (turban tumor syndrome)	Cyld	BM119209	1.7 ± 0.1	1.0 ± 0.3	1.1 ± 0.0	Ubiquitination
Protein trafficking/ER homeostasis						
stromal cell-derived factor 2-like 1	Sdf2l1	NM_022324	9.1 ± 0.1	0.9 ± 0.3	1.6 ± 0.0	Protein O-glycosylation
ORM1-like 2 (S. cerevisiae)	Ormdl2	BC002146	3.2 ± 0.1	1.0 ± 0.2	1.0 ± 0.2	Protection from ER stress
nucleobindin 2	Nucb2	NM_016773	2.6 ± 0.2	1.2 ± 0.3	1.3 ± 0.0	ER calcium regulation
Rab38, member of RAS oncogene family	Rab38	AV364767	2.6 ± 0.1	1.0 ± 0.1	0.9 ± 0.1	Membrane trafficking of enzymes
ATPase, Ca++ transporting, cardiac, slow twitch 2	Atp2a2	NM_009722	2.0 ± 0.0	0.9 ± 0.0	1.2 ± 0.0	Calcium homeostasis
ADP-ribosylation factor 2	Arf2	NM_007477	1.6 ± 0.1	1.0 ± 0.2	0.9 ± 0.0	Endomembrane protein trafficking
Biosynthesis						
mevalonate (diphospho) decarboxylase	Mvd	NM_138656	2.5 ± 0.2	1.0 ± 0.1	0.7 ± 0.1	Cholesterol biosynthesis
natural killer tumor recognition sequence	Nktr	BB317504	1.9 ± 0.1	1.0 ± 0.0	1.3 ± 0.1	Carbohydrate biosynthesis
GDP-mannose 4, 6-dehydratase	Gmds	AI747296	1.8 ± 0.2	1.1 ± 0.3	0.9 ± 0.0	Carbohydrate biosynthesis
pyridoxal (pyridoxine, vitamin B6) kinase	Pdxk	BG063905	1.6 ± 0.0	1.0 ± 0.0	1.2 ± 0.1	Vitamin biosynthesis
N-acetylneuraminic acid synthase	Nans	BI151886	1.6 ± 0.1	1.0 ± 0.1	1.0 ± 0.0	Sialic acid biosynthesis
Transport						
solute carrier family 2, member 6	Slc2a6	BB196807	4.4 ± 0.2	1.0 ± 0.2	1.0 ± 0.1	Glucose transporter
solute carrier family 39, member 14	Slc39a14	BB399837	1.7 ± 0.1	1.0 ± 0.2	1.1 ± 0.0	Zinc transporter
solute carrier family 26, member 6	Slc26a6	NM_134420	1.6 ± 0.1	1.0 ± 0.1	1.3 ± 0.0	Transporter; unknown specificity
potassium channel tetramerisation domain 7	Kctd7	AV273256	1.5 ± 0.1	1.0 ± 0.1	1.1 ± 0.1	Potential potassium channel
Nucleic acid regulation						
RNA binding motif protein 15B	Rbm15b	BB776868	2.4 ± 0.0	1.1 ± 0.1	1.3 ± 0.1	Nuclear RNA binding phosphoprotein
SWI/SNF related, subfamily b, member 1	Smarcb1	BB820473	1.9 ± 0.1	0.9 ± 0.1	0.8 ± 0.1	Chromatin remodeling
RNA binding motif protein 10	Rbm10	BE553944	1.6 ± 0.0	1.1 ± 0.2	1.2 ± 0.0	RNA binding; unknown function
endonuclease G-like 1	Endogl1	BB089035	1.6 ± 0.1	1.1 ± 0.1	1.3 ± 0.0	Endonuclease; possible death effector
Miscellaneous						
inhib. of Bruton agammaglobulinemia Tyr kinase	Ibtk	BM250711	2.9 ± 0.1	1.0 ± 0.1	1.9 ± 0.2	B cell development
CDK2-associated protein 2	Cdk2ap2	NM_026373	2.8 ± 0.1	1.0 ± 0.2	1.6 ± 0.0	Cell cycle
docking protein 5	Dok5	NM_029761	2.6 ± 0.1	0.8 ± 0.2	1.3 ± 0.2	MAP kinase cascades
dual adaptor P-Tyr and 3-phosphoinositides 1	Dapp1	NM_011932	2.4 ± 0.1	1.1 ± 0.3	1.3 ± 0.1	B cell signaling
male sterility domain containing 2	Mlstd2	BG094874	2.1 ± 0.1	1.0 ± 0.3	1.0 ± 0.0	Peroxisomal; lipid peroxidation
histocompatibility 2, M region locus 3	H2-M3	NM_013819	2.0 ± 0.1	1.1 ± 0.1	1.6 ± 0.1	Self recognition
period homolog 1 (Drosophila)	Per1	AF022992	1.7 ± 0.1	1.0 ± 0.1	0.9 ± 0.0	Circadian cycle
Unknown function						
zinc finger protein 324	Zfp324	BB277175	4.5 ± 0.0	1.2 ± 0.3	1.8 ± 0.1	
Rab9 effector protein with kelch motifs	Rabepk	AA217054	4.3 ± 0.1	0.9 ± 0.1	1.1 ± 0.1	
zinc finger protein 57	Zfp57	BB549686	2.1 ± 0.1	1.1 ± 0.1	1.3 ± 0.1	
Zinc finger protein of the cerebellum 5	Zic5	AV322605	2.0 ± 0.1	1.0 ± 0.3	1.2 ± 0.1	
cyclin M2	Cnnm2	BB278418	1.9 ± 0.1	1.0 ± 0.2	1.3 ± 0.0	
transmembrane protein 50B	Tmem50b	BC004841	1.7 ± 0.2	1.0 ± 0.3	0.7 ± 0.0	
storkhead box 2	Stox2	BM114398	1.5 ± 0.1	0.9 ± 0.2	1.1 ± 0.0	
Zinc finger, MYND domain containing 19	Zmynd19	AW125726	1.5 ± 0.2	1.0 ± 0.2	1.2 ± 0.0	

Figure 2-9. Transcriptional profiling reveals defective induction of a subset of ER stress-dependent genes in *Atf6*α*-/-* fibroblasts. (A) and (B) Cluster analysis of gene expression and transcriptional profile analysis were performed as described in the Experimental Procedures. Graphic representation of the average expression level of 8334 significantly expressed genes in untreated (A) and 249 stress regulated genes in tunicamycin-treated (B) wild-type and *Atf6*α*-/-* MEFs is shown. Each vertical bar represents a single gene. Green coloration indicates relatively low level expression, and red indicates a relatively high level of expression of a given mRNA. (C) List of genes upregulated (>1.5-fold, $p<0.05$) by TM in wild-type cells that are less induced in *Atf6*α*-/-* fibroblasts (<2/3 induction level, $p<0.05$). Data are presented as means ± SDM of the expression level relative to wild-type nontreated cells; thus the expression values for these genes in *Atf6*α*-/-* cells in the absence of stress are essentially identical to those in wild-type cells. The highlighted values indicate those genes whose stress responsiveness is completely lost in *Atf6*α*-/-* MEFs.

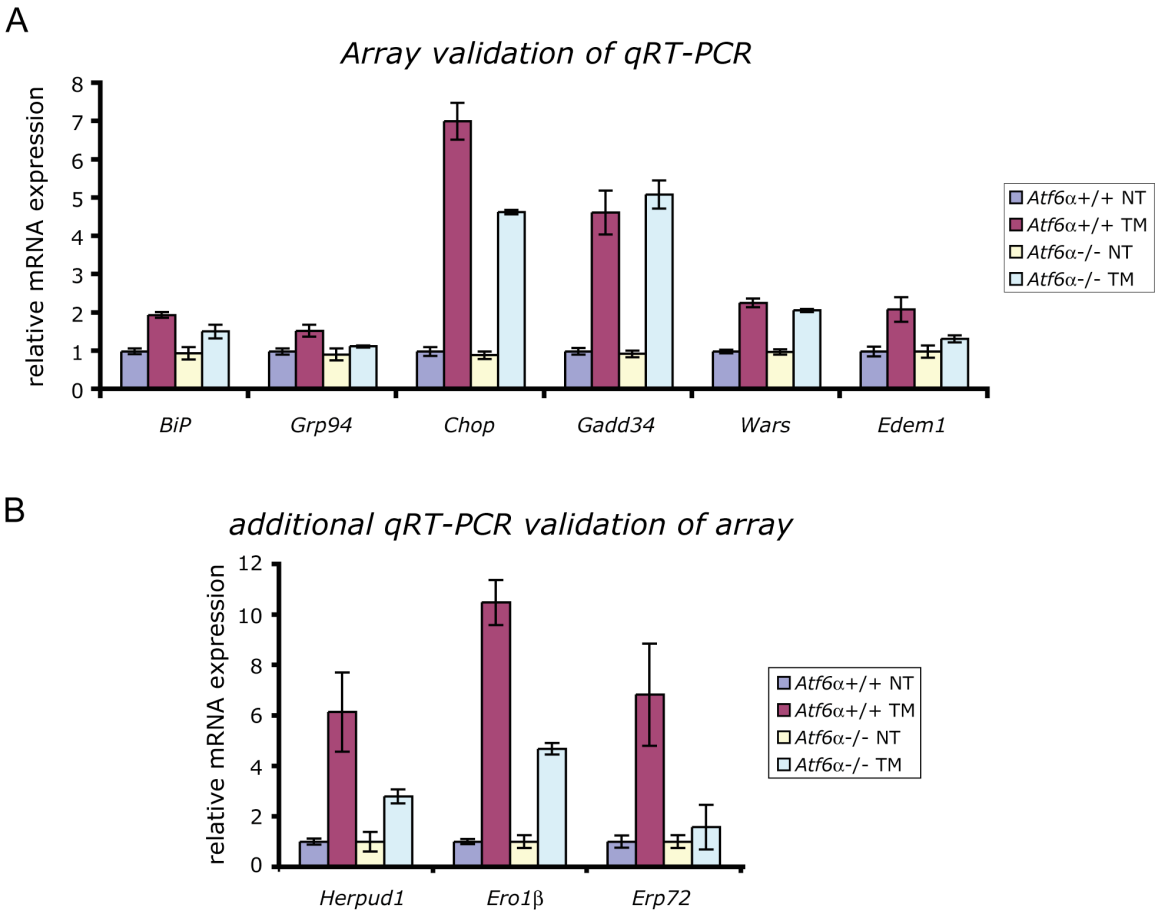

Figure 2-10. Additional validation of microarray data. (A) The average expression levels of *BiP*, *Grp94*, *Chop*, *Gadd34*, *Wars*, and *Edem1* from microarray analysis are shown, normalized against nontreated wild-type cells. Error bars represent means ± SDM. Note that the expression values for all of these genes in the absence of stress is not significantly different between wild-type and *Atf6*α-/- cells. (B) The induction levels of additional genes identified as *Atf6*α-dependent (Figure 2-9C) were determined upon treatment of wild-type and *Atf6*α-/- MEFs with 50 ng/ml TM for 24 hours, followed by quantitative real-time RT-PCR and normalization exactly as in Figure 2-3A.

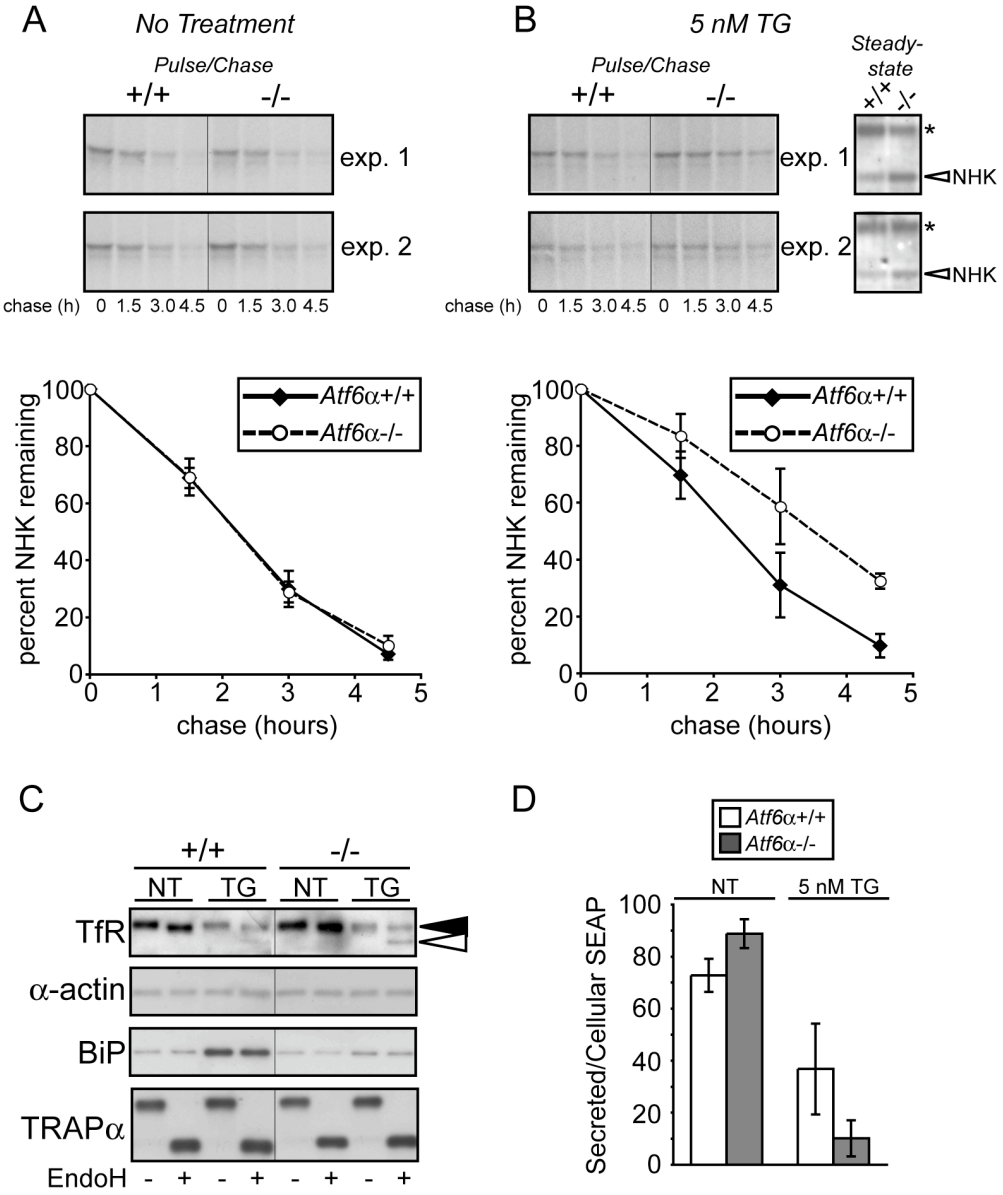

Figure 2-11. *Atf6*α deficient cells are defective in ER protein processing. (A) and (B) Wild-type and *Atf6*α-/- MEFs transfected with NHK were otherwise untreated (A) or pretreated with 5 nM TG overnight (B), pulse-labeled for 1 hr and then chased for the indicated times. NHK was isolated by immunoprecipitation. The results of two experiments are shown in each case. The rate of NHK degradation was quantitated from three experiments and is shown ± SDM in the graphs below the autoradiographs. In (B), a portion of the IP input was probed by immunoblot to detect NHK (arrowhead). The asterisk represents a nonspecific band that demonstrates equivalent total protein loading. (C) *Atf6*α+/+ and -/- MEFs were left untreated or treated overnight with 5 nM TG. Lysates were then divided into aliquots for digestion with EndoH as indicated, and probed by immunoblot. The EndoH-resistant (closed arrowhead) and EndoH-sensitive (open arrowhead) species of transferrin receptor (TfR) are shown. Deglycosylation of the ER-resident protein TRAPα is also shown. (D) *Atf6*α+/+ and -/- MEFs were transfected with constitutively-expressed SEAP and treated for 24 hours in the presence or absence of 5 nM TG. Media and lysates were collected and SEAP activity was measured by a luminescence assay. The ratio of secreted to cellular SEAP activity is provided. Error bars represent means ± SDM from three independent plates.

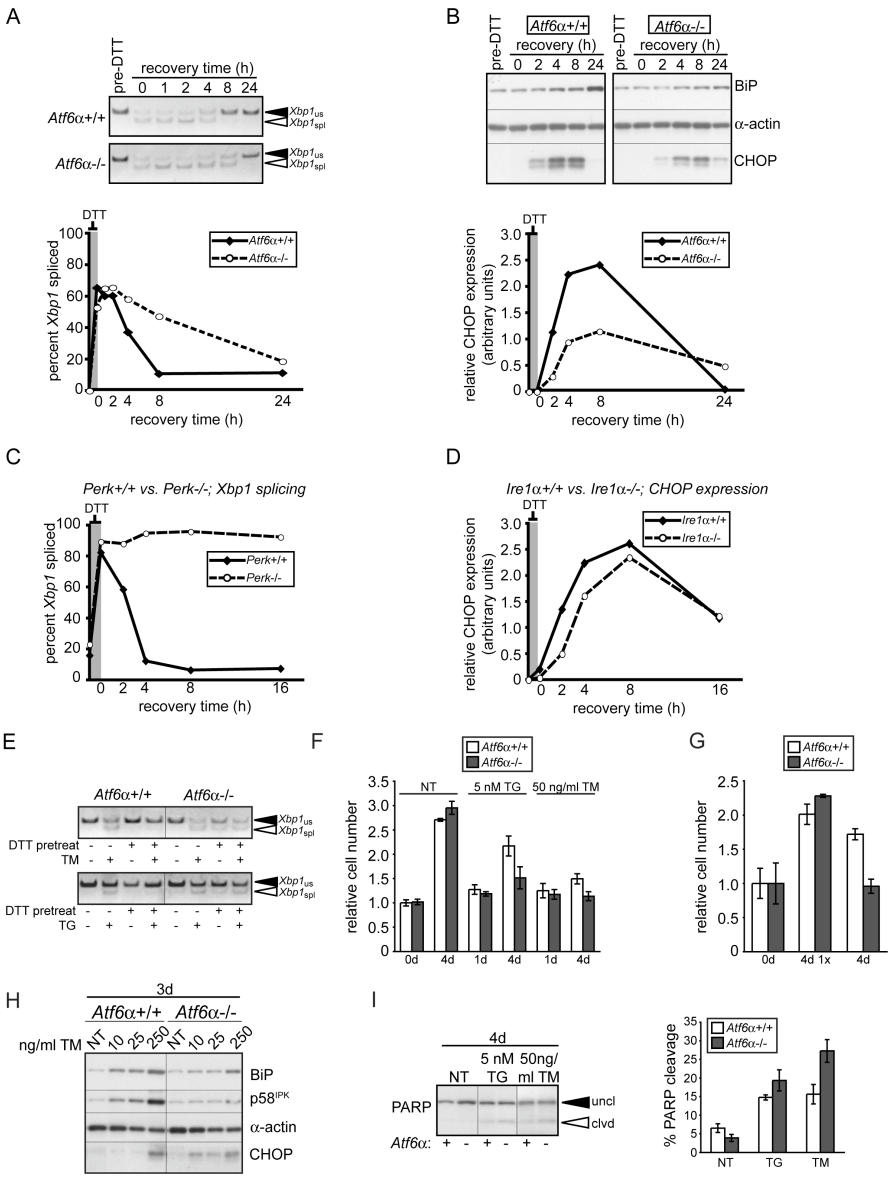

Figure 2-12. *Atf6α-/-* MEFs do not efficiently adapt to chronic ER stress. (A) Wild-type and *Atf6*α-/- MEFs were treated with 10 mM DTT for 1 hr followed by chase in DTT-free media. Total RNA was isolated at the indicated time points during recovery, for RT-PCR amplification of *Xbp1* mRNA as in Figure 2-7C. The extent of *Xbp1* mRNA splicing relative to the unspliced form was quantitated by densitometry, and is shown beneath the gel. (B) Cells were treated as in (A), and cellular lysates were probed for expression of BiP, CHOP and α-actin by immunoblot. The expression level of CHOP protein normalized against α-actin is quantitated and shown beneath the blots. In both (A) and (B), essentially identical data were obtained in independent cell lines. Note that CHOP induction depends upon multiple transcriptional and translational steps, and so is not first seen until approximately two hours after removal of DTT. (C) Total RNA was isolated from *Perk*+/+ and -/- MEFs treated and assayed as in (A), except that 1 mM DTT was used. (D) Protein lysates were collected from *Ire1*α+/+ and -/- MEFs treated and assayed as in (B). (E) Wild-type and *Atf6*α-/- MEFs were treated with 10 mM DTT for 1 hr and recovered for 16 hrs. Cells were then rechallenged as indicated with 50 ng/ml TM for 8 hours or 5 nM TG for 2 hours. Total RNA was isolated for RT-PCR amplification of *Xbp1* mRNA as in Figure 2-7C. (F) Proliferation during chronic stress is impaired by *Atf6*α deletion. Wild-type and *Atf6*α-/- MEFs were treated with 5 nM TG or 50 ng/ml TM for 1 or 4 days, or left untreated. Cell lysates were collected and cell number was estimated by protein concentration (see experimental procedures). Cell number is expressed relative to untreated *Atf6*α+/+ cells at day 0. (G) Wild-type and *Atf6*α-/- MEFs were treated with 10 mM DTT for 1 hr and allowed to recover for 11 hours before retreatment. This process was repeated over 4 days, after which lysates were collected to estimate cell proliferation as in (F). Alternatively, cells were treated only once with DTT and allowed to recover for the remainder of the time-course (4d 1x). (H) Lysates were prepared from either wild-type or *Atf6*α-/- MEFs treated with TM of the indicated concentrations for 3 days as in (F), and probed for expression of BiP, CHOP, p58^{IPK} and α-actin by immunoblot. (I) Cells were treated for 4 days with 5 nM TG or 250 ng/ml TM, and PARP cleavage was assessed and quantitated by densitometry. The graph presents PARP cleavage from three independent plates, ± SDM. The PARP immunoblot corresponding to treatment of both genotypes with 250 ng/ml TM was taken from a longer exposure because of protein underloading.

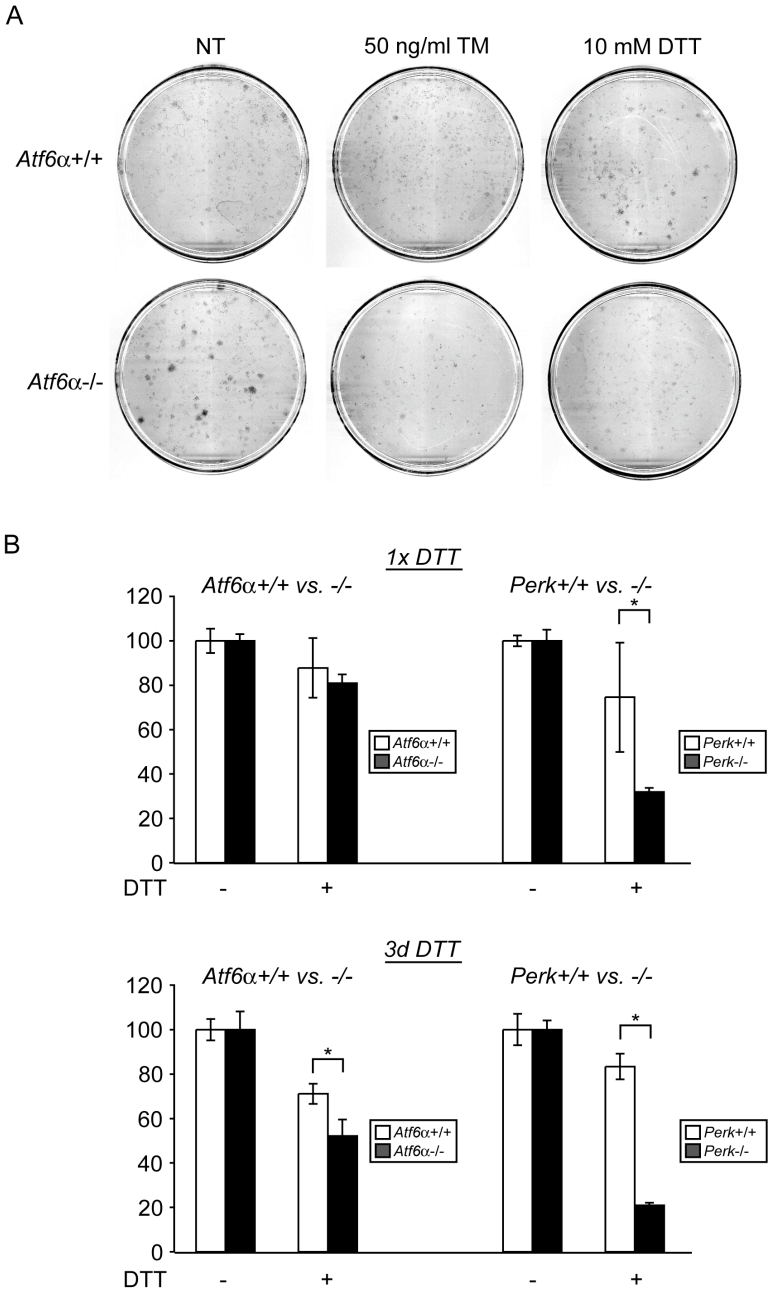

Figure 2-13. Impaired adaptation to chronic stress in *Atf6*α-/- cells. (A) Wild-type and *Atf6*α-/- MEFs were seeded in equal numbers on 10 cm plates and treated either for three days with 50 ng/ml TM or vehicle, or for one hour out of every twelve hours, for three days, with 10 mM DTT. Cells were then allowed to recover for seven days, after which colonies were visualized using crystal violet staining. Representative data from three independent experiments are shown. In the absence of stress, *Atf6*α-/- cells form somewhat larger colonies than wild-type cells. Nonetheless, their growth in markedly impaired by both TM and DTT, while that of wild-type cells is affected very little. (B) Wild-type and *Atf6*α-/- cells, and also *Perk*+/+ and *Perk*-/- MEFs, were seeded onto 96 well plates and treated for either one hour (top panel), or repeatedly for three days (one hour out of every 24 hours—bottom panel) with 10 mM DTT. Cell viability/proliferation was then assessed three days after the first treatment by MTT reduction, which measures respiratory capacity. Error bars represent means ± SDM from six wells. Asterisks represent p values less than 0.001, using a two-tailed student's t-test.

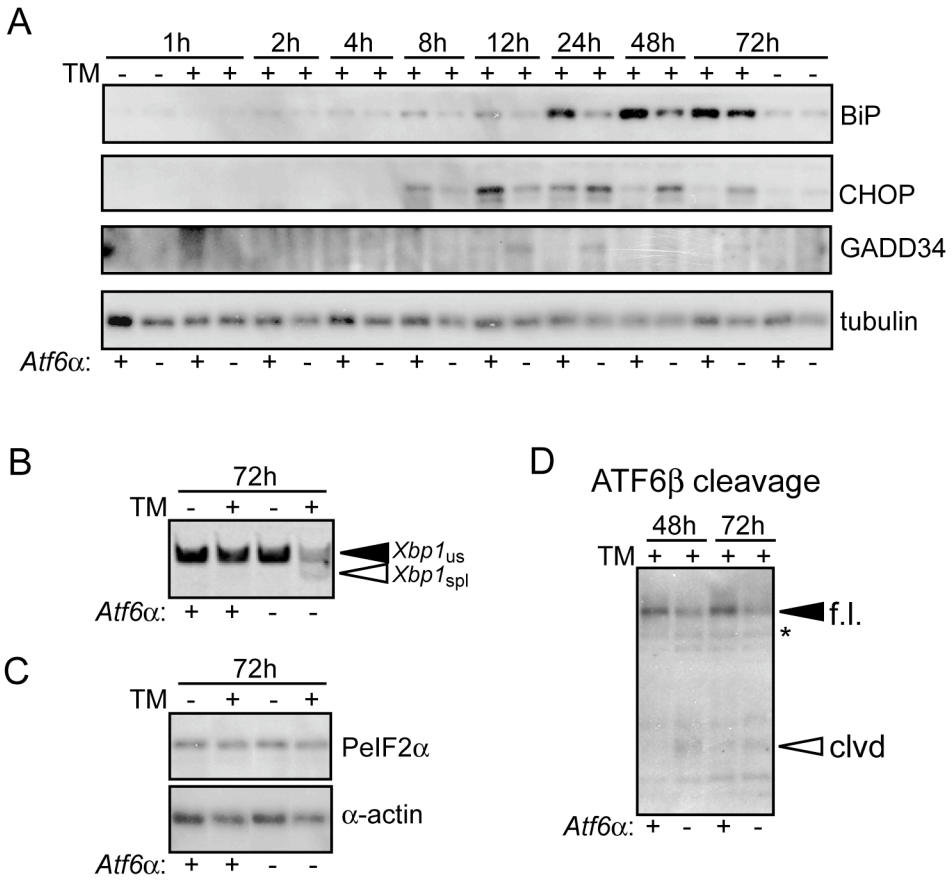

Figure 2-14. Persistence of UPR signaling in *Atf6*α-/- cells exposed to chronic stress. (A) Cells were treated with TM for up to 72 hours, with stressor refreshed daily, and lysates were harvested at the indicated times for immunoblot. (B) RNA was isolated from cells treated for 72 hours as in (A) and *Xbp1* mRNA splicing was assessed by RT-PCR as in Figure 2-7C. (C) The extent of eIF2α phosphorylation in cells treated for 72 hours as in (A) was probed by immunoblot. Treatment of cells with a more robust stress produced enhanced reactivity with this antibody (see Figure 2-15A; also data not shown), confirming the functionality of the reagent. (D) Cells exposed to TM for 48 or 72 hours as in (A) were probed for cleavage of ATF6β as in Figure 2-7A. The low concentration of stressor used (necessary for cells to survive treatment for more than 24 hours) makes the cleaved form of ATF6β fairly faint. Nonetheless, a greater ratio of cleaved to uncleaved ATF6β can be seen at both time-points in *Atf6*α-/- cells. Asterisk represents a nonspecific band.

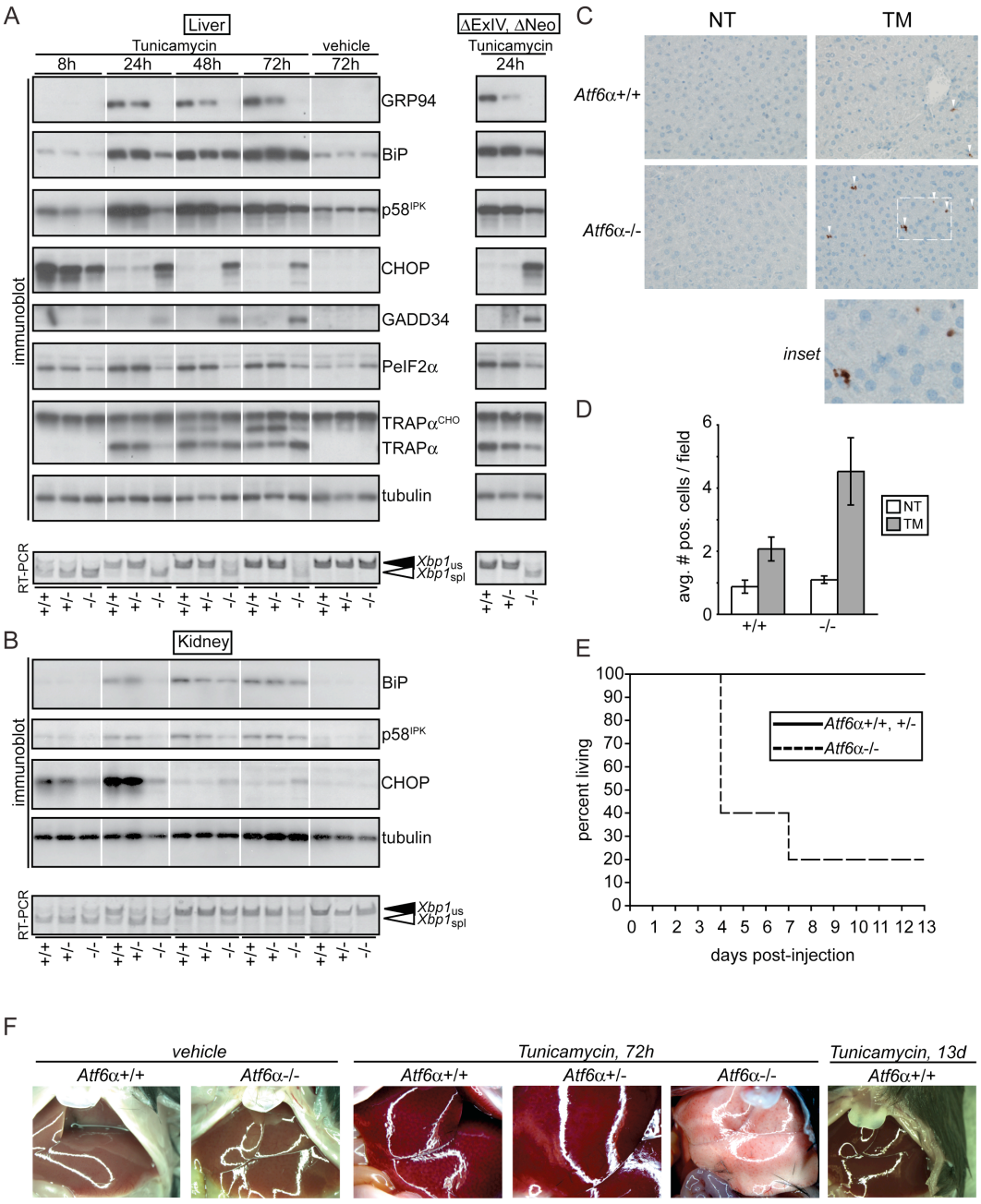

Figure 2-15. ATF6α regulates stress-dependent chaperone expression in vivo. (A) and (B) Wild-type and *Atf6α* heterozygous and homozygous mutant mice were injected intraperitoneally with TM (1 mg/kg body weight) or vehicle. Protein lysates from liver (A) and kidney (B), isolated 8, 24, 48, or 72 hours after injection, were probed by immunoblot as indicated. Efficacy of the TM was reflected in inhibition of TRAPα glycosylation (TRAPα versus TRAPα^{CHO}). RNA was prepared from the same liver tissue samples and assayed by RT-PCR of *Xbp1* mRNA as in Figure 2-7C. The right panel shows liver samples taken from mice mated with FLP recombinase-expressing animals to delete the neomycin cassette, 24 hours after injection with TM. (C) Paraffin-embedded sections (4 μm) of the fixed livers of unchallenged and TM challenged animals (18h) were stained with an antibody that recognizes the cleaved form of caspase-3, and were visualized at 400x magnification to detect apoptotic cells. Representative staining is shown in (C), with caspase-3-positive cells indicated by arrowheads. Inset shows a magnified view of the area outlined in the white box. The percentage of stained cells in each microscopic field is shown in (D). Error bars represent means ± SEM (n=3 animals). (E) *Atf6α*-/- (n = 5) or wild-type and heterozygous control (n = 8) mice were injected with TM as above, and lethality was followed over 13 days. (F) Livers of mice injected with TM were visualized in situ.

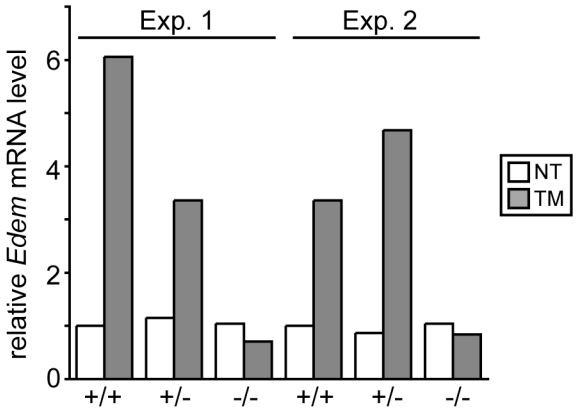

Figure 2-16. Lack of upregulation of *Edem1* in *Atf6*α-/- **mice.** The expression level of *Edem* mRNA was determined by real-time RT-PCR of livers from vehicle- or TM-injected animals (containing the neomycin cassette). Data were normalized against β-*actin* expression. The results of two independent experiments are shown.

References

1. Marciniak, SJ and Ron, D, (2006) Endoplasmic reticulum stress signaling in disease. Physiol Rev 86: 1133-49.

2. Wu, J and Kaufman, RJ, (2006) From acute ER stress to physiological roles of the Unfolded Protein Response. Cell Death Differ 13: 374-84.

3. Harding, HP, Zhang, Y, Bertolotti, A, Zeng, H and Ron, D, (2000) Perk is essential for translational regulation and cell survival during the unfolded protein response. Mol Cell 5: 897-904.

4. Harding, HP, Zhang, Y and Ron, D, (1999) Protein translation and folding are coupled by an endoplasmic-reticulum-resident kinase. Nature 397: 271-4.

5. Novoa, I, Zhang, Y, Zeng, H, Jungreis, R, Harding, HP and Ron, D, (2003) Stress-induced gene expression requires programmed recovery from translational repression. Embo J 22: 1180-7.

6. Hollien, J and Weissman, JS, (2006) Decay of endoplasmic reticulum-localized mRNAs during the unfolded protein response. Science 313: 104-7.

7. Kang, SW, Rane, NS, Kim, SJ, Garrison, JL, Taunton, J and Hegde, RS, (2006) Substrate-specific translocational attenuation during ER stress defines a pre-emptive quality control pathway. Cell 127: 999-1013.

8. Haze, K, Yoshida, H, Yanagi, H, Yura, T and Mori, K, (1999) Mammalian transcription factor ATF6 is synthesized as a transmembrane protein and activated by proteolysis in response to endoplasmic reticulum stress. Mol Biol Cell 10: 3787-99.

9. Hong, M, Luo, S, Baumeister, P, Huang, JM, Gogia, RK, Li, M et al., (2004) Underglycosylation of ATF6 as a novel sensing mechanism for activation of the unfolded protein response. J Biol Chem 279: 11354-63.

10. Nadanaka, S, Yoshida, H and Mori, K, (2006) Reduction of disulfide bridges in the lumenal domain of ATF6 in response to glucose starvation. Cell Struct Funct 31: 127-34.

11. Okada, T, Haze, K, Nadanaka, S, Yoshida, H, Seidah, NG, Hirano, Y et al., (2003) A serine protease inhibitor prevents endoplasmic reticulum stress-induced cleavage but not transport of the membrane-bound transcription factor ATF6. J Biol Chem 278: 31024-32.

12. Shen, J, Chen, X, Hendershot, L and Prywes, R, (2002) ER stress regulation of ATF6 localization by dissociation of BiP/GRP78 binding and unmasking of Golgi localization signals. Dev Cell 3: 99-111.

13. Wang, Y, Shen, J, Arenzana, N, Tirasophon, W, Kaufman, RJ and Prywes, R, (2000) Activation of ATF6 and an ATF6 DNA binding site by the endoplasmic reticulum stress response. J Biol Chem 275: 27013-20.

14. Ye, J, Rawson, RB, Komuro, R, Chen, X, Dave, UP, Prywes, R et al., (2000) ER stress induces cleavage of membrane-bound ATF6 by the same proteases that process SREBPs. Mol Cell 6: 1355-64.

15. Haze, K, Okada, T, Yoshida, H, Yanagi, H, Yura, T, Negishi, M et al., (2001) Identification of the G13 (cAMP-response-element-binding protein-related protein) gene product related to activating transcription factor 6 as a transcriptional activator of the mammalian unfolded protein response. Biochem J 355: 19-28.

16. Thuerauf, DJ, Morrison, L and Glembotski, CC, (2004) Opposing roles for ATF6alpha and ATF6beta in endoplasmic reticulum stress response gene induction. J Biol Chem 279: 21078-84.

17. Thuerauf, DJ, Marcinko, M, Belmont, PJ and Glembotski, CC, (2007) Effects of the Isoform-specific Characteristics of ATF6{alpha} and ATF6beta on Endoplasmic Reticulum Stress Response Gene Expression and Cell Viability. J Biol Chem 282: 22865-78.

18. Harding, HP, Novoa, I, Zhang, Y, Zeng, H, Wek, R, Schapira, M et al., (2000) Regulated translation initiation controls stress-induced gene expression in mammalian cells. Mol Cell 6: 1099-108.

19. Lu, PD, Harding, HP and Ron, D, (2004) Translation reinitiation at alternative open reading frames regulates gene expression in an integrated stress response. J Cell Biol 167: 27-33.

20. Scheuner, D, Song, B, McEwen, E, Liu, C, Laybutt, R, Gillespie, P et al., (2001) Translational control is required for the unfolded protein response and in vivo glucose homeostasis. Mol Cell 7: 1165-76.

21. Calfon, M, Zeng, H, Urano, F, Till, JH, Hubbard, SR, Harding, HP et al., (2002) IRE1 couples endoplasmic reticulum load to secretory capacity by processing the XBP-1 mRNA. Nature 415: 92-6.

22. Lee, K, Tirasophon, W, Shen, X, Michalak, M, Prywes, R, Okada, T et al., (2002) IRE1-mediated unconventional mRNA splicing and S2P-mediated ATF6 cleavage merge to regulate XBP1 in signaling the unfolded protein response. Genes Dev 16: 452-66.

23. Shen, X, Ellis, RE, Lee, K, Liu, CY, Yang, K, Solomon, A et al., (2001) Complementary signaling pathways regulate the unfolded protein response and are required for C. elegans development. Cell 107: 893-903.

24. Yoshida, H, Matsui, T, Yamamoto, A, Okada, T and Mori, K, (2001) XBP1 mRNA is induced by ATF6 and spliced by IRE1 in response to ER stress to produce a highly active transcription factor. Cell 107: 881-91.

25. Xu, C, Bailly-Maitre, B and Reed, JC, (2005) Endoplasmic reticulum stress: cell life and death decisions. J Clin Invest 115: 2656-64.

26. Rutkowski, DT, Arnold, SM, Miller, CN, Wu, J, Li, J, Gunnison, KM et al., (2006) Adaptation to ER stress is mediated by differential stabilities of pro-survival and pro-apoptotic mRNAs and proteins. PLoS Biol 4: e374.

27. Baumeister, P, Luo, S, Skarnes, WC, Sui, G, Seto, E, Shi, Y et al., (2005) Endoplasmic reticulum stress induction of the Grp78/BiP promoter: activating mechanisms mediated by YY1 and its interactive chromatin modifiers. Mol Cell Biol 25: 4529-40.

28. Okada, T, Yoshida, H, Akazawa, R, Negishi, M and Mori, K, (2002) Distinct roles of activating transcription factor 6 (ATF6) and double-stranded RNA-activated protein kinase-like endoplasmic reticulum kinase (PERK) in transcription during the mammalian unfolded protein response. Biochem J 366: 585-94.

29. Yoshida, H, Haze, K, Yanagi, H, Yura, T and Mori, K, (1998) Identification of the cis-acting endoplasmic reticulum stress response element responsible for transcriptional induction of mammalian glucose-regulated proteins. Involvement of basic leucine zipper transcription factors. J Biol Chem 273: 33741-9.

30. Harding, HP, Zhang, Y, Zeng, H, Novoa, I, Lu, PD, Calfon, M et al., (2003) An integrated stress response regulates amino acid metabolism and resistance to oxidative stress. Mol Cell 11: 619-33.

31. Lee, AH, Iwakoshi, NN and Glimcher, LH, (2003) XBP-1 regulates a subset of endoplasmic reticulum resident chaperone genes in the unfolded protein response. Mol Cell Biol 23: 7448-59.

32. Hendershot, LM, (2004) The ER function BiP is a master regulator of ER function. Mt Sinai J Med 71: 289-97.

33. Fawcett, TW, Martindale, JL, Guyton, KZ, Hai, T and Holbrook, NJ, (1999) Complexes containing activating transcription factor (ATF)/cAMP-responsive-element-binding protein (CREB) interact with the CCAAT/enhancer-binding protein (C/EBP)-ATF composite site to regulate Gadd153 expression during the stress response. Biochem J 339 (Pt 1): 135-41.

34. Ma, Y, Brewer, JW, Diehl, JA and Hendershot, LM, (2002) Two distinct stress signaling pathways converge upon the CHOP promoter during the mammalian unfolded protein response. J Mol Biol 318: 1351-65.

35. Yan, W, Frank, CL, Korth, MJ, Sopher, BL, Novoa, I, Ron, D et al., (2002) Control of PERK eIF2alpha kinase activity by the endoplasmic reticulum stress-induced molecular chaperone P58IPK. Proc Natl Acad Sci U S A 99: 15920-5.

36. Yoshida, H, Matsui, T, Hosokawa, N, Kaufman, RJ, Nagata, K and Mori, K, (2003) A time-dependent phase shift in the mammalian unfolded protein response. Dev Cell 4: 265-71.

37. Marciniak, SJ, Yun, CY, Oyadomari, S, Novoa, I, Zhang, Y, Jungreis, R et al., (2004) CHOP induces death by promoting protein synthesis and oxidation in the stressed endoplasmic reticulum. Genes Dev 18: 3066-77.

38. Li, M, Baumeister, P, Roy, B, Phan, T, Foti, D, Luo, S et al., (2000) ATF6 as a transcription activator of the endoplasmic reticulum stress element: thapsigargin stress-induced changes and synergistic interactions with NF-Y and YY1. Mol Cell Biol 20: 5096-106.

39. Yamamoto, K, Yoshida, H, Kokame, K, Kaufman, RJ and Mori, K, (2004) Differential contributions of ATF6 and XBP1 to the activation of endoplasmic reticulum stress-responsive cis-acting elements ERSE, UPRE and ERSE-II. J Biochem (Tokyo) 136: 343-50.

40. Gal-Yam, EN, Jeong, S, Tanay, A, Egger, G, Lee, AS and Jones, PA, (2006) Constitutive nucleosome depletion and ordered factor assembly at the GRP78 promoter revealed by single molecule footprinting. PLoS Genet 2: e160.

41. Sifers, RN, Brashears-Macatee, S, Kidd, VJ, Muensch, H and Woo, SL, (1988) A frameshift mutation results in a truncated alpha 1-antitrypsin that is retained within the rough endoplasmic reticulum. J Biol Chem 263: 7330-5.

42. Luo, S, Baumeister, P, Yang, S, Abcouwer, SF and Lee, AS, (2003) Induction of Grp78/BiP by translational block: activation of the Grp78 promoter by ATF4 through and upstream ATF/CRE site independent of the endoplasmic reticulum stress elements. J Biol Chem 278: 37375-85.

43. Hung, CC, Ichimura, T, Stevens, JL and Bonventre, JV, (2003) Protection of renal epithelial cells against oxidative injury by endoplasmic reticulum stress preconditioning is mediated by ERK1/2 activation. J Biol Chem 278: 29317-26.

44. Lu, PD, Jousse, C, Marciniak, SJ, Zhang, Y, Novoa, I, Scheuner, D et al., (2004) Cytoprotection by pre-emptive conditional phosphorylation of translation initiation factor 2. Embo J 23: 169-79.

45. Hetz, C, Bernasconi, P, Fisher, J, Lee, AH, Bassik, MC, Antonsson, B et al., (2006) Proapoptotic BAX and BAK modulate the unfolded protein response by a direct interaction with IRE1alpha. Science 312: 572-6.

46. Zinszner, H, Kuroda, M, Wang, X, Batchvarova, N, Lightfoot, RT, Remotti, H et al., (1998) CHOP is implicated in programmed cell death in response to impaired function of the endoplasmic reticulum. Genes Dev 12: 982-95.

47. Carrasco, DR, Sukhdeo, K, Protopopova, M, Sinha, R, Enos, M, Carrasco, DE et al., (2007) The differentiation and stress response factor XBP-1 drives multiple myeloma pathogenesis. Cancer Cell 11: 349-60.

48. Reimold, AM, Iwakoshi, NN, Manis, J, Vallabhajosyula, P, Szomolanyi-Tsuda, E, Gravallese, EM et al., (2001) Plasma cell differentiation requires the transcription factor XBP-1. Nature 412: 300-7.

49. Nagasawa, K, Higashi, T, Hosokawa, N, Kaufman, RJ and Nagata, K, (2007) Simultaneous induction of the four subunits of the TRAP complex by ER stress accelerates ER degradation. EMBO Rep 8: 483-9.

50. Hiraoka, M, Abe, A, Lu, Y, Yang, K, Han, X, Gross, RW et al., (2006) Lysosomal phospholipase A2 and phospholipidosis. Mol Cell Biol 26: 6139-48.

51. Schuster-Gossler, K, Lee, AW, Lerner, CP, Parker, HJ, Dyer, VW, Scott, VE et al., (2001) Use of coisogenic host blastocysts for efficient establishment of germline chimeras with C57BL/6J ES cell lines. Biotechniques 31: 1022-4, 1026.

52. Seong, E, Saunders, TL, Stewart, CL and Burmeister, M, (2004) To knockout in 129 or in C57BL/6: that is the question. Trends Genet 20: 59-62.

53. Gentleman, RC, Carey, VJ, Bates, DM, Bolstad, B, Dettling, M, Dudoit, S et al., (2004) Bioconductor: open software development for computational biology and bioinformatics. Genome Biol 5: R80.

54. Luo, S and Lee, AS, (2002) Requirement of the p38 mitogen-activated protein kinase signalling pathway for the induction of the 78 kDa glucose-regulated protein/immunoglobulin heavy-chain binding protein by azetidine stress: activating transcription factor 6 as a target for stress-induced phosphorylation. Biochem J 366: 787-95.

55. Rubinson, DA, Dillon, CP, Kwiatkowski, AV, Sievers, C, Yang, L, Kopinja, J et al., (2003) A lentivirus-based system to functionally silence genes in primary mammalian cells, stem cells and transgenic mice by RNA interference. Nat Genet 33: 401-6.

CHAPTER III

ENDOPLASMIC RETICULUM STRESS AND INFLAMMATION

Part I. UPR and the acute phase response

Abstract

CREBH was recently identified as an ER stress-induced basic leucine Zipper (bZIP) transcription factor that shares significant structural homology with ATF6α. Here we found that in response to bacterial lipopolysaccharide (LPS) or ER stressor tunicamycin (TM) challenge, the expression and secretion of acute phase response (APR) markers were significantly reduced in CREBH knockdown mice compared to control mice. Our preliminary data also demonstrated reduced serum levels of APR markers in TM-injected *Atf6α*-/- mice and defective hepatic induction of APR markers in LPS-injected conditional *Ire1α*-/- mice compared to control mice. These findings elucidate an intimate relationship between inflammatory responses and ER stress responses.

Introduction

ATF6α is activated by regulated intramembrane proteolysis (RIP) in response to ER stress to initiate the UPR [1-3]. ATF6α is a type II ER transmembrane protein that contains a basic leucine zipper (bZiP) domain in the cytosol and a stress-sensing domain in the ER lumen [1]. Under normal conditions, ATF6α is retained in the ER through interaction with the ER protein chaperone BiP/GRP78 [2]. Upon accumulation of unfolded or misfolded proteins in the ER lumen, ATF6α is released from BiP and transits to the

Golgi compartment where it is cleaved by the processing enzymes S1P and S2P. The cleaved ATF6α cytosolic domain traffics to the nucleus to activate transcription of UPR target genes.

Recently, researchers identified several new members of the membrane-bound transcription factor family that are structurally similar to ATF6α. These new members, including Luman, OASIS and CREBH, all possess a transcription activation domain, a bZiP domain in close proximity to a hydrophobic transmembrane domain, and a domain that resides in the ER lumen [4-7]. CREBH was identified as a hepatocyte-specific bZiP transcription factor belonging to the cyclic AMP response element binding protein transcription factor (CREB/ATF) family [4]. Recent reports suggested that CREBH requires proteolytic cleavage for its activation [4,6]. However, the stimuli that activate CREBH, the mechanism of CREBH cleavage, and the physiological role that CREBH provides in the liver are unknown.

The innate immune response is an ancient metazoan adaptation mechanism initiated by chemical structures presented by invading microorganisms or revealed by damage to the host. The systemic inflammatory component of innate immunity is called the acute phase response (APR) [8-10]. C-reactive protein (CRP) is the major component of the acute phase response in humans, whereas it is a minor one in the mouse. In contrast, serum amyloid P-component (SAP), the structural homolog pentraxin of CRP, is the major component of the acute phase response in the mouse, but is a minor one in humans [11-14]. In mice, both SAP and CRP are inducible by stimulation with inflammatory stimuli such as LPS and cytokines IL6 and/or IL1β [15]. Another acute phase protein (APP), serum amyloid A (SAA), has been identified in all vertebrates investigated to date and are

highly conserved. Its mRNA can increase by as much as 1000-fold during inflammation [16].

We have demonstrated that the expression levels of *Crp, Sap* and *Saa3* mRNAs are significantly reduced in embryonic livers of transgenic CREBH knockdown mice and CREBH plays an essential role in the activation of the acute phase response. We found that besides inflammatory stimuli such as LPS and cytokines IL6 and/or IL1β, the ER stress inducer tunicamycin (TM) can activate the APR *in vivo*. Our preliminary data also suggest that the activation of the APR is defective in both *Atf6*α-/- and conditional-*Ire1*α-/- mice.

These studies provide molecular links between intracellular stress and inflammation, and indicate that pharmacological intervention to prevent UPR activation may be beneficial to control inflammatory responses in disease states.

Results and Discussion

Generation of CREBH knockdown mice

CREBH is an ER-localized liver-specific basic leucine zipper (bZIP) transcription factor of the CREB/ATF family and shares significant homology with ATF6α (Figure 3-1A). Upon ER stress, membrane-anchored CREBH is cleaved by Golgi-resident site-1 and site-2 proteases to liberate an amino-terminal cytosolic fragment that transits to the nucleus. Instead of inducing the expression of UPR genes, cleaved CREBH activates a subset of acute phase response genes to initiate an inflammatory response. Furthermore, CREBH binds to a promoter element in specific acute phase responsive genes and induces transcription of the human CRP gene and the murine SAP gene upon ER stress in hepatocytes.

To explore the physiological function of CREBH, we silenced the *CREBH* gene in the mouse by using a lentivirus-based system that expresses CREBH-specific hairpin small interfering RNAs (siRNAs). CREBH-specific RNAi lentivirus was injected into single-cell mouse embryos to generate CREBH-knockdown mice. As a control, empty vector lentivirus was also injected into single-cell mouse embryos. The mice were screened by examining expression of CREBH and green fluorescence protein (GFP), a marker for expression from the lentiviral vector (Figure 3-1B). CREBH siRNA specifically targeted and degraded *CREBH* mRNA in the livers of the knockdown mice. Histopathological analysis of the CREBH knockdown embryos at E14.5 did not reveal any morphological or developmental defects (Figure 3-1C).

To identify potential target genes for CREBH action in the liver, we performed gene chip analysis of RNA samples from CREBH knockdown or control fetal livers at gestation stage E14.5. At this time in embryogenesis, the *CREBH* gene is highly expressed. Knockdown of the CREBH gene in the fetal liver reduced expression of genes involved in the APR and lipid metabolism (data not shown). Northern blot and quantitative real-time RT-PCR analyses confirmed that expression of mRNAs encoding CRP and its structural homologue pentraxin, SAP, were significantly reduced in the fetal livers of the CREBH knockdown mice compared to the RNAi control mice (Figure 3-2A). Additionally, the expression levels of mRNAs encoding SAA3 and apolipoprotein B-100 (ApoB) were reduced by 3-5 fold in the CREBH knockdown mice compared to that of the control mice. In contrast, mRNA levels of other major APR proteins including serum amyloid A 1 (SAA1), serum amyloid A2 (SAA2), fibrinogen and α1-acid

glycoprotein were similar in CREBH knockdown and control fetal livers (data not shown).

In mice, both SAP and CRP are inducible by stimulation with pro-inflammatory cytokines or bacterial LPS during the APR. The reduced mRNA levels of *Crp* and *Sap* in CREBH knockdown mice suggested that CREBH might be required to activate the APR. To test this hypothesis, we examined the response of CREBH knockdown mice to stimuli of inflammatory cytokines, LPS or TM. The basal serum levels of SAP and CRP in the CREBH knockdown mice were detectable, but lower than those in the control RNAi mice. At 24 hours after injection of LPS or IL6 plus IL1β, serum levels of SAP in the control RNAi mice were significantly increased, to a level of approximately 4.5- and 9-times that of the untreated control mice. In contrast, serum levels of SAP in the CREBH knockdown mice were only slightly increased after challenged with LPS or IL6 plus IL1β. Injection of TM increased serum levels of SAP in the control mice approximately 12-fold whereas TM injection increased serum SAP in the CREBH knockdown mice approximately 2-fold (Figure 3-2B). Furthermore, while injection of pro-inflammatory cytokines, LPS or TM increased serum levels of CRP approximately 2-fold in control RNAi mice, there was no such increase in the treated CREBH knockdown mice (Figure 3-2C). These results support the hypothesis that CREBH is required to potently activate transcription of the *SAP* and *CRP* genes in response to ER stress as well as pro-inflammatory cytokines *in vivo*.

Together, our studies delineate a molecular mechanism for activation of a novel ER-localized transcription factor CREBH that is essential for transcriptional induction of

innate immune response genes, and reveal an unprecedented link by which ER stress initiates an acute inflammatory response.

ATF6 alpha is essential to acute phase response markers secretion in response to an ER stress-induced inflammatory response

In Chapter II, we demonstrated that wild-type and heterozygous mutant mice can survive challenges with TM whereas most of *Atf6α-/-* mice succumbed to the same dose TM injection within a week (Figure 2-15). Studies with CREBH RNAi transgenic mice shown that TM can effectively induce the acute phase response *in vivo*. We therefore monitored the acute phase response markers in the TM-challenged wild-type, *Atf6α+/-* and *Atf6α-/-* mice. SAP, one of major murine APR markers, was significantly induced in the sera of the TM-challenged wild-type and heterozygous mice (4-6 folds induced at 24 hrs post-injection compared to the vehicle-injected control mice) whereas such induction was absent in the TM-injected *Atf6α-/-* mice (Figure 3-3B). At the same time, we detected significant amount of SAP protein in the liver samples of *Atf6α-/-* mice at 24, 48 and 72 hrs post TM-injection by western blot analysis. In contrast, the hepatic levels of SAP in both wild-type and heterozygous mutant *Atf6α* mice were marginally detectable only at 24hrs time point (Figure 3-3A).

When the animals were challenged with the inflammatory stimuli LPS, which leads to an even higher induction of SAP (around 10 times more compared to that of TM challenged wild-type mice), SAP was significantly induced to similar levels in both livers and sera of all the wild-type, *Atf6α+/-* and *Atf6α-/-* mice that were injected with LPS (Figure 3-4).

The serum levels of another APR marker, CRP, were induced approximately 2-folds in LPS or TM challenged wild-type and *Atf6α*+/- mice, whereas such increase was only observed in the LPS treated *Atf6α*-/- mice but not in the TM challenged *Atf6α*-/- mice (data not shown).

Further experiments are necessary to elucidate the molecular mechanism(s) for the preliminary observations in *Atf6α*-/- mice. We have demonstrated that efficiency of protein secretion is reduced in the presence of an exogenous stress in *Atf6α*-/- cells, (Figure 2-11). So it is tempting to speculate that while hepatocytes in *Atf6α*-/- mice are capable of upregulating *Sap* and *Crp* expression upon both TM and LPS challenges, the former severely disturbs ER homeostasis and in the absence of ATF6α, the processing and secretion of SAP are impaired. With less secretion of SAP into the blood, *Atf6α*-/- mice lost the defense from the acute phase response and the defects in the protective APR may partly result in the lethality of *Atf6α*-/- mice injected with the normally sublethal dose of TM.

IRE1α/XBP1 pathway activates the inflammatory response upon intracellular stress

Where ER stress activates both ATF6α and CREBH through regulated intramembrane proteolysis (RIP), ER stress induces IRE1α-dependent splicing of *Xbp1* mRNA to produce an active transcription factor. XBP1 is another ER stress-inducible bZIP transcription factor of CREB/ATF family. We determined whether IRE1α/XBP1 UPR subpathway is required for expression of acute phase proteins in the liver in response to inflammatory stimuli. Mice were engineered with temporally-controlled deletion or tissue-specific deletion of the IRE1α gene. A *loxP*-flanked IRE1α transgene was introduced into IRE1α knock-out mice [17] to rescue embryonic lethality associated

with homozygous deletion of the IRE1α gene. To generate temporally-controlled (*Ire1*α-/-:tg/+:Mx1-cre) or hepatocyte-specific (*Ire1*α-/-:tg/+:Alb-cre) IRE1α conditional knockout mice, the IRE1α transgene-rescued mice with homozygous deletion of the endogenous IRE1α gene were mated with transgenic mice expressing recombinase CRE under the control of the Mx1 promoter or the albumin promoter. We first injected *Ire1*α+/-:tg/+:Mx1-cre mice and *Ire1*α-/-:tg/+:Mx1-cre mice intraperitoneally with poly I-C to delete IRE1α transgene to produce animals with *Ire1*α+/- and *Ire1*α-/- genotypes, respectively. After 4 weeks of Poly I-C injection, southern blot analysis demonstrated ~82% of the transgene was deleted in the whole liver tissue of *Ire1*α+/-:tg/+:Mx1-cre mice or *Ire1*α-/-:tg/+:Mx1-cre mice. To test whether IRE1α is required for the liver inflammatory response, Poly I-C-injected *Ire1*α+/-:tg/+:Mx1-cre mice and *Ire1*α-/-:tg/+:Mx1-cre mice were challenged with LPS (3 μg/gram body weight) for 24 hours. Total RNAs were isolated from the livers at 24 hours post-injection, and subjected to quantitative real-time PCR analysis to determine levels of *Ire1α, Sap* and *Saa3* mRNAs. As shown in Figure 3-6, *Ire1α* mRNA levels in IRE1α-deleted animals were dramatically reduced compared to those of *Ire1*α+/-:tg/+:Mx1-cre mice. Prior to LPS injection**,** the basal levels of *Sap* and *Saa3* mRNAs in the liver were very low. At 24 hours after LPS challenge, the levels of *Sap* and *Saa3* mRNAs in the control mice were dramatically increased, whereas the levels of *Sap* and *Saa3* mRNA in the IRE1α-deleted mice were only marginally increased after LPS challenge (Figure 3-5). This suggests that IRE1α is required for transcriptional induction of the major acute phase proteins SAP and SAA3 in the liver in response to inflammatory stimuli. Following these results, we challenged *Ire1*α+/-:tg/+:Alb-cre and *Ire1*α-/-:tg/+:Alb-cre mice with the same

inflammatory stimuli by intraperitoneal injection of LPS (3μg/gram body weight for 24 hours). Similar to the temporally-controlled IRE1α-deleted animals, the expression levels of the *Sap* and *Saa3* mRNAs in the animals with liver-specific deletion of the IRE1α gene were significantly reduced in response to LPS challenge (data not shown), thus further confirming the requirement of the major ER stress transducer IRE1α for the acute inflammatory response in the liver.

Our observations from conditional *Ire1α-/-* mice support the hypothesis that ER homeostasis, as well as the protein folding status in the ER, may signal an inflammatory response. Our findings suggest that, under many physiological and pathological conditions, ER stress-triggered activation of CREBH and IRE1α significantly contribute to the acute inflammatory response.

Experimental Procedures:

Generation of CREBH knockdown mice

Generation of RNA interference transgenic mice was performed as described previously [18]. Briefly, vectors that express hairpin siRNAs under the control of the mouse U6 promoter were constructed by inserting pairs of annealed DNA oligonucleotides into the LentiLox3.7 vector (kindly provided by Dr. Luk Van Parijs) between the HpaI and XhoI restriction sites. The sequence used for CREBH RNAi is: TCGAGAAAAAAGACATAGCGGCTGGAAAGATCTCTTGAATCTTTCCAGCCGC TATGTCA. The clones and packaging vectors including VSVG, RSV-REV, pMDL g/p RRE were co-transfected into 293T cells. The supernatants containing virus were concentrated by ultracentrifugation. A small volume of high-titer RNAi lentivirus (approximately $5x10^6$ IU ml^{-1}) was transferred into the perivitelline space of single-cell

C57BL/6J mouse embryos through microinjection. The injected single-cell embryos were implanted into pseudopregnant recipient mice for generating CREBH knockdown embryos and pups.

Generation of transgenic rescued *Ire1α*-/- mice

To generate transgenic mice that express wild type IRE1α in all tissues, we used the pCX-EGFP vector (gift of Dr Masaru Okabe, Osaka University) that contains the cytomegalovirus enhancer, chicken β-actin promoter, β-actin intron, enhanced green fluorescence protein (*EGFP*), and followed by bovine globin polyadenylation signal [19]. The 2.7 kb mouse *Ire1α* cDNA from pcDNA3.1-mIRE1α [20] was inserted into between Sal I and Xma I site of pDNR-CMV plasmid (CLONTECH) to generate pDNR-CMV-LoxP-mIRE1α which has one *loxP* site in front of mouse *Ire1α* cDNA. To generate pCMV-LoxP-mIRE1α-LoxP which is surrounded by two *loxP* sites, the Not I fragment from pDNR-CMV was inserted into the site of Xma I of pDNR-CMV-LoxP-mIRE1α. To generate pCMV-LoxP-mIRE1α-LoxP-EGFP, the Not I and Sal I fragment of pCMV-LoxP-mIRE1α-LoxP was then inserted into pEGFP-N1 to get EGFP sequence behind of *Ire1α* cDNA. The 3.9 kb (LoxP-mIRE1α-LoxP-EGFP) fragment digested with Not I from pCMV-LoxP-mIRE1α-LoxP-EGFP was inserted into pCX-EGFP digested with EcoR I to generate pCX-LoxP-mIRE1α-LoxP-EGFP. The 6.5 kb fragment of the (LoxP-mIRE1α-LoxP-EGFP) transgenic construct was obtained by digestion of pCX-LoxP-mIRE1α-LoxP-EGFP plasmid with Ssp I and Sfi I restriction enzymes, followed by gel purification. The transgenic construct was microinjected into C57BL/6xSJL fertilized embryos and implanted into pseudopregnant females.

Transgenic founder mice were identified by a PCR based genotyping of tail DNAs with the following three different primer sets: For Enhancer-promoter primers (~370 bp fragments), Forward: cgacattgattattgactag, Reverse: gtaatagcgatgactaatac; For GFP primers (~200 bp fragment), Forward: tatatcatggccgacaagca, Reverse: gaactccagcaggaccatgt; For mIRE1α-EGFP primers (~600 bp fragment), Forward: gatggactggcgggagaacatc, Reverse: gcggacttgaagaagtcgtg. From 15 PCR positive-transgenic founders, one transgenic founder (#402) was chosen. The transgene was confirmed by Southern blot analysis. The expressed *LoxP-mIRE1α-LoxP-EGFP* mRNAs were confirmed by Northern blot analysis in most tissues.

The IRE1α knockout (*Ire1*α-/-:Tg/+) mice expressing the transgenic *LoxP-IRE1α-LoxP-EGFP* mRNA were generated by crossing the transgenic *Ire1*α+/+:Tg/+ mice strain into heterozygous *Ire1*α+/- mice. Presence of the *LoxP-IRE1α-LoxP-EGFP* transgene was determined by PCR methods described above. Presence of the *Ire1α* mutant allele was identified by a PCR based genotyping with the following two different primer sets: For NEO cassette primers (~500 bp fragments), Forward: aggatctcctgtcatctcaccttgctcctg, Reverse: aagaactcgtcaagaaggcgatagaaggcg; For Exon14/15 primers (~850 bp fragment from wild type allele or ~200 bp fragment from transgene). After the *Ire1*α-/-:Tg/+ mice were generated, the strain was maintained by interbreeding of *Ire1*α-/-:Tg/+ mice.

To delete the transgene in hepatocytes, Albumin-*Cre* transgenic mice were breed with the transgenic *Ire1*α-/-:Tg/+ mice. The Alb-*Cre* transgene led to a hepatocyte-specific deletion, starting from late gestation and leading to nearly complete deletion in adult mice (*Ire1α-/-*:tg/+:Alb-cre).

To achieve temporally-controlled deletion of the IRE1α in the transgenic *Ire1*α-/-:Tg/+ mice, Mx1-*Cre* transgenic mice were breed with the transgenic *Ire1*α-/-:Tg/+ mice. Then we injected *Ire1*α+/-:tg/+:Mx1-cre and *Ire1*α-/-:tg/+:Mx1-cre mice intraperitoneally with poly I-C (300μg/mouse) every 48 hrs for total 4 times to delete IRE1α transgene to produce animals with IRE1α+/- and IRE1α-/- genotypes, respectively. The deletion is nearly complete 4 weeks after Poly I-C injection.

Administration of proinflammatory cytokines, LPS, and TM and measurement of serum CRP and SAP in mice

Proinflammatory cytokines recombinant murine IL6 (BD Pharmingen), recombinant murine IL1β (R&D System, Mineapolis, MN) and bacterial LPS (Sigma, St. Louis, MO) were re-suspended in sterile pyrogen-free 0.9% NaCl (Abbott Laboratories, North Chicago, IL). Mice at age of 3-month were given a single intraperitoneal injection of IL6 (25ng/gram body weight) plus IL1β (25ng/gram body weight) or LPS (3mg/kg body weight). Mice were injected intraperitoneally with TM (2mg/kg body weight for CREBH knockdown and control RNAi mice and 1mg/kg body weight for wild-type, heterozygous and homozygous *Atf6α* mice) in 150mM dextrose solution. Sera from blood samples were collected from the mice by cardiac puncture at indicated times after injection, using BD Microtainer with serum separator™ (BD, Franklin Lakes, NJ, USA). For CREBH knockdown and control RNAi mice, serum levels of murine CRP were determined using a murine CRP ELISA kit (ALPCO Diagnostics, Windham, NH, USA). Serum levels of murine SAP were determined by ELISA analysis using sheep anti-Mouse SAP as the capture antibody (Alpha Diagnostic Intl., San Antonio, Texas), and murine SAP reference serum was purchased from the same company. For wild-type,

heterozygous and homozygous mutant *Atf6α* mice, serum levels of murine CRP and SAP were determined using murine CRP and SAP ELISA kits (Immunology Consultants Laboratory, Inc. Newberg, OR, USA).

Tissue preparation and analysis

Livers were isolated from challenged mice at indicated times. Briefly, tissue was homogenized using an electronic homogenizer in RIPA buffer containing protease inhibitors, and centrifuged twice at 15,000rpm for 10 minutes in a microfuge at 4°C.

Histological analysis

CREBH knockdown and control RNAi embryos were fixed in 4% paraformalin for embedding in paraffin. Sections of 4μm were cut and mounted on slides. Sections were stained by conventional hematoxylin and eosin staining for light microscopic observation.

Western Blot Analysis

Sera or liver RIPA lysates were diluted into 1%SDS, 0.1M Tris pH8.8 prior to addition of loading buffer and electrophoresis. Antibodies were supplied by BD Biosciences (BiP, used at 1/5,000; San Diego, California, United States), Santa Cruz Biotechnology (tubulin, used at 1/5000; Santa Cruz, California, United States), R&D system (Rat-anti-mouse SAP monoclonal antibody, Cat#: MAB2558, Minneapolis, MN) and Stressgen (CNX, used at 1/20,000).

Northern Blot Analysis and Quantitative Real-time RT-PCR

RNA was isolated using TRIzol RNA reagent (Invitrogen) according to the manufacturer's protocols. Northern blot analysis was performed according to standard procedures [21]. ^{32}P-labeled probes were prepared using a random prime labeling system

(Amersham Pharmacia, Piscataway, NJ, USA). A 210 bps murine CREBH cDNA fragment, a 250 bps murine CRP cDNA fragment and a 260 bps murine SAP cDNA fragment were amplified from murine total RNA by a reverse transcription-PCR system (Roche Applied Science), respectively, and were used as probes for Northern blot analysis. Total RNA (15μg) per sample purified from tissues was used for Northern blot analysis. Quantitative real-time RT-PCR was performed as previously described [22]. Additional real-time primer sequences were as follows: *Ire1*α: catgctcaaggacatggcta and gctcaggggtaagtgatga; *Sap*: tgtctgggattgagatcttacaaca and ctgccgccttgacctcttac; *saa3*: cgggacatggagcagagg and ttgccactccggccc.

Part II. Lipopolysaccharide+Galactosamine (LPS+GalN) induced acute liver injury requires phosphorylation of the alpha subunit of eukaryotic translation initiation factor 2

Abstract

The PERK/eIF2α pathway couples protein synthesis with ER protein folding capacity. Mice with a hepatocyte-specific homozygous mutation at the PERK-phosphorylation site in eIF2α(Ser51Ala) exhibited significantly reduced liver injury upon LPS + Galactosamine (LPS+GalN) challenge compared to control mice. This *in vivo* protection was correlated with the defective upregulation of CHOP expression upon LPS+GalN challenges. These findings suggest that pharmacological modulation of eIF2α phosphorylation may provide therapeutic benefit during fulminate hepatitis or hemorrhagic shock.

Introduction

The liver plays an important physiological role in detoxification, in particular, hepatocytes are involved in the clearance of endotoxin [23]. In experimental shock models, various agents can lead to hepatocyte damage and liver failure. Lipopolysaccharide (LPS), present in the cell wall of gram-negative bacteria, can induce endotoxemia and cause multi-organ failure including severe hepatic damage, which is characterized by hepatocyte apoptosis and followed by massive hepatic necrosis and subsequent liver failure [24]. LPS interacts with toll-like receptor 4 (TLR4) on macrophages, and promotes secretion of pro-inflammatory cytokines and chemokines [25,26]. Among these cytokines and chemokines, TNFα does not induce liver injury in normal hepatocytes *in vivo* because of the strong activation of cytoprotective pathways such as NF-κB [27]. However,

hepatic TNFα toxicity is induced when hepatic gene transcription is blocked by coadministration of galactosamine (GalN), which mimics fulminate hepatitis in human [28,29].

It has been previously reported that phosphorylation at Ser 51 on the α-subunit of eukaryotic translation initiation factor 2 (eIF2α) may play a pro-apoptotic role in certain physiological and pathological conditions [30-33], although the detailed mechanisms for these observations have not been elucidated. In higher eukaryotes, eIF2 is required to deliver $_{met}tRNA^{i}$ to the 40 S ribosomal subunit [34]. Phosphorylation of eIF2α at Ser51 inhibits the guanine nucleotide exchange factor eIF2B to recycle the eIF2 complex to its active GTP-bound form. The formation of the ternary translation initiation complex eIF2-GTP-$tRNA^{Met}$ is required for AUG initiation codon recognition and joining the 60S ribosomal subunit that occurs during initiation phase of polypeptide chain synthesis. Therefore, phosphorylation of eIF2αreduces the efficiency of AUG initiation codon recognition and attenuates translation initiation. However, reduced AUG initiation codon recognition can increase the initiation efficiency at selective AUG codons, thereby altering translation initiation for specific mRNAs. ATF4 is the best characterized example of an mRNA for which translation requires eIF2α phosphorylation. ATF4 is a basic leucine Zipper (bZIP) transcription factor that can form homodimers or heterdimers with other bZIP transcription factors. Array studies in *Atf4*-/- mice demonstrated that ATF4 most likely regulates expression of genes that encode proteins responding to cellular stress in general.

Recent studies on the unfolded protein response (UPR) have presented a new perspective on the physiological role of eIF2α phosphorylation. In response to the

accumulation of unfolded proteins in the ER, the rate of general translation initiation is attenuated, the expression of ER resident protein chaperones and protein foldases is induced, the ER compartment proliferates, and ER-associated degradation (ERAD) is activated to eliminate the irreparably misfolded proteins [35]. When the pro-survival efforts are exhausted, ER-stress-related apoptosis commences. Among all these cellular responses, eIF2α phosphorylation not only directly functions as an emergency brake on translation initiation, it also activates C/EBP homologous protein (CHOP)/growth arrest and DNA damage-inducible gene 153 (GADD153) through upregulation of ATF4. CHOP is a member of the C/EBP transcription factor family, and its expression correlates with ER-stress-mediated apoptosis [22]. More recent reports suggest that CHOP may repress anti-apoptotic BCL2 expression leading to the oxidative stress induced cell death [36] and CHOP-/- mice are protected from LPS-induced lung inflammation [37].

Homozygous eIF2α S51A knockin mutant MEFs that are defective in eIF2α phosphorylation were protected from TNFα-induced apoptosis *in vitro* [33]. Homozygous eIF2α mutant mice die neonatally [38]. In this study we investigated the physiological role the phosphorylation of eIF2α *in vivo.* The lethality of the eIF2α Ser51Ala homozygous knock-in mouse was rescued by expression of a conditional wild-type eIF2α transgene that can be deleted by Cre recombinase expression. Deletion of the transgenic eIF2α cDNA by albumin promoter-driven Cre expression creates hepatocyte-specific homozygous Ser51Ala mutation (eIF2α$^{A/A}$:tg/+:Alb-cre). eIF2α$^{A/A}$:tg/+:Alb-cre mice displayed significantly reduced liver injury upon LPS+GalN challenge compared to control mice. This protection correlated with the defective upregulation of CHOP expression in the LPS+GalN challenged eIF2α$^{A/A}$:tg/+:Alb-cre mice. Our findings

suggest that pharmacological inhibition of eIF2α phosphorylation may provide therapeutic benefit during fulminate hepatitis or hemorrhagic shock.

Results and Discussion

Generation of hepatocyte-specific eIF2α Ser51Ala knock-in mice

A *loxP* flanked eIF2α wild-type cDNA transgene was introduced into eIF2α Ser51Ala knockin mice (Figure 3-6A and Back and Kaufman, et. al. unpublished data). The wild-type cDNA transgene rescued the lethality and eIF2$\alpha^{A/A}$:tg/+ mice were born in the expected genotypic ratios and show no obvious developmental defects. eIF2$\alpha^{A/A}$:tg/+ mice were crossed into Alb-*cre* transgenic mice expressing Cre recombinase under the hepatocyte-specific albumin promoter control [39] to generate eIF2$\alpha^{A/A}$:tg/+:Alb-cre mice. Cre-mediated deletion was confirmed by the expression of the deletion-reporter GFP in the transgene vector, (Figure 3-6 B and C) and deletion efficiency was assessed by Southern blotting of genomic DNA from the liver and primary hepatocytes (Figure 3-6D). In livers from neonates, the efficiency of albumin-cre mediated recombination was approximately 50% [39], but increased to more than 80% in hepatocytes isolated from mice at 4 months of age (Fig 3-6D and E). This is consistent with previously reports using this *cre*-strain from other groups [40,41]. Western blot analysis of the whole liver lysates further confirmed that the phosphorylation of eIF2α at Ser51 is effectively disrupted by 3 months in this strain (Figure 3-6F). eIF2$\alpha^{A/A}$:tg/+:Alb-cre mice were born at Mendelian frequencies and exhibited no developmental abnormalities or morbidity. This observation is consistent with previous reports that heterozygous eIF2$\alpha^{S/A}$ mice showed no apparent defects [38].

Disruption of eIF2α phosphorylation ameliorates acute liver injury induced by LPS+GalN challenge *in vivo*

It has been reported that when cells were treated with LPS or its principal mediator *in vivo*, TNFα, eIF2α phosphorylation can be induced in cells, such as macrophages, fibroblasts, Jurkat T cells, promonocytic U937 cells and fibrosarcoma L929 cells [32,33,42,43]. To study these effects *in vivo*, we intraperitoneally injected LPS to GalN-sensitized control (eIF2α$^{S/A}$:tg/+:Alb-cre and eIF2α$^{A/A}$:tg/+) and eIF2α$^{A/A}$:tg/+:Alb-cre mice. Previous reports shown that co-administration of GalN blocked transcription in the liver and precluded the protection from anti-apoptotic NF-κB target genes. In the livers of LPS+GalN-challenged control mice, the phosphorylation of eIF2α at Ser 51 in the whole liver was significantly induced at 5.5 hrs post injection compared to PBS-injected mice, whereas in livers isolated from LPS+GalN-challenged eIF2α$^{A/A}$:tg/+:Alb-cre mice, phosphorylation of eIF2α was barely detectable. The low level detection of eIF2α phosphorylation could be due to other cell types present in the liver tissue (Figure 3-7).

It was previously demonstrated that homozygous eIF2α mutant MEFs are resistant to the apoptotic effects of TNFα *in vitro* [33]. We further analyzed tissue injury in LPS+GalN-challenged control (eIF2α$^{S/A}$:tg/+:Alb-cre and eIF2α$^{A/A}$:tg/+) and eIF2α$^{A/A}$:tg/+:Alb-cre mice. The livers of LPS+GalN-challenged control mice displayed extensive apoptosis and hemorrhagic necrosis at 5.5 hrs (figure 3-8A, C). In contrast, concomitant with the absence of the eIF2α phosphorylation, less tissue injury was observed in the livers from the eIF2α$^{A/A}$:tg/+:Alb-cre mice challenged with LPS+GalN. Histological analysis of liver sections from LPS+GalN-challenged eIF2α$^{A/A}$:tg/+:Alb-cre

mice demonstrated less hepatocyte apoptosis and hemorrhagic necrosis compared to that observed in control mice (figure 3-8A-C). As a marker for liver damage, we analyzed serum levels of Alanine aminotransferase (ALT). Serum ALT levels in the LPS+GalN-challenged eIF2$\alpha^{A/A}$:tg/+:Alb-cre mice were lower than that of LPS+GalN-challenged eIF2$\alpha^{S/A}$:tg/+:Alb-cre and eIF2$\alpha^{A/A}$:tg/+ mice (Figure 3-8D), further confirming that the absence eIF2α phosphorylation in hepatocytes ameliorates acute liver injury induced by LPS+GalN-challenge *in vivo*. We also explored Caspase 3 cleavage, a marker of apoptosis, by western blot analysis. There was detectable caspase 3 cleavage in the livers of eIF2$\alpha^{A/A}$:tg/+:Alb-cre mice challenged with LPS+GalN, although less than that observed in the control mice (Figure 3-8E). This observation is consistent with the histological analysis where hepatic apoptosis is detectable but to a lesser extent in the eIF2$\alpha^{A/A}$:tg/+:Alb-cre mice compared to the challenged control mice.

CHOP upregulation is defective in the LPS+GalN-challenged eIF2$\alpha^{A/A}$:tg/+:Alb-cre mice

Upon eIF2α phosphorylation increased ATF4 translation leads to transcriptional activation of *Chop*. Increased CHOP expression correlates with apoptosis, at least in the context of UPR [22]. We hypothesize that the protective phenotype we observed in the LPS+GalN-challenged eIF2$\alpha^{A/A}$:tg/+:Alb-cre mice may be caused by defects in upregulation of CHOP expression in the absence of eIF2α phosphorylation. Western blot analysis demonstrated that the CHOP protein level was very low in vehicle injected mice (undetectable by western blot) but significantly upregulated in the LPS+GalN-challenged control mice (eIF2$\alpha^{S/A}$:tg/+:Alb-cre and eIF2$\alpha^{A/A}$:tg/+). In contrast, CHOP upregulation was much reduced or absent in livers of LPS+GalN-injected eIF2$\alpha^{A/A}$:tg/+:Alb-cre mice

(Figure 3-9A). Analysis by real-time RT-PCR demonstrated that *Chop* mRNA was upregulated when the control mice were challenged by LPS alone. On the contrary, the expression of *Chop* mRNA was not induced in the LPS challenged eIF2$\alpha^{A/A}$:tg/+:Alb-cre liver. Since GalN inhibits transcription in hepatocytes by UTP depletion, the expression levels of *Chop* mRNA were fairly low at 5.5 hrs post LPS+GalN injection in both control and eIF2$\alpha^{A/A}$:tg/+:Alb-cre mice (Figure 3-9B). The upregulation of CHOP protein level in the LPS+GalN challenged control mice could be due to rapid induction of *Chop* mRNA that occurred prior to GalN-induced transcription inhibition.

Perspectives and future directions

Previous reports suggested that PKR-mediated eIF2α phosphorylation and general translational inhibition can activate apoptosis in response to different stimuli [32,33,42]. We therefore tested the relationship between general translational inhibition and the protective phenotype in the hepatocytes of the eIF2$\alpha^{A/A}$:tg/+:Alb-cre mice. When general translation was blocked by cycloheximide (CHX) pretreatment, the control (eIF2$\alpha^{S/A}$:tg/+:Alb-cre and eIF2$\alpha^{A/A}$:tg/+) and eIF2$\alpha^{A/A}$:tg/+:Alb-cre mice challenged with LPS+GalN showed similar levels of ALT (data not shown). These data suggest that the protective effect of the Ser51Ala mutation upon LPS+GalN induced liver injury is mediated, at least partly, through translational inhibition. Further analysis is required to elucidate how general translation inhibition mediates the LPS+GalN-induced liver injury.

The liver injury induced by LPS+GalN depends on the cross talk between macrophages and hepatocytes (Figure 3-10). In the eIF2$\alpha^{A/A}$:tg/+:Alb-cre mice, we observed that serum levels of TNFα and IL-6 were comparable to that of the control mice (data not shown), which is expected since the eIF2α transgene expression is not deleted

in macrophages. We also observed similar level of mRNA expression of TNFα, IL-6 and IL-1β in the whole liver tissue (data not shown). We observed similar level of JNK activation in both genotypes upon treatment (data not shown). These data suggest that protective phenotype in eIF2α$^{A/A}$:tg/+:Alb-cre mice is achieved at the hepatocytes level.

Our data here demonstrated that general translation inhibition and upregulation of pro-apoptotic marker CHOP through eIF2α phosphorylation plays an important role in hepatic apoptosis induced by LPS+GalN *in vivo* and suggested that regulation of eIF2α phosphorylation could provide an attractive target for therapeutic intervention.

Experimental Procedures

Generation of hepatocyte-specific eIF2α Ser51Ala knock-in mice

To generate conditional transgenic rescued eIF2α mice, a vector was constructed with the sequence of *eIF2α* cDNA flanked by *loxP* sites, for *in vivo* specific-promoter-*Cre* recombinase-mediated deletion. The 4.4 kb transgenic fragment of the (LoxP-meIF2α-LoxP-EGFP) also contains EGFP as a deletion reporter. The transgenic construct was microinjected into C57BL/6xSJL fertilized embryos and implanted into pseudopregnant females. From 21 PCR positive-transgenic founder mice, one transgenic founder mouse (#137) was chosen. Southern blot analysis confirmed this founder mouse has ~ 1 copy of transgene construct and northern blot analysis confirmed the expression of the transgenic LoxP-meIF2α–LoxP-EGFP mRNA in most tissues. The transgene was introduced into homozygous eIF2α S51A mutation background by crossing the transgenic mice strain with heterozygous eIF2α-S51A mice.

To delete the transgene in hepatocytes, Albumin-*Cre* transgenic mice were breed with the transgenic homozygous eIF2α S51A mice (eIF2α$^{A/A}$:tg/+). The Alb-*Cre*

transgene led to a hepatocyte-specific deletion, starting from late gestation and leading to nearly complete deletion in adult mice (eIF2$\alpha^{A/A}$:tg/+:Alb-cre).

Liver injury models

Mice were challenged by intraperitoneally injection with LPS (*Escherichia coli O55:B5*, Sigma-Aldrich) alone (4.5 μg/g body weight) or co-injection with LPS (100 ng/g body weight) and GalN (700 μg/g body weight) or co-injection with LPS (100 ng/g body weight), GalN (700 μg/g body weight) and CHX (Sigma-Aldrich) (40μg/g body weight). Mice were sacrificed, blood was collected by cardiac puncture, and livers were surgically removed. Serum was separated using BD Microtainer with serum separator™ (BD, Franklin Lakes, NJ, USA).

Isolation of hepatocytes

Primary mouse hepatocytes were isolated by collagenase perfusion. Mouse liver was perfused retrograde with Krebs Ringer buffer followed by perfusion of the liver with Liberase Blendzyme 3 solution (Roche). Isolated hepatocytes were washed intensely with Dulbecco's Modified Eagle Medium (Invitrogen). After determination of viability by trypan blue staining (>95%), 8×10^5 cells were plated collagen-coated dishes in M199 media (Invitrogen) with 10% heat inactivated FBS and 1% penicillin G/streptomycin at 37°C in a 5% CO2 incubator. The medium was freshed after over night incubation.

Histology and immnunohistochemistry

Liver tissues from adult mice were fixed in 10% buffered formalin solution (Sigma) for over 12 hrs at 4 °C, dehydrated, embedded in paraffin, and sectioned at 4 μm thickness. To detect Enhanced green fluorescence protein (EGFP), mouse anti-EGFP (1/500 dilution, Clontech) was used and followed by FITC conjugated goat anti-mouse

antibody (1/500 dilution, Jackson ImmunoResearch Laboratories, Inc.). The images were captured with a cooled charge-coupled device camera and a Zeiss LSM 510 confocal microscope (Jena, Germany). For light microscopic observation, sections were stained by conventional hematoxylin and eosin staining. TUNEL staining was performed using ApopTag® Peroxidase In Situ Apoptosis Detection Kit (CHEMICON), according to manufacturer's instructions. The images were captured with an Olympus BX51 microscope. The intrinsic EGFP expression from dissected liver was analyzed using a Leica MZFLIII stereo-dissecting microscope (Leica Corp., Deerfield, IL). All data were processed with Adobe photoshop software (Mountain View,Calif.).

Southern blot analysis

Southern blot analysis were followed as previously described [17,44]. ^{32}P-labeled probes were prepared using a random prime labeling system (Amersham Pharmacia). For Southern blot analysis, a 1 kb Bgl II fragment containing 0.8 kb PCR product containing the EGFP cDNA from pCX-LoxP-eIF2α-LoxP-EGFP vector (for Figure 3-6) was used. The PCR was done with Forward primer: 5'-GTCGACCGGTCGCCACCA-3' and Reverse primer: 5'-AGATCTCAGTGGTATTTG-3'.

RNA analysis

RNA was isolated using TRIzol RNA reagent (Invitrogen) according to the manufacturers' protocols. Real-time RT-PCR analysis, including primer sequences and applicable control/piloting experiments, has been described [22].

Tissue preparation and analysis

Liver isolated from challenged or control mice, was homogenized using an electronic homogenizer in RIPA buffer containing protease inhibitors, and centrifuged

twice at 15,000 rpm for 10 minutes in a microfuge at 4°C. Samples were diluted into 1% SDS, 0.1 M Tris pH 8.8 prior to addition of loading buffer and electrophoresis. Antibody sources have been previously described [22].

Alanine aminotranferase (ALT) assay

Serum ALT was measured at the U-M Animal Diagnostic Lab by the IDEXX VetTest Chemistry Analyzer from IDEXX Laboratories (www.idexx.com).

Statistical analysis

Data are expressed as mean±SD, unless otherwise indicted.

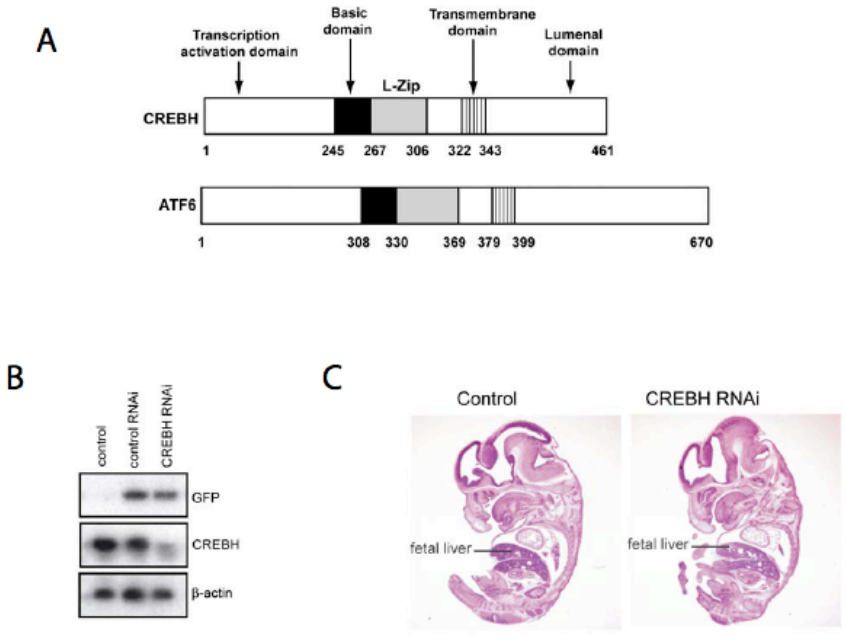

Figure 3-1. Generation of CREBH knockdown mice. (A) Structural comparison of CREBH and ATF6. The domains are indicated by residue numbers of amino acids. (B) Identification of CREBH knockdown mice. Total RNAs were isolated from the livers of the CREBH RNAi or the control RNAi mice, and subjected to Northern blot analysis for detecting levels of *GFP* mRNA and *CREBH* mRNA, respectively. (C) Morphology of CREBH knockdown embryos at gestation stage E14.5. The paraffin-embedded embryo sections were stained with hematoxylin and eosin. Magnification: 20 X.

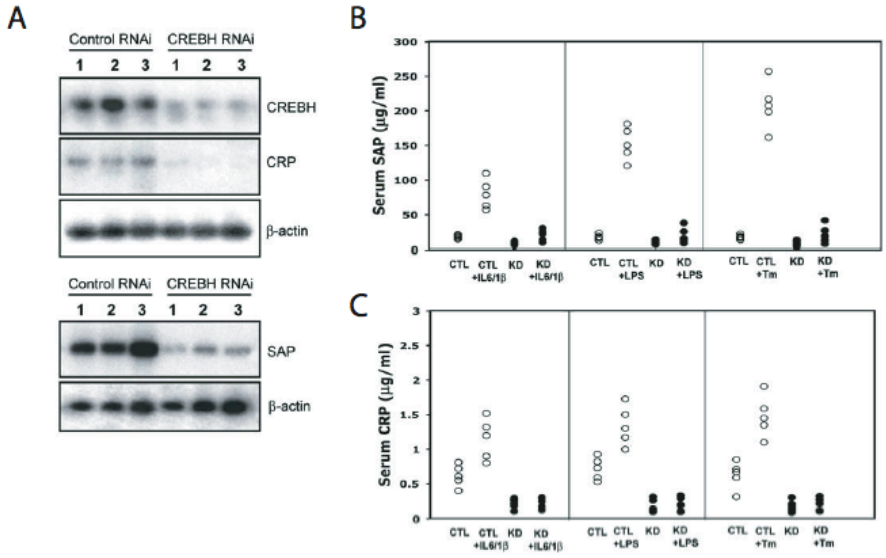

Figure 3-2. CREBH is required to up-regulate expression of the CRP and SAP genes. (A) Northern blot analysis of levels of *CREBH*, *CRP* and *SAP* mRNA in the livers of the CREBH knockdown or the control mice. (B-C) SAP and CRP induction requires CREBH. CREBH knockdown and control RNAi mice at 3-months of age were challenged with IL6 (25 ng/gram body weight) plus IL1β (25 ng/gram body weight), LPS (3 μg/gram body weight) or TM (2 mg/kg body weight). Serum levels of SAP and CRP in the mice were determined before injection and at 24 hours after injection. Data points are serum levels of SAP or CRP for individuals, $n = 5$ CREBH knockdown or 5 control RNAi mice per injection. The differences in CREBH knockdown and control mice are statistically significant ($P < 0.001$). CTL, control RNAi mice; KD, CREBH knockdown mice.

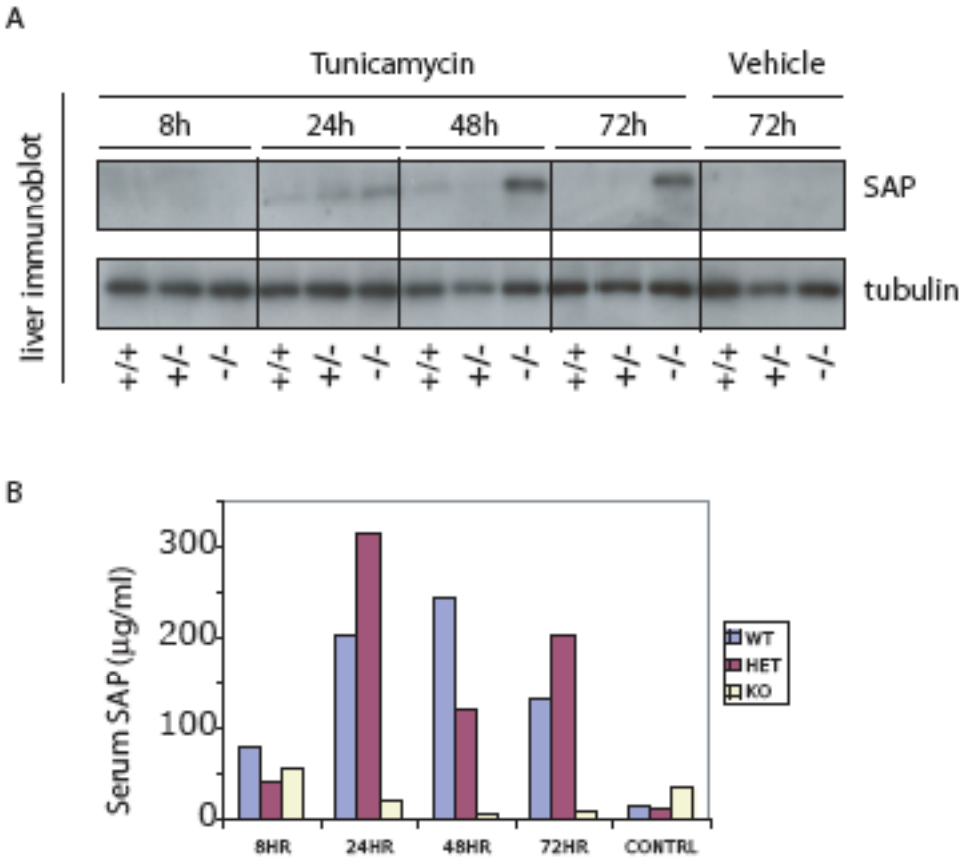

Figure 3-3. Attenuated secretion of SAP in TM challenged *Atf6α-/-* mice. (A) Wild-type and *Atf6α* heterozygous and homozygous mutant mice were injected intraperitoneally with TM (1 mg/kg body weight) or vehicle. Protein lysates from livers isolated at 8, 24, 48 or 72 hours after injection, were probed by immunoblot as indicated. (B) Serum levels of SAP were determined by ELISA. (One animal per time point)

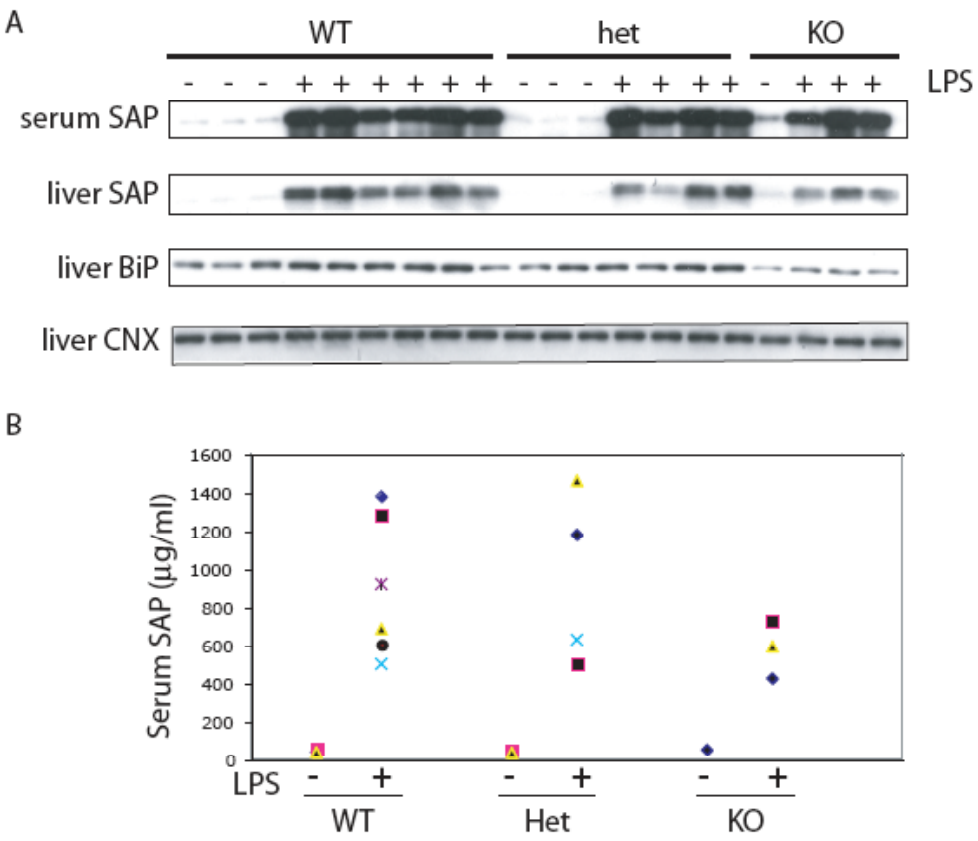

Figure 3-4. *Atf6α*-deficient mice are responsive to LPS challenge. (A) Wild-type and *Atf6α* heterozygous and homozygous mutant mice were injected intraperitoneally with LPS (3 mg/kg body weight) or vehicle. Protein lysates from livers or sera isolated 24 hours after injection, were probed by immunoblots as indicated. (B) Serum levels of SAP were determined by ELISA. Data points are for individuals.

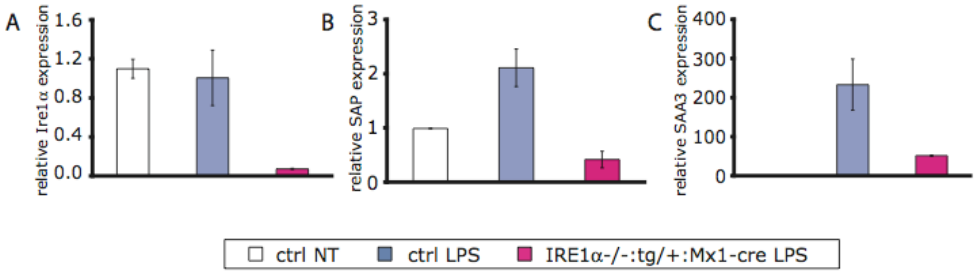

Figure 3-5. *Ire1α*-deficient mice are defective in up-regulation of acute phase response marker genes upon LPS challenge. Ire1α-/-:tg/+:Mx1-cre mice were injected intraperitoneally with poly IC (300 μg/mouse) every 48 hours for 4 times to induce *in vivo cre*-mediated deletion. Control mice and *Ire1α*-deficient mice were injected intraperitoneally with LPS (3 mg/kg BW). Total RNAs isolated from the livers 24hrs post injection were subjected to real-time RT-PCR analysis for expression levels of *Ire1α* (A), *SAP* (B) and *SAA3* (C). n = 5-6 control or 2-3 *Ire1α*-deleted LPS injected mice. Ctrl, control mice. Error bars represent means ± SEM from individual animals.

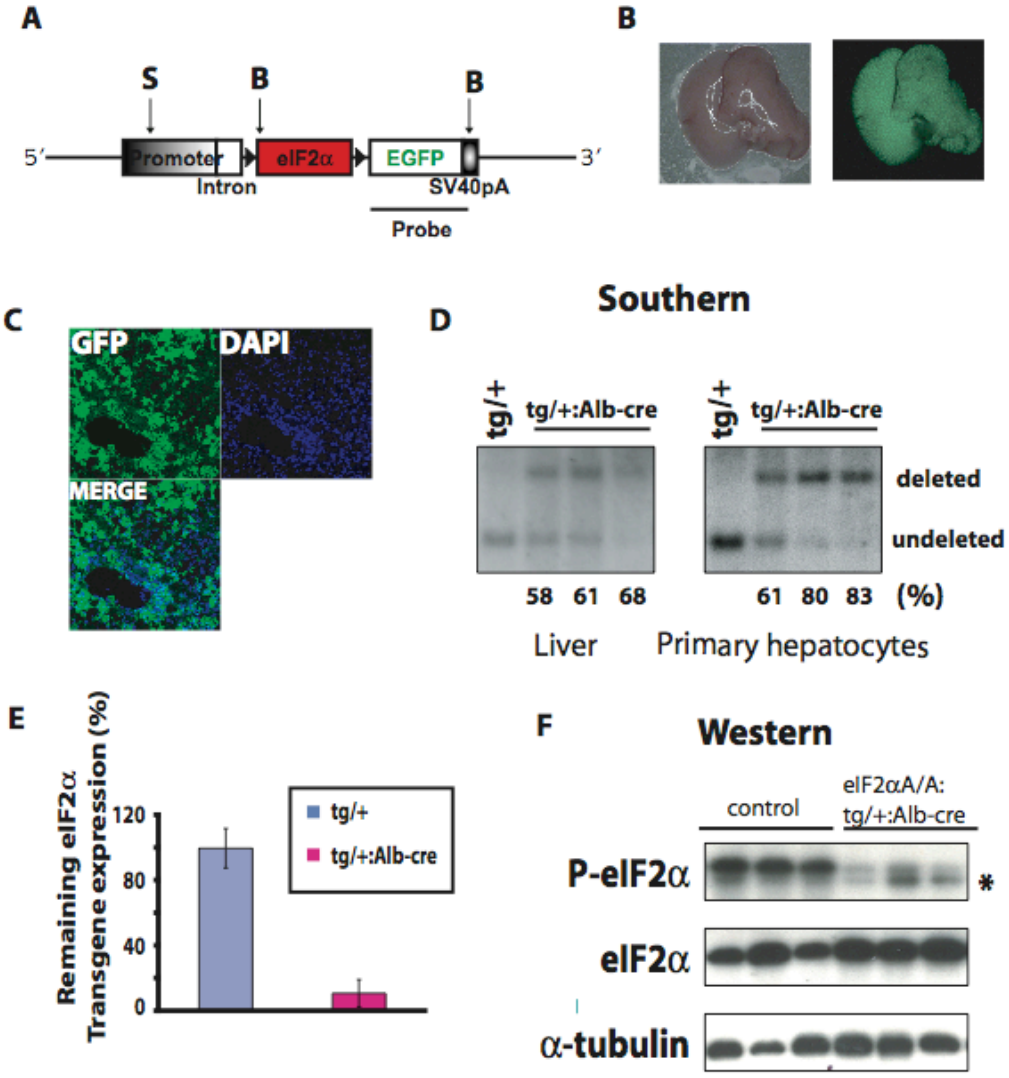

Figure 3-6. Generation of hepatocyte-specific eIF2α Ser51Ala knockin mice. (A) Schematic drawings of the structure of eIF2α transgene. The *loxP* (►) sites, the restriction sites used for Southern analysis (BglII: B, SpeI: S) and the probe are indicated. (B) Whole liver samples from 4 week old eIF2α$^{A/A}$:tg/+:Alb-cre mice were assessed for GFP expression under light (left panel) or fluorescence macroscope (right panel) using Leica MZFL III sterero/dissecting fluorescent microscope. Representative pictures are shown. (C) Paraffin-embedded sections (4μm) of the fixed livers of 4 month old eIF2α$^{A/A}$:tg/+:Alb-cre mice were stained for EGFP and DAPI and visualized at 200× magnification. Representative staining is shown. (D) Genomic DNA extracted out of whole liver tissue of 3 month old mice (left panel)/or primary hepatocytes from 4 month old mice (right panel), were subjected to southern blot analysis. The extent of *Cre*-mediated deletion was quantitated by densitometry and is shown underneath the blots. (E) Total RNA was isolated from 3 month old tg/+ (n=2) or tg/+:Alb-cre (n=5) mice and the expression level of the eIF2α transgene was quantitated by real-time RT-PCR, normalized against *18S* rRNA expression. Error bars represent means± SDM from individual animals. (F) Protein lysates of whole liver tissue, isolated from 3 month old control (eIF2α$^{S/A}$:tg/+:Alb-cre or eIF2α$^{A/A}$:tg/+) and eIF2α$^{A/A}$:tg/+:Alb-cre mice were probed by immunoblot with antibodies specific for phosphorylated eIF2α, total eIF2α or α-tubulin as a loading control. The asterisk indicates a non-specific background band. (A-E were contributed by S. Back)

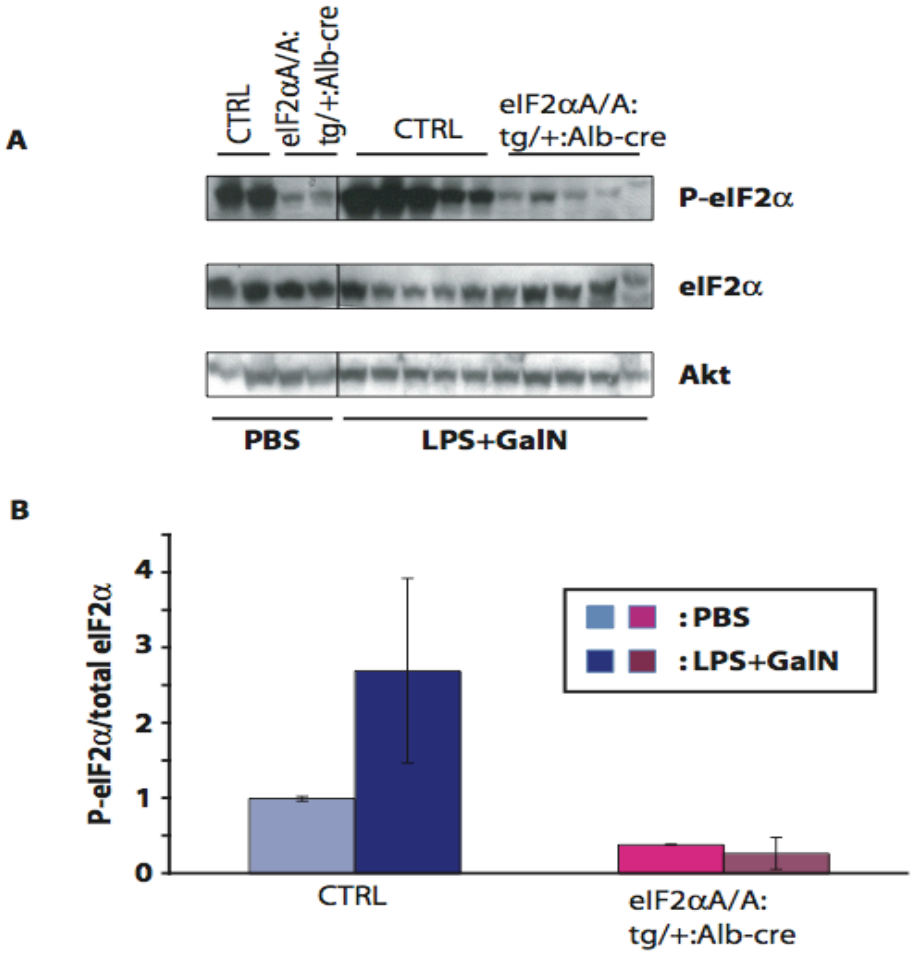

Figure 3-7. LPS+GalN challenge induces eIF2α phosphorylation in vivo. (A) Control (eIF2α$^{S/A}$:tg/+:Alb-cre and eIF2α$^{A/A}$:tg/+) and eIF2α$^{A/A}$:tg/+:Alb-cre mice were co-injected intraperitoneally with LPS (0.1 μg/g body weight) plus GalN (0.7mg/g body weight) or PBS. Protein lysates from livers isolated 5.5 hours after injection, were probed for phosphorylated eIF2α, total eIF2α and total AKT as a loading control. (B) The extent of phosphorylated eIF2α relative to total eIF2α was quantitated and is shown ± SDM in the graphs below the blots.

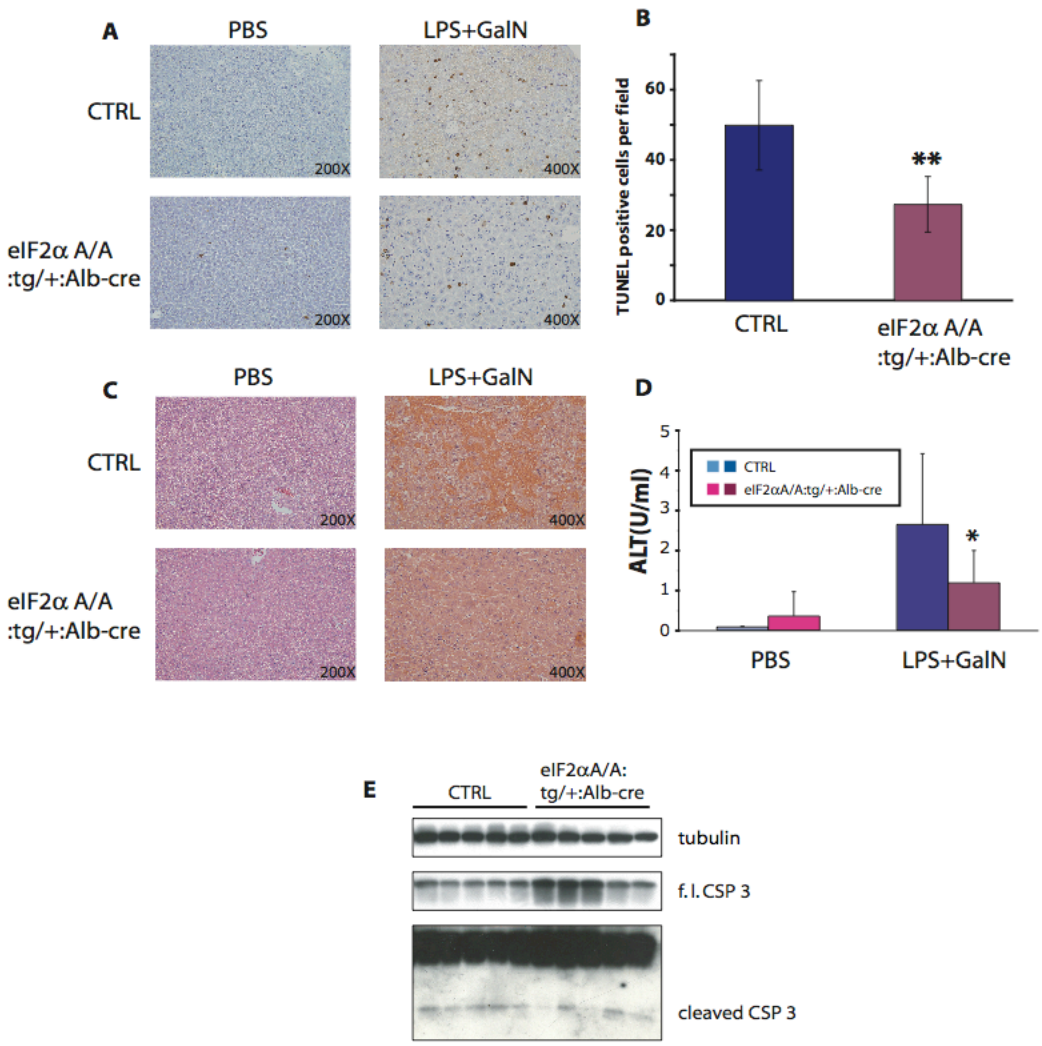

Figure 3-8. Disruption of eIF2α phosphorylation ameliorates acute liver injury induced by LPS+GalN challenge. Control (eIF2α$^{S/A}$:tg/+:Alb-cre and eIF2α$^{A/A}$:tg/+) and eIF2α$^{A/A}$:tg/+:Alb-cre mice were injected intraperitoneally with PBS, or LPS (0.1μg/g body weight) plus GalN (0.7mg/g body weight). Liver was surgically isolated 5.5 hrs post injection. Paraffin-embedded sections (4 μm) of the fixed livers were assayed for apoptosis by TUNEL (A) or stained with hematoxylin-eosin (C). Representative staining is shown and the magnifications are indicated. The number of apoptotic positive cells in each microscopic field was scored double-blindly and is shown in (B). Error bars represent means ± SDM (n=3-4, ** indicates statistical significance: $P<0.05$). The liver injury was measured by determining serum ALT levels (D). Error bars represent means ± SDM of independent animals (PBS injected, n=2, LPS+GalN coinjected, n=6, * indicates statistical significance: $P<0.1$). (E) Protein lysates from the livers of LPS+GalN challenged control (eIF2α$^{S/A}$:tg/+:Alb-cre and eIF2α$^{A/A}$:tg/+) and eIF2α$^{A/A}$:tg/+:Alb-cre mice were probed for full-length caspase-3, cleaved form of caspase 3 and tubulin as a loading control.

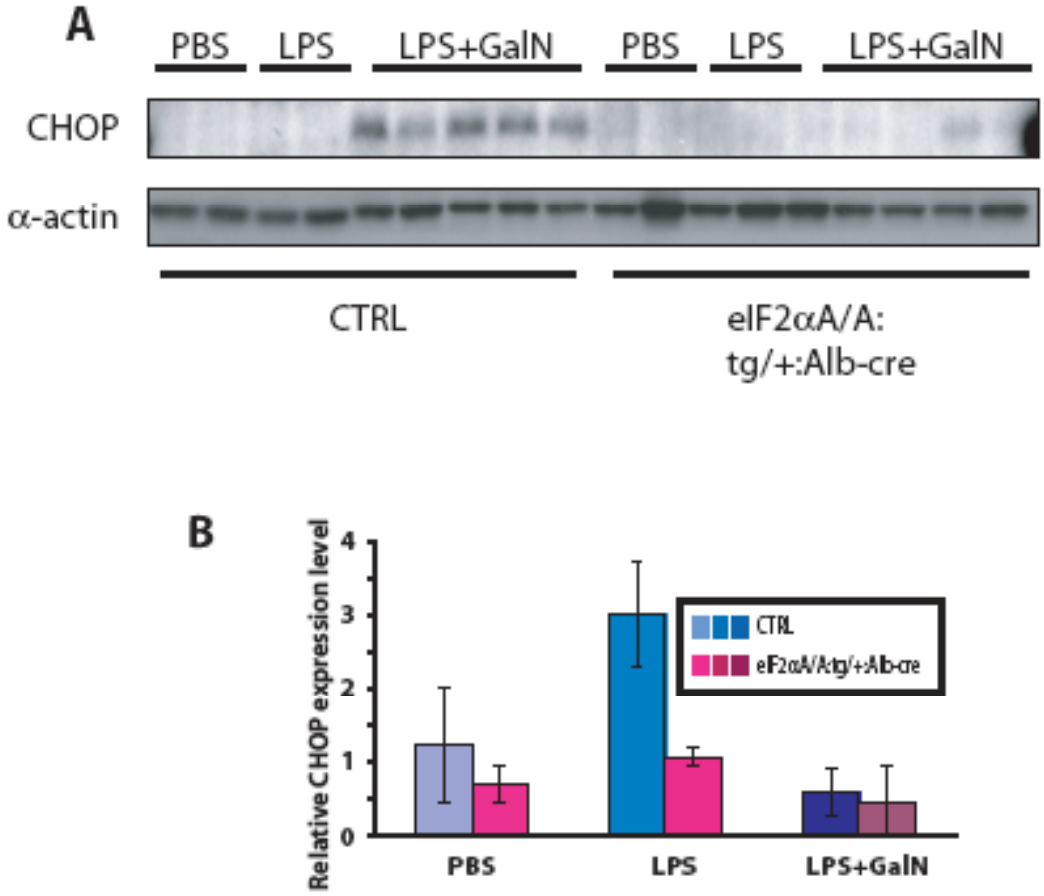

Figure 3-9. CHOP upregulation is defective in the LPS+GalN challenged eIF2α$^{A/A}$:tg/+:Alb-cre mice. (A) Control (eIF2α$^{S/A}$:tg/+:Alb-cre and eIF2α$^{A/A}$:tg/+) and eIF2α$^{A/A}$:tg/+:Alb-cre mice were injected intraperitoneally with PBS, LPS alone (4.5μg/g body weight) or LPS (0.1μg/g body weight) plus GalN (0.7mg/g body weight). Livers were surgically isolated 5.5 hrs post injection. Protein lysates were probed for CHOP, α-actin as a loading control. (B) Total RNA was independently prepared from the same liver tissue samples and the expression level of the CHOP mRNA was quantitated by real-time RT-PCR, normalized against *18S* rRNA expression. Error bars represent means ± SDM from individual animals (PBS injected, n=2, LPS injected, n=3-4, LPS+GalN co-injected, n=6).

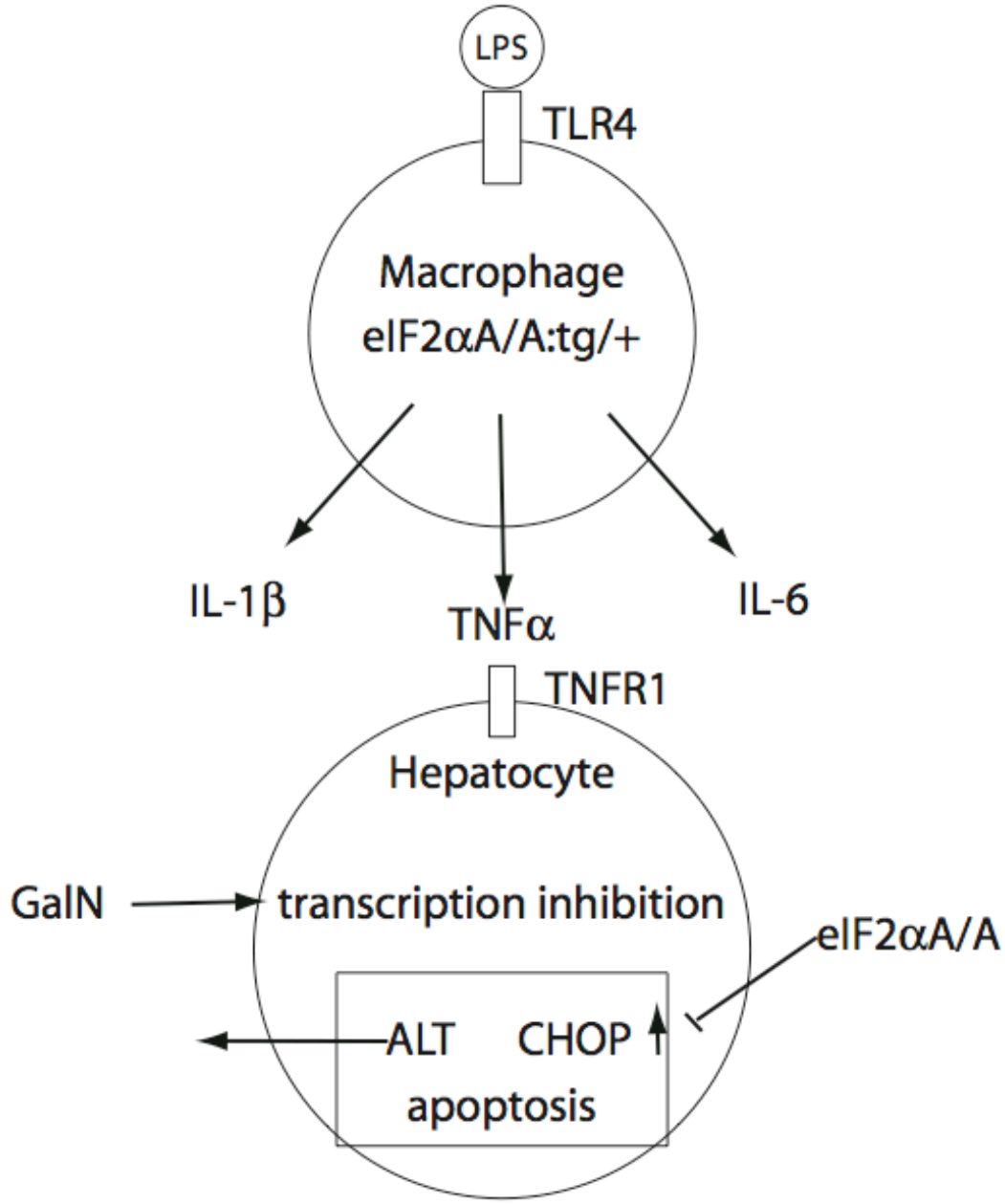

Figure 3-10. Diagrammatic representation of the cross talk of macrophages and hepatocytes during LPS+GalN induced liver apoptosis in eIF2α$^{A/A}$:tg/+:Alb-cre mice.

References:

1. Haze, K, Yoshida, H, Yanagi, H, Yura, T and Mori, K, (1999) Mammalian transcription factor ATF6 is synthesized as a transmembrane protein and activated by proteolysis in response to endoplasmic reticulum stress. Mol Biol Cell 10: 3787-99.

2. Shen, J, Chen, X, Hendershot, L and Prywes, R, (2002) ER stress regulation of ATF6 localization by dissociation of BiP/GRP78 binding and unmasking of Golgi localization signals. Dev Cell 3: 99-111.

3. Ye, J, Rawson, RB, Komuro, R, Chen, X, Dave, UP, Prywes, R et al., (2000) ER stress induces cleavage of membrane-bound ATF6 by the same proteases that process SREBPs. Mol Cell 6: 1355-64.

4. Omori, Y, Imai, J, Watanabe, M, Komatsu, T, Suzuki, Y, Kataoka, K et al., (2001) CREB-H: a novel mammalian transcription factor belonging to the CREB/ATF family and functioning via the box-B element with a liver-specific expression. Nucleic Acids Res 29: 2154-62.

5. Raggo, C, Rapin, N, Stirling, J, Gobeil, P, Smith-Windsor, E, O'Hare, P et al., (2002) Luman, the cellular counterpart of herpes simplex virus VP16, is processed by regulated intramembrane proteolysis. Mol Cell Biol 22: 5639-49.

6. Chin, KT, Zhou, HJ, Wong, CM, Lee, JM, Chan, CP, Qiang, BQ et al., (2005) The liver-enriched transcription factor CREB-H is a growth suppressor protein underexpressed in hepatocellular carcinoma. Nucleic Acids Res 33: 1859-73.

7. Kondo, S, Murakami, T, Tatsumi, K, Ogata, M, Kanemoto, S, Otori, K et al., (2005) OASIS, a CREB/ATF-family member, modulates UPR signalling in astrocytes. Nat Cell Biol 7: 186-94.

8. Gabay, C and Kushner, I, (1999) Acute-phase proteins and other systemic responses to inflammation. N Engl J Med 340: 448-54.

9. Medzhitov, R and Janeway, CA, Jr., (2002) Decoding the patterns of self and nonself by the innate immune system. Science 296: 298-300.

10. Yoo, JY and Desiderio, S, (2003) Innate and acquired immunity intersect in a global view of the acute-phase response. Proc Natl Acad Sci U S A 100: 1157-62.

11. Bodmer, B and Siboo, R, (1977) Isolation of mouse C-reactive protein from liver and serum. J Immunol 118: 1086-9.

12. Whitehead, AS, Zahedi, K, Rits, M, Mortensen, RF and Lelias, JM, (1990) Mouse C-reactive protein. Generation of cDNA clones, structural analysis, and induction of mRNA during inflammation. Biochem J 266: 283-90.

13. Le, PT, Muller, MT and Mortensen, RF, (1982) Acute phase reactants of mice. I. Isolation of serum amyloid P-component (SAP) and its induction by a monokine. J Immunol 129: 665-72.

14. Baumann, H and Gauldie, J, (1990) Regulation of hepatic acute phase plasma protein genes by hepatocyte stimulating factors and other mediators of inflammation. Mol Biol Med 7: 147-59.

15. Ochrietor, JD, Harrison, KA, Zahedi, K and Mortensen, RF, (2000) Role of STAT3 and C/EBP in cytokine-dependent expression of the mouse serum amyloid P-component (SAP) and C-reactive protein (CRP) genes. Cytokine 12: 888-99.

16. Uhlar, CM and Whitehead, AS, (1999) Serum amyloid A, the major vertebrate acute-phase reactant. Eur J Biochem 265: 501-23.

17. Lee, K, Tirasophon, W, Shen, X, Michalak, M, Prywes, R, Okada, T et al., (2002) IRE1-mediated unconventional mRNA splicing and S2P-mediated ATF6 cleavage merge to regulate XBP1 in signaling the unfolded protein response. Genes Dev 16: 452-66.

18. Rubinson, DA, Dillon, CP, Kwiatkowski, AV, Sievers, C, Yang, L, Kopinja, J et al., (2003) A lentivirus-based system to functionally silence genes in primary mammalian cells, stem cells and transgenic mice by RNA interference. Nat Genet 33: 401-6.

19. Okabe, M, Ikawa, M, Kominami, K, Nakanishi, T and Nishimune, Y, (1997) 'Green mice' as a source of ubiquitous green cells. FEBS Lett 407: 313-9.

20. Miyoshi, K, Katayama, T, Imaizumi, K, Taniguchi, M, Mori, Y, Hitomi, J et al., (2000) Characterization of mouse Ire1 alpha: cloning, mRNA localization in the brain and functional analysis in a neural cell line. Brain Res Mol Brain Res 85: 68-76.

21. Sambrook, J, Fritsch, EF and Sambrook, J, (1989) Molecular cloning : a laboratory manual. (Cold Spring Harbor Laboratory, Cold Spring Harbor, N.Y.).

22. Rutkowski, DT, Arnold, SM, Miller, CN, Wu, J, Li, J, Gunnison, KM et al., (2006) Adaptation to ER stress is mediated by differential stabilities of pro-survival and pro-apoptotic mRNAs and proteins. PLoS Biol 4: e374.

23. Jirillo, E, Caccavo, D, Magrone, T, Piccigallo, E, Amati, L, Lembo, A et al., (2002) The role of the liver in the response to LPS: experimental and clinical findings. J Endotoxin Res 8: 319-27.

24. Heumann, D and Roger, T, (2002) Initial responses to endotoxins and Gram-negative bacteria. Clin Chim Acta 323: 59-72.

25. Beutler, B, (2000) Endotoxin, toll-like receptor 4, and the afferent limb of innate immunity. Curr Opin Microbiol 3: 23-8.

26. Butchar, JP, Parsa, KV, Marsh, CB and Tridandapani, S, (2006) Negative regulators of toll-like receptor 4-mediated macrophage inflammatory response. Curr Pharm Des 12: 4143-53.

27. Karin, M and Lin, A, (2002) NF-kappaB at the crossroads of life and death. Nat Immunol 3: 221-7.

28. Lehmann, V, Freudenberg, MA and Galanos, C, (1987) Lethal toxicity of lipopolysaccharide and tumor necrosis factor in normal and D-galactosamine-treated mice. J Exp Med 165: 657-63.

29. Galanos, C, Freudenberg, MA and Reutter, W, (1979) Galactosamine-induced sensitization to the lethal effects of endotoxin. Proc Natl Acad Sci U S A 76: 5939-43.

30. Yeung, MC, Chang, DL, Camantigue, RE and Lau, AS, (1999) Inhibitory role of the host apoptogenic gene PKR in the establishment of persistent infection by encephalomyocarditis virus in U937 cells. Proc Natl Acad Sci U S A 96: 11860-5.

31. Kaufman, RJ, (1999) Double-stranded RNA-activated protein kinase mediates virus-induced apoptosis: a new role for an old actor. Proc Natl Acad Sci U S A 96: 11693-5.

32. Saelens, X, Kalai, M and Vandenabeele, P, (2001) Translation inhibition in apoptosis: caspase-dependent PKR activation and eIF2-alpha phosphorylation. J Biol Chem 276: 41620-8.

33. Scheuner, D, Patel, R, Wang, F, Lee, K, Kumar, K, Wu, J et al., (2006) Double-stranded RNA-dependent protein kinase phosphorylation of the alpha-subunit of eukaryotic translation initiation factor 2 mediates apoptosis. J Biol Chem 281: 21458-68.

34. Dever, TE, (2002) Gene-specific regulation by general translation factors. Cell 108: 545-56.

35. Wu, J and Kaufman, RJ, (2006) From acute ER stress to physiological roles of the Unfolded Protein Response. Cell Death Differ 13: 374-84.

36. McCullough, KD, Martindale, JL, Klotz, LO, Aw, TY and Holbrook, NJ, (2001) Gadd153 sensitizes cells to endoplasmic reticulum stress by down-regulating Bcl2 and perturbing the cellular redox state. Mol Cell Biol 21: 1249-59.

37. Endo, M, Mori, M, Akira, S and Gotoh, T, (2006) C/EBP homologous protein (CHOP) is crucial for the induction of caspase-11 and the pathogenesis of lipopolysaccharide-induced inflammation. J Immunol 176: 6245-53.

38. Scheuner, D, Song, B, McEwen, E, Liu, C, Laybutt, R, Gillespie, P et al., (2001) Translational control is required for the unfolded protein response and in vivo glucose homeostasis. Mol Cell 7: 1165-76.

39. Postic, C and Magnuson, MA, (2000) DNA excision in liver by an albumin-Cre transgene occurs progressively with age. Genesis 26: 149-50.

40. Maeda, S, Chang, L, Li, ZW, Luo, JL, Leffert, H and Karin, M, (2003) IKKbeta is required for prevention of apoptosis mediated by cell-bound but not by circulating TNFalpha. Immunity 19: 725-37.

41. Horie, Y, Suzuki, A, Kataoka, E, Sasaki, T, Hamada, K, Sasaki, J et al., (2004) Hepatocyte-specific Pten deficiency results in steatohepatitis and hepatocellular carcinomas. J Clin Invest 113: 1774-83.

42. Hsu, LC, Park, JM, Zhang, K, Luo, JL, Maeda, S, Kaufman, RJ et al., (2004) The protein kinase PKR is required for macrophage apoptosis after activation of Toll-like receptor 4. Nature 428: 341-5.

43. Xue, X, Piao, JH, Nakajima, A, Sakon-Komazawa, S, Kojima, Y, Mori, K et al., (2005) Tumor necrosis factor alpha (TNFalpha) induces the unfolded protein response (UPR) in a reactive oxygen species (ROS)-dependent fashion, and the UPR counteracts ROS accumulation by TNFalpha. J Biol Chem 280: 33917-25.

44. Back, SH, Lee, K, Vink, E and Kaufman, RJ, (2006) Cytoplasmic IRE1alpha-mediated XBP1 mRNA splicing in the absence of nuclear processing and endoplasmic reticulum stress. J Biol Chem 281: 18691-706.

CHAPTER IV

CONCLUSIONS, PERSPECTIVES AND FUTURE DIRECTIONS

Introduction

In 1989, an Australian group reported severe dilation of cisternae of the rough endoplasmic reticulum (ER) in hepatocytes and reduced concentrations of serum proteins in tunicamycin-injected Guinea pigs [1]. At the time, the researchers did not know the exact molecular mechanism for this hepatic toxicity. Two decades and more than 5000 unfolded protein response (UPR) and ER stress related papers later, it is fairly safe to infer at least one of the major toxicological/pathological causes for this observation is ER stress in the hepatocytes and disturbed protein secretion from the ER *in vivo*.

In the last twenty years, tremendous progress has been made in the UPR field. The unfolded protein response was first studied in yeast, in which Ire1p/Hac1p is the only UPR signaling pathway [2,3]. Genomic analysis suggests that although *atf-6* and *pek* emerged within the *Caenorhabditis elegans* UPR, the most significant UPR regulation occurs through the *ire-1/xbp-1* pathway in the worm [4]. In higher eukaryotes, the UPR expanded to a signal transduction nexus: IRE1 and ATF6 both contain alpha and beta isoforms. Several basic leucine zipper (b-ZIP)-containing transcription factors that share homology with ATF6, such as Luman [5], are reported to be ER stress responsive. To cope with different types of ER stress in different tissues, vertebrates have also evolved tissue-specific UPR regulators. For example, transcription factors regulated in a similar manner

to ATF6 are CREBH, OASIS and Tisp40, that are selectively expressed in hepatocytes, astrocytes and spermatids, respectively [6-8]. More recent studies in plants and drosophila [9,10] further support the notion that the UPR signal transduction pathway is essential for, most likely, all eukaryotes to cope with stress in the ER.

Our current knowledge of UPR signaling has benefited from studies in plants, yeast, *C. elegans, drosophila* and genetically manipulated rodent models harboring mutations in selective UPR components. Murine genetic models have most significantly contributed to understanding the physiological roles of the UPR. Although deletion of some of the UPR signaling pathways results in embryonic lethality, mice have recently been engineered with conditionally-targeted gene mutations or conditional transgenes to rescue null mutations to circumvent the embryonic or neonatal lethality and to define the physiological role of each UPR subpathway.

In this thesis study, we have deleted the *Atf6*α gene in the mouse and, for the first time, identified the unique role for this third UPR subpathway in ER function. Data generated from this loss-of-function model in pure genetic background clarified some long-debated questions on the role of ATF6α.

ATF6alpha is not essential for basal chaperone expression and embryonic and postnatal development

The first surprising observation was that homozygous *Atf6*α-deficient mice are born at the expected Mendelian ratio and show no obvious developmental defects. This is in contrast to the embryonic lethality observed in *Ire1*α-/or *Xbp1*-deficient mice and neonatal homozygous mutant eIF2α Ser51Ala phosphorylation-resistant knock-in mice. Further characterization demonstrated that ATF6α plays an essential role in adapting to

chronic stress, and that IRE1α and PERK may compensate for ATF6α deficiency during murine embryonic development. Recently, several proteins that share significant structural homology with ATF6αwere identified that are activated through stress-induced regulated intramembrane proteolysis. These tissue-specific or ubiquitously expressed transcription factors may collaborate to manage vital functions throughout development.

ATF6alpha optimizes protein processing in the ER

Our studies using genetically-deficient murine embryonic fibroblasts (MEFs) have also elucidated novel features of the role of ATF6α in the ER stress response. Our gene expression studies confirmed previous findings that suggested that ATF6α regulates ER chaperone upregulation upon ER stress [11,12]. However, our microarray analyses demonstrated a much more significant role for ATF6α during the ER stress response as ATF6α regulates almost every aspect of the ER function including protein folding, protein degradation, protein trafficking, protein secretion and ER biogenesis. Although regulation of ER-associated degradation (ERAD) gene expression was previously considered to be IRE1α-dependent [13], our findings show that ATF6α is also required for the stress-induced up-regulation of ERAD. Further characterization revealed that protein processing and secretion were also defective when *Atf6α-/-* cells were subjected to ER stress, suggesting that ATF6α function may be vital when professional secretory cells are exposed to ER stress *in vivo.*

As a major secretory organ, the liver regulates glucose homeostasis, lipid metabolism and drug detoxification. Our preliminary data have shown that when challenged by a high-fat diet, *Atf6α*-deficient mice have lower levels of blood high-

density lipoprotein (HDL) and total cholesterol, compared to wild-type mice (Data not shown), reminiscent of previous reports that ATF6α may antagonize the lipogenic functions of sterol-response-element binding protein 2 (SREBP2) in the liver [14]. Further study is ongoing to determine how the absence of ATF6α affects metabolic functions of the liver. We have shown that when *Atf6α*-deficient mice are challenged with tunicamycin (1mg/kg body weight), the secretion of acute phase response markers SAP and CRP from hepatocytes is defective. The defects in this protective response may be one reason why the *Atf6α*-deficient mice succumb to the injection of sub-lethal doses of tunicamycin.

Crosstalk between ATF6alpha and other UPR subpathways

As the last available loss-of-function model among the three proximal ER stress sensors, *Atf6α*-deficient cells and mice have provided new insights into the crosstalk between each of the UPR subpathways and have contributed to a more complete understanding of UPR signal transduction (Figure 4-1). Upon severe and acute ER stress, wild-type and *Atf6α-/-* cells exhibit similar activation of PERK, IRE1α/XBP1 and ATF6β (Figure 2-7). However, in contrast to wild-type cells and/or mice, when *Atf6α-/-* cells and/or mice were subjected to chronic or repetitive ER stress, the IRE1α/XBP1 pathway was continuously activated. We interpret this finding that the mutant cells are unable to adapt to the chronic stress (Figure 2-14 and Figure 2-15). This notion is supported by the observation that upon chronic stress, *Atf6α-/-* cells displayed more CHOP expression, more PARP cleavage and less BiP expression compared to the wild type cells. In contrast to IRE1α/XBP1, the phosphorylation of eIF2α was more efficiently down-regulated in mutant cells than in wild-type control cells (Figure 2-15).

The reduced eIF2α phosphorylation may be a consequence of the increased expression of GADD34, a regulatory subunit of the type 1 Ser/Thr phosphatase PP1, in the mutant cells. GADD34 was previously proposed to be regulated through CHOP and function as a negative regulator of the PERK/eIF2α signaling pathway [15].

GADD34 protein upregulation is observed in TM-injected *Atf6*α-/- animals but not in wild-type or heterozygous controls (Figure 2-15). This result mirrors an elevation of *Gadd34* mRNA and protein in *Atf6*α-/- MEFs (Figures 2-3A and 2-14). CHOP is also elevated in *Atf6*α-/- cells and animals at later points after ER stress. Both CHOP and GADD34 are short-lived at the mRNA and protein levels [16], which suggests that their persistence in *Atf6*α-/- animals and cells reflects active and ongoing synthesis. Therefore, absent both eIF2α phosphorylation and ATF6α, which have been proposed as the regulators of CHOP expression, we conclude that there is an additional as yet unidentified regulator of CHOP. The putative role of such a regulator might be to ensure the perpetuation of an apoptotic signal during unresolved stress, as a way of circumventing GADD34-mediated negative feedback of eIF2α signaling.

An appealing candidate for this CHOP regulator would be XBP1. Even though there is no direct data to support that this bZIP transcription factor is involved in CHOP activation, in the *Atf6α-/-* cells splicing of *Xbp1* mRNA persists upon chronic stress (Figure 2-15) and overexpression of XBP1 can rescue UPRE-reporter activation in the absence of ATF6α (Figure 2-6). To study how the IRE1α/XBP1 subpathway may compensate ATF6α, a tempting solution is to cross *Atf6α*-null allele into IRE1α knockout background. However in order to circumvent the technical challenges from *Ire1α-/-* mice embryonic lethality, we could either work with dominant-negative-IRE1α-

stable-transfected *Atf6α-/-* cell lines or isolate fibroblasts from *Atf6α-/-:Ire1α*-fe/fe embryos, in which the expression of *Ire1α*could be later deleted by adenoviral-*cre* expression.

siRNA knockdown of *Atf6β* in *Atf6α-/-* cells had no effect on the stress-dependent upregulation of BiP and CHOP, which is consistent with previous reports that the protein has a non-redundant role with ATF6α [17,18]. Our preliminary analyses on the homozygous *Atf6β-/-* MEFs suggested that this protein may play an important role in maintaining calcium homeostasis. To avoid the limitation of RNAi and elucidate the potential functional overlapping between these two isoforms, we are currently underway to generate double knockout mice deficient in both *Atf6α* and *Atf6β*.

Physiological roles of ATF6alpha

Experimental studies in cultured cells have revealed roles for each of the UPR sensors protection against ER stress. However, ER stress that is encountered during physiological, pathological and developmental contexts *in vivo* is likely quite distinct from the relatively artificial conditions of the pharmacologically severe and acute induction of ER stress that investigators have used to dissect UPR subpathways *in vitro*. It is presently unknown how the UPR can mount a protective response during such fundamental processes as the differentiation, development, and maintenance of professional secretory cell function. Since deletions in IRE1α versus PERK have such divergent phenotypes in the mouse suggests that signaling through each UPR subpathway *in vivo* is highly-dependent upon the nature of the stress, as well as the cell type. Since mice with deletions in each of the three of the proximal sensors of ER stress are now available, future studies will be able to more directly address the physiological roles of

each of these subpathways. Importantly, our unpublished results have already provided new insights into the role of ATF6α in particular in the differentiation and maintenance of professional secretory cells, and how this pathway interfaces with other UPR signaling pathways during ER stress.

I. ATF6alpha in B cell differentiation

One well-studied experimental model of the ER stress response in the differentiation of professional secretory cells is that of mature B lymphocytes upon differentiation into antibody-producing plasma cells when challenged by antigen or bacterial toxins such as lipopolysaccharide (LPS). Studies have demonstrated that the expansion of the secretory apparatus and upregulation of ER chaperones require proper UPR signaling. It is known that both IRE1α and XBP1 are required for B cell differentiation [19,20], though PERK appears dispensable for the process [21]. On the other hand, it remains elusive what is the nature of the stimulus that leads to UPR activation during the process and how selective UPR subpathways can be activated without leading to UPR-mediated cell death.

To investigate the role of ATF6α in plasma cell differentiation, we isolated primary splenic B cells from wild-type and *Atf6α-/-* mice. When challenged with LPS, BiP was robustly upregulated after 48 hours in wild-type B cells. In contrast, both the basal level and the upregulation of BiP were significantly reduced in the absence of ATF6α (Figure 4-2). Furthermore, CHOP, which has been suggested to be a marker for ER stress-induced cell death, was significantly upregulated in *Atf6α-/-* B cells after 48 and 72hrs differentiation whereas CHOP expression is only marginally detectable in the wild type cells (Figure 4-2). It is conceivable that the defective chaperone gene

expression in the *Atf6α-/-* B cells cannot support the high-level antibody production and secretion, and as a consequence, activates an apoptotic cell death program. However, the levels of IgM and IgG1 secretion in the cell culture media were comparable between the genotypes from these preliminary experiments (data not shown). It is possible that reduced, but not completely abrogated, BiP expression in *Atf6α-/-* B cells is sufficient to support antibody processing and secretion under these conditions. It is also conceivable that, similar to what we observed in MEFs, the defect in the protein processing and secretion will only be readily detectable in the context of additional ER stress (Figure 2-11). It will be necessary to evaluate additional markers of plasma cell differentiation to clarify the consequence of the defective chaperone upregulation in the absence of ATF6α.

II. ATF6alpha in the pancreas

Numerous studies support the idea that ER stress, together with oxidative stress, play important roles in pancreatic beta cell function and etiology of type-II diabetes [22]. Previous studies have shown that polymorphisms in the human Atf6α promoter may be linked with type 2 diabetes [23]. Our preliminary data have suggested that the insulin secretion upon fasting and re-feeding is defective in *Atf6α-/-* mice (data not shown). However, there is little difference in the glucose tolerance test (GTT) between wild-type and *Atf6α-/-* mice, either on a regular CHOW diet or high-fat diet (data not shown). It may be important to impose greater levels of ER stress on the beta cell to uncover a specific requirement for ATF6α. Future studies should challenge the *Atf6α-/-* mice with streptozotocin (STZ), which is believed to damage beta cells through oxidative stress [24]. This could also shed insight into how Reactive Oxygen Species (ROS) disturb ER

homeostasis, especially in stress-sensitive cells. While analysis of beta cell function in older animals is underway, we measured expression of the ER chaperone BiP in the whole pancreas (Figure 4-3). The basal level of BiP expression was reproducibly reduced in the pancreas from the *Atf6α*-/- mice. However, the reduced BiP may reflect decreased BiP expression in pancreatic acinar cells, which constitute approximately 80% of the cells of the pancreas. Earlier reports on *Perk*-/- and tissue-specific *Xbp1* transgenic-rescued *Xbp1*-deficient mice suggest that PERK and XBP1 are essential for the function of the exocrine pancreas [25,26]. Even though *Atf6α*-deficient mice do not display any obvious digestive defects (similar body weight up to 7 months of age), have similar basal levels of amylase and trypsin expression, and have normal acinar cell-ultrastructure (data not shown), the decreased expression of BiP suggests some alteration ER function may exist in the *Atf6α*-/- pancreas. Clinical studies have suggested acinar cell defects in alcohol-related acute pancreatitis in human [27]. One way to burden the *Atf6α*-/- pancreatic acinar cells is to challenge the mice with ethanol, which will also provide a valuable model to study the role of ATF6α in alcohol-induced liver disease.

Beyond ER stress

Twenty years of work on elucidating the mechanisms and roles of UPR signaling has provided many unexpected insights into the significance of these pathways in human disease. More detailed clinical studies are required to elucidate the relationship between ER stress, oxidative stress, and the role of the UPR in cancer, metabolic disease, neurological diseases, genetic disease, and infectious diseases will undoubtedly provide new insights. All these questions could only be answered when researchers from different fields collaborate closely and combine the power of various models.

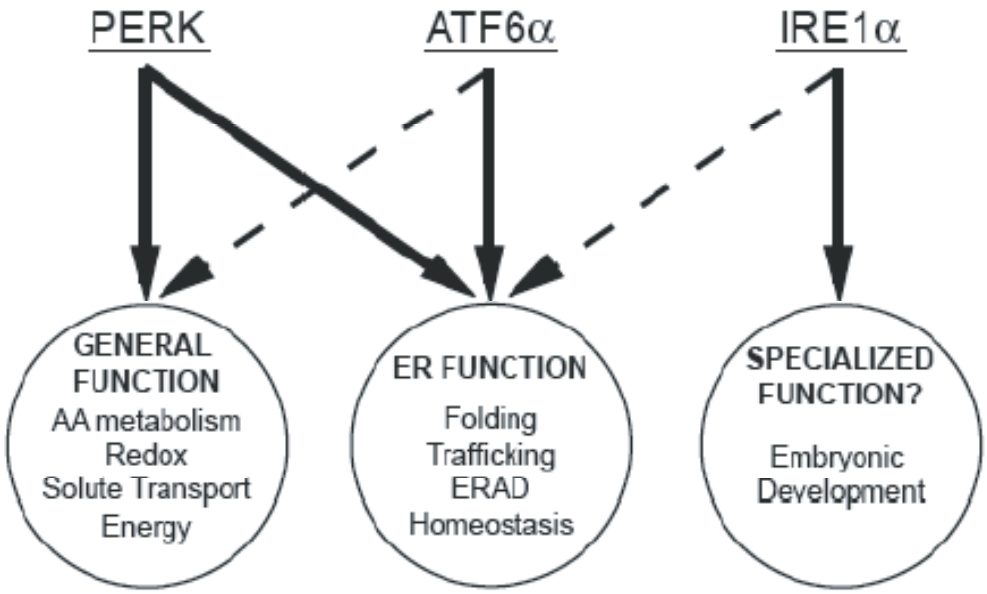

Figure 4-1. A schematic diagram depicting the relative roles of PERK, ATF6α and IRE1α in regulating the functions responsible for adaptation to stress. Solid lines indicate potentially major involvement of a sensor, and dashed lines minor involvement. Note the degree of redundancy in the control of genes regulating ER function.

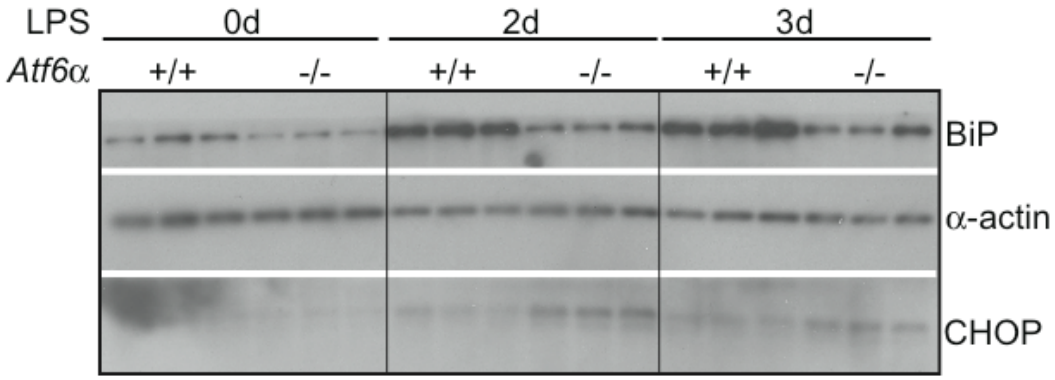

Figure 4-2 *Atf6α*-/- primary splenic B cells do not efficiently adapt to physiological stress during plasma cell differentiation. Primary splenic B cells were isolated from wild-type and *Atf6α*-/- mice spleens as described [28] and treated for indicated time with LPS, a direct plasma cell differentiation stimulus. Protein lysates were then extracted and probed for BiP, CHOP and α-actin as a loading control.

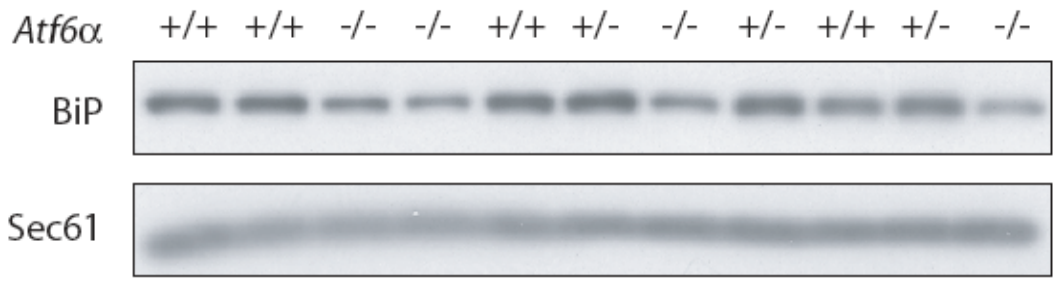

Figure 4-3. Basal pancreatic expression level of BiP is lower in *Atf6α*-/- mice. Protein lysates from total pancreases of wild-type and *Atf6α*- heterozygous and homozygous mutant mice were probed for BiP to compare the basal expression level of this ER chaperone, with Sec61 as a loading control.

References:

1. Finnie, JW and O'Shea, JD, (1989) Acute hepatotoxicity with resultant pulmonary and cerebral embolism in guinea pigs given tunicamycin. Pathology 21: 194-9.

2. Cox, JS, Chapman, RE and Walter, P, (1997) The unfolded protein response coordinates the production of endoplasmic reticulum protein and endoplasmic reticulum membrane. Mol Biol Cell 8: 1805-14.

3. Kawahara, T, Yanagi, H, Yura, T and Mori, K, (1997) Endoplasmic reticulum stress-induced mRNA splicing permits synthesis of transcription factor Hac1p/Ern4p that activates the unfolded protein response. Mol Biol Cell 8: 1845-62.

4. Shen, X, Ellis, RE, Sakaki, K and Kaufman, RJ, (2005) Genetic Interactions Due to Constitutive and Inducible Gene Regulation Mediated by the Unfolded Protein Response in C. elegans. PLoS Genet 1: e37.

5. DenBoer, LM, Hardy-Smith, PW, Hogan, MR, Cockram, GP, Audas, TE and Lu, R, (2005) Luman is capable of binding and activating transcription from the unfolded protein response element. Biochem Biophys Res Commun 331: 113-9.

6. Kondo, S, Murakami, T, Tatsumi, K, Ogata, M, Kanemoto, S, Otori, K et al., (2005) OASIS, a CREB/ATF-family member, modulates UPR signalling in astrocytes. Nat Cell Biol 7: 186-94.

7. Omori, Y, Imai, J, Watanabe, M, Komatsu, T, Suzuki, Y, Kataoka, K et al., (2001) CREB-H: a novel mammalian transcription factor belonging to the CREB/ATF family and functioning via the box-B element with a liver-specific expression. Nucleic Acids Res 29: 2154-62.

8. Nagamori, I, Yabuta, N, Fujii, T, Tanaka, H, Yomogida, K, Nishimune, Y et al., (2005) Tisp40, a spermatid specific bZip transcription factor, functions by binding to the unfolded protein response element via the Rip pathway. Genes Cells 10: 575-94.

9. Urade, R, (2007) Cellular response to unfolded proteins in the endoplasmic reticulum of plants. Febs J 274: 1152-71.

10. Ryoo, HD and Steller, H, (2007) Unfolded protein response in Drosophila: why another model can make it fly. Cell Cycle 6: 830-5.

11. Okada, T, Yoshida, H, Akazawa, R, Negishi, M and Mori, K, (2002) Distinct roles of activating transcription factor 6 (ATF6) and double-stranded RNA-activated protein kinase-like endoplasmic reticulum kinase (PERK) in transcription during the mammalian unfolded protein response. Biochem J 366: 585-94.

12. Yoshida, H, Haze, K, Yanagi, H, Yura, T and Mori, K, (1998) Identification of the cis-acting endoplasmic reticulum stress response element responsible for transcriptional induction of mammalian glucose-regulated proteins. Involvement of basic leucine zipper transcription factors. J Biol Chem 273: 33741-9.

13. Yoshida, H, Matsui, T, Hosokawa, N, Kaufman, RJ, Nagata, K and Mori, K, (2003) A time-dependent phase shift in the mammalian unfolded protein response. Dev Cell 4: 265-71.

14. Zeng, L, Lu, M, Mori, K, Luo, S, Lee, AS, Zhu, Y et al., (2004) ATF6 modulates SREBP2-mediated lipogenesis. Embo J 23: 950-8.

15. Novoa, I, Zeng, H, Harding, HP and Ron, D, (2001) Feedback inhibition of the unfolded protein response by GADD34-mediated dephosphorylation of eIF2alpha. J Cell Biol 153: 1011-22.

16. Rutkowski, DT, Arnold, SM, Miller, CN, Wu, J, Li, J, Gunnison, KM et al., (2006) Adaptation to ER stress is mediated by differential stabilities of pro-survival and pro-apoptotic mRNAs and proteins. PLoS Biol 4: e374.

17. Thuerauf, DJ, Morrison, L and Glembotski, CC, (2004) Opposing roles for ATF6alpha and ATF6beta in endoplasmic reticulum stress response gene induction. J Biol Chem 279: 21078-84.

18. Thuerauf, DJ, Marcinko, M, Belmont, PJ and Glembotski, CC, (2007) Effects of the Isoform-specific Characteristics of ATF6{alpha} and ATF6beta on Endoplasmic Reticulum Stress Response Gene Expression and Cell Viability. J Biol Chem 282: 22865-78.

19. Zhang, K, Wong, HN, Song, B, Miller, CN, Scheuner, D and Kaufman, RJ, (2005) The unfolded protein response sensor IRE1alpha is required at 2 distinct steps in B cell lymphopoiesis. J Clin Invest 115: 268-81.

20. Iwakoshi, NN, Lee, AH and Glimcher, LH, (2003) The X-box binding protein-1 transcription factor is required for plasma cell differentiation and the unfolded protein response. Immunol Rev 194: 29-38.

21. Gass, JN, Gifford, NM and Brewer, JW, (2002) Activation of an unfolded protein response during differentiation of antibody-secreting B cells. J Biol Chem 277: 49047-54.

22. Harding, HP and Ron, D, (2002) Endoplasmic reticulum stress and the development of diabetes: a review. Diabetes 51 Suppl 3: S455-61.

23. Chu, WS, Das, SK, Wang, H, Chan, JC, Deloukas, P, Froguel, P et al., (2007) Activating transcription factor 6 (ATF6) sequence polymorphisms in type 2 diabetes and pre-diabetic traits. Diabetes 56: 856-62.

24. Lukic, ML, Stosic-Grujicic, S and Shahin, A, (1998) Effector mechanisms in low-dose streptozotocin-induced diabetes. Dev Immunol 6: 119-28.

25. Lee, AH, Chu, GC, Iwakoshi, NN and Glimcher, LH, (2005) XBP-1 is required for biogenesis of cellular secretory machinery of exocrine glands. Embo J 24: 4368-80.

26. Harding, HP, Zeng, H, Zhang, Y, Jungries, R, Chung, P, Plesken, H et al., (2001) Diabetes mellitus and exocrine pancreatic dysfunction in perk-/- mice reveals a role for translational control in secretory cell survival. Mol Cell 7: 1153-63.

27. Cosen-Binker, LI and Gaisano, HY, (2007) Recent insights into the cellular mechanisms of acute pancreatitis. Can J Gastroenterol 21: 19-24.

28. Iwakoshi, NN, Lee, AH, Vallabhajosyula, P, Otipoby, KL, Rajewsky, K and Glimcher, LH, (2003) Plasma cell differentiation and the unfolded protein response intersect at the transcription factor XBP-1. Nat Immunol 4: 321-9.